

The Voltage Gated Sodium Channel  $\beta 1/\beta 1B$  subunits: Emerging Therapeutic Targets in  
the Heart

Zachary James Williams

Dissertation submitted to the faculty of the Virginia Polytechnic Institute and State  
University in partial fulfillment of the requirements for the degree of

Doctor of Philosophy in  
Translational Biology, Medicine, and Health

Robert G Gourdie, Chair  
Sharon Swanger  
Steven Poelzing  
Webster Santos

December 4, 2023  
Roanoke, Virginia

Keywords: Voltage-gated sodium channels, SCN1B ( $\beta 1/\beta 1B$ ), peptide therapeutics,  
arrhythmia, sudden cardiac death

# The Voltage Gated Sodium Channel $\beta 1/\beta 1B$ subunits: Emerging Therapeutic Targets in the Heart

Zachary James Williams

## ABSTRACT

Voltage-gated sodium channels are composed of pore-forming  $\alpha$ -subunits, and modulatory and multifunctional associated  $\beta$  subunits. While much of the field of cardiac electrophysiology and pathology has focused on treating and preventing cardiac arrhythmias by targeting the  $\alpha$  subunit, there is also evidence that targeting the  $\beta$  subunits, particularly SCN1B, the gene that encodes  $\beta 1$  and an alternatively spliced variant  $\beta 1B$ , has therapeutic potential. The first attempt at targeting the  $\beta 1$  subunit was with the generation of and treatment with an SCN1B Ig domain mimetic peptide  $\beta adp1$ . Here we describe further investigation into the function and mode-of-action of both  $\beta adp1$  and novel peptides derived from the original  $\beta adp1$  sequence. We find that in a heterologous expression system  $\beta adp1$  initially disrupts  $\beta 1$ -mediated trans-homophilic adhesion, but after approximately 30 hours eventually increases adhesion. Novel mimetic dimers increase  $\beta 1$  adhesion up to 48 hours post-treatment. Furthermore, it appears that  $\beta adp1$  may increase  $\beta 1$  adhesion by upregulating the intramembrane proteolysis of  $\beta 1$ , a process which has important downstream implications and effects on translation. Despite these exciting findings, we were unable to translate them into a primary culture of cardiac cells with endogenous expression of  $\beta 1$  because we found that both neonatal rat cardiomyocytes and isolated adult mouse cardiomyocytes do not express  $\beta 1$  at detectable levels, whereas they do appear to express  $\beta 1B$ . In summary, we show exciting findings on the function and mode-of-action of SCN1B mimetic peptides and their therapeutic potential in targeting the  $\beta 1$  subunit, but further work is needed to determine the translatability of our findings to *in vivo* models and eventually to humans.

The Voltage Gated Sodium Channel  $\beta 1/\beta 1B$  subunits: Emerging Therapeutic Targets in  
the Heart

Zachary James Williams

GENERAL AUDIENCE ABSTRACT

Voltage-gated sodium channels have two main parts: the pore-forming  $\alpha$ -subunits and the modulatory  $\beta$  subunits. Most research in heart function and issues has focused on fixing problems with the  $\alpha$  subunit. However, there's evidence that working on the  $\beta$  subunits, specifically the SCN1B gene that makes  $\beta 1$  and another version called  $\beta 1B$ , could be helpful. Previously, researchers used a peptide that is designed exactly like a part of  $\beta 1$ , called  $\beta adp1$ , to target the  $\beta 1$  subunit. In our study, we explore more about how  $\beta adp1$  works and test new peptides based on  $\beta adp1$ . We found that  $\beta adp1$  initially disrupts trans-homophilic adhesion, where 2  $\beta 1$  subunits interact with each other across the space between 2 cells, but after about 30 hours, it actually increases adhesion. New mimetic dimers also boost adhesion up to 48 hours later. It seems like  $\beta adp1$  might enhance adhesion by triggering a process called intramembrane proteolysis of  $\beta 1$ , which has important effects on translation. Despite these exciting findings, we couldn't confirm the presence of this protein in heart cells because we discovered that certain heart cells don't have enough  $\beta 1$ , although they do have  $\beta 1B$ . In conclusion, our study shows promising results about how SCN1B mimetic peptides work and their potential for treating arrhythmia. However, more research is needed to see if these findings apply to real-life situations and eventually to help people with cardiac conduction abnormalities.

## Dedication

This and all my work, past and future, is first dedicated to my wife Jaci, who is everything to me and without whom I never would have made it to the light at the end of the tunnel. She was beside me from start to finish for my PhD journey.

Second, I dedicate this work to my two boys, Asher and Ezra, who have made the difficult days easier and who bring smiles and joy with them wherever they go. I pray they see the hard work and long days pay off in the future and that I can set an example of finishing what you start.

## Acknowledgements

I would first like to acknowledge my advisor, Rob Gourdie. He has a knack for teaching and guiding in all aspects of science training, whether it be experimentation, writing, presenting work to others, or gleaning knowledge from confusing and unexpected results. Even with all the various interruptions to my experiments and writing that occurred over the course of my PhD (including but not limited to: a pandemic and the birth of my two children) he stuck with me during the slow months and the packed months. I am honored to have completed my dissertation work in his esteemed lab.

Second, I would like to acknowledge Jane Jourdan, the Gourdie lab manager, who has an astounding breadth of knowledge in biochemical techniques and is a well of general scientific understanding and experimentation. She has been vital to the design and completion of many of the experiments described herein.

I want to thank my committee members, Steve Poelzing, Webster Santos, and Sharon Swanger, for their astute questions and suggestions that have shaped and guided the direction my research took, which has led to this dissertation and work that I am proud to have completed.

I want to thank many of the people who assisted in any aspect of preparing, completing, or presenting this work. Linda Collins, who is always a bright spot in my day and helps

with anything from wrangling the busy PIs all into one room at the same for a committee meeting or is simply asking how my children are doing when she knows they have been sick. All previous lab members who I have bounced ideas off, presented my work to countless times in lab meeting, and received valuable feedback from: Randy Strauss, Daniel Hoagland, Spencer Marsh, Kevin Pridham, Ruhul Amin, Xiaobo Wu, Claire Beard, Alan Dogan, and Anna Buhle. Many others outside my lab who have listened to me describe my work and offered sound advice or resources: Mason Wheeler, Mike Zeitz, William Adams, Jamie Smyth, Jessica Pfleger, Yassine Sassi, Anita Alvarez-Laviada, and Julia Gorelik.

Lastly, I want to thank my family, my mom, dad, and siblings, Joshua, John and Kayla for never doubting me.

## Attributions

Several colleagues aided in the formulation of hypotheses or experimental design for two of the chapters in this dissertation or provided resources such as specific isolated cell types. A brief description of each author's contribution to those chapters is given here.

### **Chapter 2: Development and Characterization of the Mode-of-Action of Inhibitory and Agonist Peptides Targeting the Voltage-Gated Sodium Channel SCN1B/ $\beta$ 1 Subunit:**

Zachary Williams, Steve Poelzing, and Rob Gourdie designed the research question and the project. Anita Alvarez-Laviada collected original experimental data consisting of the neonatal rat ventricular myocyte patch clamping while Zachary Williams collected all other experimental data. Zachary Williams analyzed data, drafted the text and drafted the figures. All authors contributed to text and figure revision.

### **Chapter 3: New insights on the expression of SCN1B splice variants $\beta$ 1 and $\beta$ 1B in cardiac cells:**

Zachary Williams, Steve Poelzing, and Rob Gourdie designed the research question and the project. Mason Wheeler and Jamie Renick provided isolated neonatal rat cardiomyocytes and fibroblasts. Xiaobu Wu provided isolated adult mouse cardiomyocytes. Zachary Williams analyzed data, drafted the text and drafted the figures and collected all original experimental data.

Table of Contents

**Chapter 1: Introduction: Emerging insights in Voltage-gated sodium channel  $\beta$  subunits** ..... **1**

Introduction..... 1

$\beta$  subunit structure and  $\alpha$  interaction ..... 2

**Figure 1: VGSC  $\beta$  subunits sequence alignment**..... 4

$\beta$  subunits as adhesion molecules..... 5

**Figure 2: VGSC  $\beta$  subunit adhesion interaction and multimer formation**..... 6

Regulated Intramembrane Proteolysis of  $\beta$  subunits ..... 10

$\beta$  subunit associated pathologies..... 12

$\beta$  subunit cardiac pathologies ..... 12

**Figure 3: SCN1B mutations and associated pathologies**..... 13

$\beta$  subunit brain pathologies..... 16

References..... 19

**Chapter 2: Development and Characterization of the Mode-of-Action of Inhibitory and Agonist Peptides Targeting the Voltage-Gated Sodium Channel SCN1B/ $\beta$ 1 Subunit ...** **35**

Abstract ..... 36

Introduction..... 37

Results ..... 40

**Figure 1: Acute effects of  $\beta$ adp1 on  $I_{Na}$ ,  $\beta$ 1 density and intercellular adhesion** .... 41

**Table 1: SCN1B mimetic peptides** ..... 44

**Figure 2: In silico modeling of binding of  $\beta$ adp1 and LQLEED monomeric inhibitory peptides to the  $\beta$ 1 Immunoglobulin domain**..... 45

**Figure 3:  $\beta$ adp1 decreases intercellular adhesion in 1610 $\beta$ 1 cells, whereas  $\beta$ adp1-related dimeric peptides PS2C and PS2L increase adhesion**..... 47

**Figure 4:  $\beta$ adp1 increases  $\beta$ 1 immunolabeling over a 48 hour Time-Course** ..... 49

**Figure 5:  $\beta$ adp1 and  $\beta$ adp1-derived monomeric and dimeric peptides increase  $\beta$ 1 immunolabeling at 48 hours of treatment** ..... 50

**Figure 6:  $\beta$ adp1 increases Regulated Intramembrane Proteolysis (RIP) of  $\beta$ 1 following 6, 24 and 48 hours of treatment**..... 52

**Figure 7: The PS2L dimer acutely increases the RIP of  $\beta$ 1, but not subsequently** . 54



<b>Figure 8: DAPT inhibition of RIP results in loss of <math>\beta</math>adp1 effects on ECIS-assayed cell adhesion</b> .....	55
Discussion .....	57
<b>Figure 9: Model for Effects of SCN1B (<math>\beta</math>1/<math>\beta</math>1B) immunoglobulin domain mimetic peptides</b> .....	58
Materials and Methods.....	66
Supplemental Figures.....	71
<b>Supplemental Figure 1: Confocal immunolabeling of NRVMs treated with scrambled control peptide for 60 minutes and immunolabeled for <math>\beta</math>1 Cx43</b> .....	71
<b>Supplemental Figure 2: Effects of <math>\beta</math>adp1 and short <math>\beta</math>adp1-based monomeric sequences on relative resistance in 1610<math>\beta</math>1 cells <math>\beta</math>adp1</b> .....	72
<b>Supplemental Figure 3: <math>\beta</math>adp1 control peptide R85D shows no effects on <math>\beta</math>1 RIP</b> .....	73
References.....	74
<b>Chapter 3: New insights on the expression of SCN1B splice variants <math>\beta</math>1 and <math>\beta</math>1B in cardiac cells</b> .....	<b>83</b>
Abstract .....	84
Introduction.....	86
Results .....	89
<b>Figure 1: <math>\beta</math>1 is undetectable in NRVMs with the <math>\beta</math>1 C-terminal antibody</b> .....	90
<b>Figure 2: <math>\beta</math>1 is not detectable in neonatal rat cardiac fibroblasts or isolated adult mouse cardiomyocytes with a C-terminal antibody</b> .....	91
<b>Figure 3: Design of <math>\beta</math>1B specific antibody and location of all antibodies</b> .....	92
<b>Figure 4: The <math>\beta</math>1B specific antibody mirrors the results in WB and IF with the N-terminal <math>\beta</math>1/<math>\beta</math>1B antibody</b> .....	94
Discussion .....	96
Materials and Methods.....	99
References.....	103
<b>Chapter 4: Conclusions and Future Directions</b> .....	<b>108</b>
Summary and Discussion.....	108
Limitations.....	111
Future Directions.....	113
References.....	116

## **Chapter 1: Introduction**

### **Emerging Insights in Voltage-Gated Sodium Channel $\beta$ subunits**

#### **1. Introduction**

Voltage-gated sodium channels (VGSCs) are vital to the continued propagation of action potentials and communication between cells in both neurons and cardiomyocytes. As their name suggests, VGSCs are sensitive to changes in membrane voltage, causing them to open and allow the passage of sodium ions across the membrane. VGSCs have two classes of subunits, the  $\alpha$  pore-forming subunit, and the non-pore-forming  $\beta$  subunits. The  $\alpha$  subunits are given the names  $\text{Na}_v1.1$ - $\text{Na}_v1.9$  while the  $\beta$  subunits are encoded by genes  $\text{SCN1B}$ - $\text{SCN4B}$  and given the names  $\beta1$ - $\beta4$  as well as an alternatively spliced variant encoded by  $\text{SCN1B}$  named  $\beta1B$ . The typical VGSC complex is formed by one  $\alpha$  subunit and two  $\beta$  subunits, but both the  $\alpha$  and  $\beta$  subunits are expressed in a tissue specific manner. Canonically,  $\text{Na}_v1.1$ - $\text{Na}_v1.3$  and  $\text{Na}_v1.6$  are expressed in the brain while  $\text{Na}_v1.6$ - $\text{Na}_v1.9$  are expressed in the peripheral nervous system (de Lera Ruiz and Kraus, 2015).  $\text{Na}_v1.4$  is expressed in skeletal muscle and  $\text{Na}_v1.5$  is the major isoform in the heart, although there is expression of  $\text{Na}_v1.1$ ,  $\text{Na}_v1.3$ , and  $\text{Na}_v1.6$  in the transverse tubules in cardiomyocytes (Maier et al., 2004). All the  $\beta$  subunits are found in excitable tissue, including the heart, the central nervous system, and the peripheral nervous system, while  $\beta1$  and  $\beta4$  are also found in skeletal muscle. The  $\beta$  subunits are also found in many non-excitable cell types as laid out by Brackenbury and Isom in a prior review (Brackenbury and Isom, 2011). The  $\beta1$  subunit is ubiquitously expressed in the brain, but is enriched subcellularly at axon initial segments and nodes of Ranvier (Hull and Isom, 2018).  $\beta1$  is

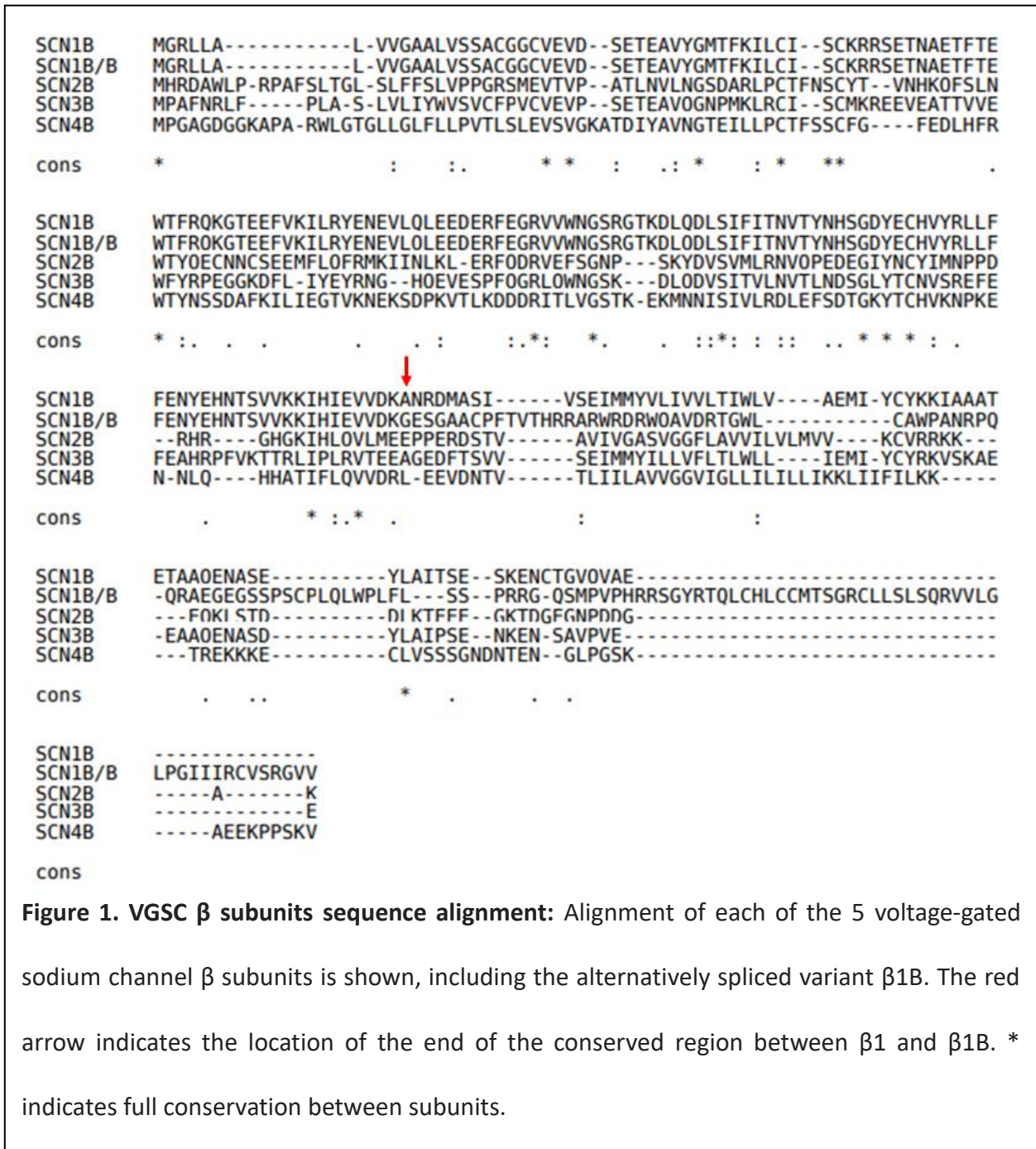
also expressed in the heart with higher expression in the atria than the ventricles and is found in the membrane both at the intercalated disk and in the t-tubules (Gaborit et al., 2007; Maier et al., 2004; Veeraraghavan et al., 2018; Zhu et al., 2021).

Although initially reported as mainly modulators of the  $\alpha$  subunit, the  $\beta$  subunits have been shown to have a wide variety of functions over the last 40 years.  $\beta 1$  was first reported in 1980 with the other  $\beta$  subunits to follow (Beneski and Catterall, 1980; Isom et al., 1994; Isom et al., 1992; Isom et al., 1995; Morgan et al., 2000; Yu et al., 2003). Since then, the  $\beta$  subunits have been shown to be involved in trafficking of the  $\alpha$  subunits to the plasma membrane (Cortada et al., 2019; Cusdin et al., 2008), modulating kinetics and gating of the  $\alpha$  subunits (Brackenbury and Isom, 2011; Edokobi and Isom, 2018), participating in adhesion interactions in a variety of contexts and with a variety of molecules (Kazarinova-Noyes et al., 2001; Malhotra et al., 2000; McEwen et al., 2009; Namadurai et al., 2015; Ratcliffe et al., 2001; Veeraraghavan et al., 2018; Xiao et al., 1999; Yereddi et al., 2013), and regulating gene expression of multiple targets, including the VGSC  $\alpha$  subunits as well as other ion channels (Bouza et al., 2021; O'Malley and Isom, 2015; Wong et al., 2005). As more work has been completed investigating the important roles of the VGSC  $\beta$  subunits, they have emerged as key therapeutic targets in a variety of pathologies and understanding their role is vital to our wider understanding of the complete function of the VGSC complex.

## **2. $\beta$ subunit structure and $\alpha$ subunit interaction**

The  $\beta$ 1- $\beta$ 4 subunits of VGSC are composed of an extracellular V-type immunoglobulin (Ig) domain, a transmembrane alpha-helical domain, and an intracellular relatively disordered Carboxy-terminal domain. The alternatively spliced variant  $\beta$ 1B encoded by the gene SCN1B and formed by a retained intron is composed of an identical Amino-terminal and Ig domain to that of  $\beta$ 1 but differs in the C-terminal region (Kazen-Gillespie et al., 2000). While the other  $\beta$  subunits are anchored in the membrane,  $\beta$ 1B lacks the same transmembrane region resulting in its secretion from the cell under most circumstances (Patino et al., 2011). However, when  $\text{Na}_v1.5$ , the major cardiac  $\alpha$  subunit, and  $\beta$ 1B are heterologously expressed together in HEK cells,  $\beta$ 1B is retained at the membrane (Patino et al., 2011), suggesting a unique function for  $\beta$ 1B in a cardiac context that needs to be further explored. It is important to note that developmentally, both  $\beta$ 1B and  $\beta$ 3 are most highly expressed in the brain during embryonic development and early postnatally, but decrease in expression during adulthood, while in the heart  $\beta$ 1B and  $\beta$ 3 expression does not decrease in adulthood (Kazen-Gillespie et al., 2000; Shah et al., 2001).

The sequences of  $\beta$ 1 and  $\beta$ 3 are most closely related to each other and bind non-covalently to their associated  $\alpha$ -subunit while  $\beta$ 2 and  $\beta$ 4 are closely related and bind to their associated  $\alpha$ -subunit covalently via a disulfide bond (Buffington and Rasband, 2013; Chen et al., 2012; Chopra et al., 2007). The protein sequences and alignment using the online T-Coffee alignment tool of each  $\beta$  subunit is shown in Figure 1 (Notredame et al., 2000). Because of the similarities in sequence and binding of the  $\beta$ -subunits with the  $\alpha$ -subunit, much of the literature has stated that a VGSC complex is typically formed of an  $\alpha$  subunit and either a  $\beta$ 1 or  $\beta$ 3 subunit and either

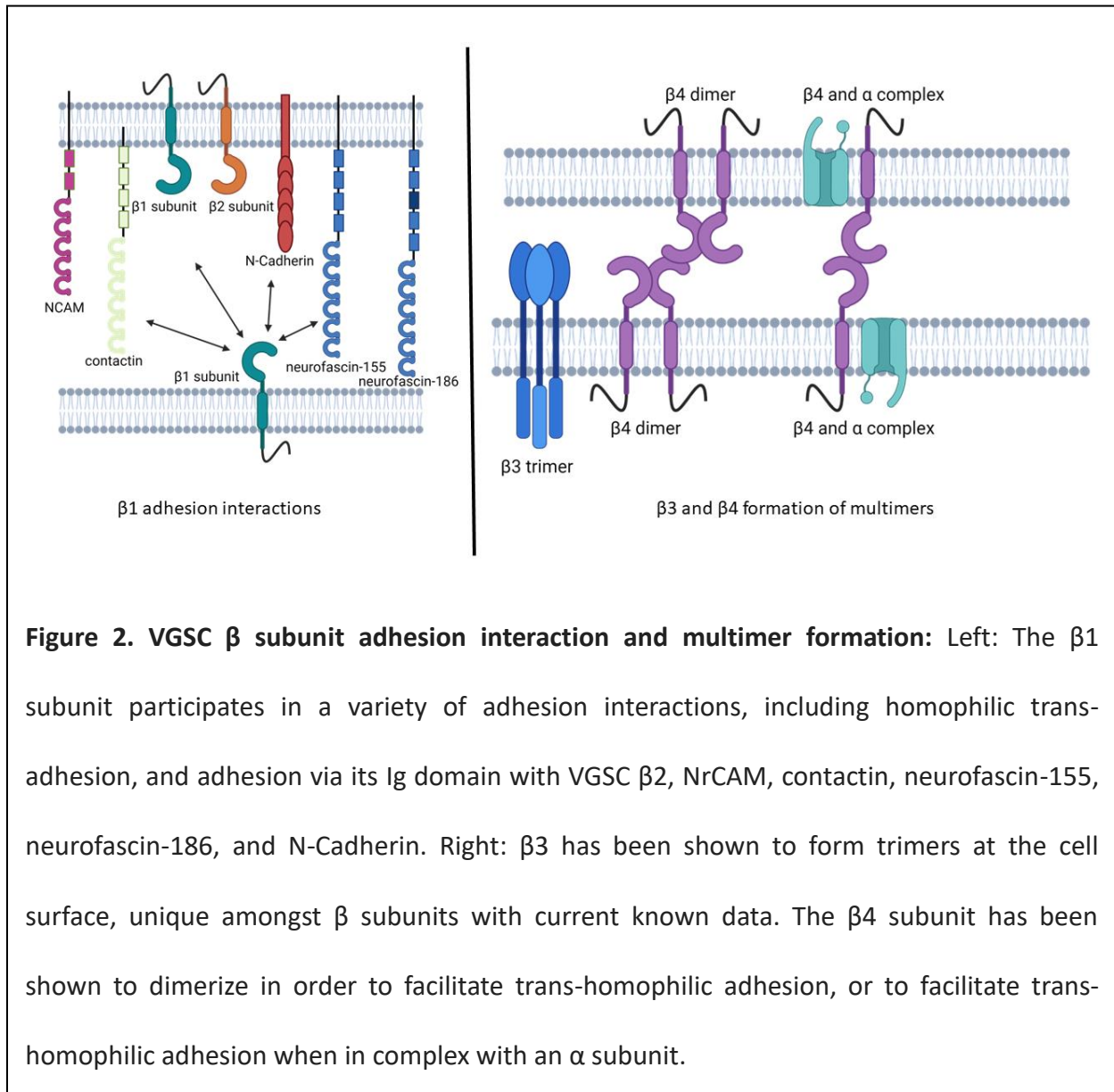


a  $\beta$ 2 or  $\beta$ 4 subunit but a recent review by Salvage et al. made the case that Nav1.5 may be able to bind both  $\beta$ 1 and  $\beta$ 3 simultaneously (Salvage et al., 2020a). The interaction of  $\beta$ 1 with Nav1.4, Nav1.6 and Nav1.7 has been resolved at high resolution (Li et al., 2023; Pan et al., 2018; Shen et al., 2019; Yan et al., 2017). Although  $\beta$ 1 interactions have been resolved with some  $\alpha$ -subunits,

the interactions are not easily modeled with the other  $\text{Na}_v$  isoforms. For example, with  $\text{Na}_v1.7$  the  $\beta1$ -subunit Ig domain has ionic and hydrogen-bonds with multiple extracellular loop regions, including D1, S5-P, DIII, S1-S2 and DIV, P-S6 (Salvage et al., 2020a). However, the  $\text{Na}_v1.5$  structure has significant key differences structurally, such as an extra N-linked glycosylation site at Asn319 not found in other  $\alpha$ -subunits that could block binding of the  $\beta1$  subunit Ig domain (Salvage et al., 2020a; Shen et al., 2019). There is further evidence that  $\text{Na}_v1.5$  also has no accessible cysteines for the Ig domains of  $\beta2$  and  $\beta4$  to form a disulfide bond with, unlike other  $\text{Na}_v$  isoforms (Pan et al., 2019; Shen et al., 2019). Altogether, this suggests that with  $\text{Na}_v1.5$ , the  $\beta$ -subunit Ig domains are less constricted and free to interact as cell-adhesion motifs. However, this relatively loose association with  $\text{Na}_v1.5$  may lead to technically difficult detection of the  $\beta1$  subunit in the heart at the protein level, as multiple papers and groups have stated that commercially available antibodies do not work in either Western Blot or IF or that the detection is weak enough that quantification is not possible (Angsutararux et al., 2021; Cervantes et al., 2022; Signore et al., 2015). It is important to again note that  $\beta1B$  also has an identical Ig domain to  $\beta1$  and is found to be retained in the membrane only when co-expressed with  $\text{Na}_v1.5$ , building the argument for a unique role for  $\beta1/\beta1B$  in a cardiac context.

### **3. $\beta$ subunits as adhesion molecules**

The  $\beta$  subunits belong to the Ig superfamily of CAMs, with  $\beta1$  and  $\beta2$  both able to interact via heterophilic adhesion to other CAM molecules.  $\beta1$  interacts with contactin, N-cadherin, NCAM, neurofascin-155, neurofascin-186, VGSC  $\beta2$ , and tenascin-R (Bouza and Isom, 2018; McEwen



and Isom, 2004).  $\beta 2$  has been shown to interact in heterophilic adhesion with  $\beta 1$ , tenascin-R, and tenascin-C (Bouza and Isom, 2018; Srinivasan et al., 1998; Xiao et al., 1999). Less is known about  $\beta 3$  and  $\beta 4$  adhesion, although  $\beta 3$  expressed in *Drosophila* S2 cells do not aggregate, suggesting a lack of trans-homophilic adhesion (McEwen et al., 2009) while  $\beta 3$  does interact with neurofascin suggesting a role in trans-heterophilic adhesion (Ratcliffe et al., 2001).  $\beta 4$  has been shown to interact in both cis- and trans-homophilic interactions, with the trans-

interaction relying on either the cis- interaction or association with the  $\alpha$  subunit (Shimizu et al., 2017). Figure 2 shows an overview of  $\beta$  subunit adhesion.

Recent findings have shown the importance specifically of  $\beta$ 1 trans-homophilic adhesion in the heart.  $\beta$ 1 has been shown to be enriched at the intercalated disc, the specialized junctions between cardiomyocytes responsible for maintaining cardiac conduction and coordinated muscle contraction (Veeraraghavan et al., 2018). More precisely,  $\beta$ 1 has been shown to localize to the perinexus, a nano-domain adjacent to gap junctions within intercalated discs in cardiomyocytes (Veeraraghavan et al., 2018). The perinexus was first described in 2011 by *Rhett et al.* as a region in the membrane surrounding gap junctions with high levels of Connexin43 (Cx43) and Zonula occludens-1 (ZO-1) interacting and regulating gap junction plaque size as well as providing a domain where ephaptic coupling of cardiomyocytes could take place (Rhett et al., 2011). A following publication found that  $Na_v1.5$  also colocalizes with Cx43 in the perinexus, providing more evidence for the perinexus playing a role in action potential conduction (Rhett et al., 2012). The theory of ephaptic coupling between cardiomyocytes has been growing in prominence over the last two decades, with multiple modeling (Greer-Short et al., 2017; Hichri et al., 2018; Kucera et al., 2002; Lin and Keener, 2010; Mori et al., 2008; Nowak et al., 2020; Nowak et al., 2021; Tsumoto et al., 2020; Tveito et al., 2017; Wei et al., 2016; Wei and Tolkacheva, 2020; Weinberg, 2017) and experimental (Adams et al., 2023; George et al., 2016; Raisch et al., 2018; Veeraraghavan et al., 2018; Veeraraghavan et al., 2015; Veeraraghavan et al., 2016) studies supporting the concept. Ephaptic coupling is a parallel method to gap junctional coupling that allows for propagation of action potentials. The proposed method is that a small extracellular space between two cells, in this case the perinexus, is highly sensitive to changes in



sodium ion ( $\text{Na}^+$ ) concentration so that when one cell is depolarized and draws in  $\text{Na}^+$  from the perinexus, the depletion of extracellular  $\text{Na}^+$  leads to local depolarization in the adjacent cell and eventually to complete depolarization as the cell begins to draw in  $\text{Na}^+$  and propagates an action potential.

For ephaptic coupling to be possible, models have shown that the width of the perinexus must be no more than 30nm (Mori et al., 2008). It has also been shown that alignment of clusters of sodium channels across the perinexus is necessary for ephaptic coupling (Hichri et al., 2018). We propose that the  $\beta 1$  subunit may be responsible for making sure both requirements are met. The  $\beta 1$  subunit is involved in cell-adhesion interactions via its extracellular Ig domain (Isom and Catterall, 1996; Malhotra et al., 2000; Veeraraghavan et al., 2018). In the perinexus,  $\beta 1$  participates in trans-homophilic adhesion interactions that can be disrupted by a  $\beta 1$  mimetic peptide,  $\beta \text{adp}1$ , resulting in a widened perinexus and decreased conduction velocity as well as increased incidence of arrhythmia in a Langendorff-perfused guinea pig model (Veeraraghavan et al., 2018). Thus,  $\beta 1$  may be responsible for regulation of perinexal width. Furthermore, modeling of the  $\beta 1$  subunit extending from the plasma membrane suggests it projects 5-10nm (Hoagland et al., 2019). This means trans-homophilic adhesion of  $\beta 1$  subunits would suggest a regulated width of 10-20nm for the perinexus, which is in the range of <30nm modeled by Mori and colleagues (Mori et al., 2008).

However, models typically show a single  $\text{Na}_v1.5$  with a single  $\beta 1$  subunit on one cardiomyocyte interacting with one  $\text{Na}_v1.5$  with a  $\beta 1$  subunit on the opposing cardiomyocyte, which presents a

problem with the alignment of sodium channels across the perinexus. These models always show a misalignment of the pore of the channel because of the location of the proposed trans-homophilic binding site (aa 66-86) of the  $\beta 1$  subunits. This does not fit with proposed models of sodium channel alignment in ephaptic coupling (Hichri et al., 2018). Other evidence suggests the alignment could be slightly different and still agree with the *in silico* data. One factor that can change how we think about the adhesion of  $\beta 1$  and alignment of the  $\alpha$  subunit is that VGSCs assemble and gate as dimers, as shown by the Deschênes group (Clatot et al., 2017) or form spontaneous supramolecular clusters in heterologous expression systems that can have individual  $\alpha$  subunits modified by  $\beta 3$  (Salvage et al., 2020b). Another factor is that the  $\beta 3$  subunit, which has the most similar homology to  $\beta 1$  has shown a trimeric assembly via its Ig domain (Namadurai et al., 2014). Although it has not been shown experimentally that  $\beta 1$  exists as a trimer at the plasma membrane, the Jackson group has made convincing arguments in multiple reviews that the structural aspects required for trimeric assembly of  $\beta 3$  subunits are also present in  $\beta 1$  subunits, including a Cys2-24 disulfide bond and a membrane-buried glutamic acid (Namadurai et al., 2015; Salvage et al., 2020a). This insight reforms the idea of  $\beta 1$  trans-homophilic adhesion from single Ig domain interactions across the perinexus to a trimer formed interface, which in turn brings 3 Nav1.5  $\alpha$  subunits together, and a much more likely direct alignment of the pores.

Contradicting this theory is a modeling paper comparing  $\beta 1$  and  $\beta 3$  dynamics and potential to form trimers (Glass et al., 2020). Glass and associates show through their simulations using the up-to-date resolved structure of Nav1.4 in complex with  $\beta 1$  (Pan et al., 2018) that the constraint

of the extracellular domain of  $\beta 1$  is much greater than that of  $\beta 3$ , suggesting that despite sequence homology,  $\beta 1$  may be unable to form trimers (Glass et al., 2020). It will be important in future experimental work to determine whether  $\beta 1$  forms trimers *in vivo* at the plasma membrane as the  $\beta$  subunits are becoming prime therapeutic targets, especially in the context of regulating perinexal width and the effect that has on cardiac conduction.

#### **4. Regulated Intramembrane Proteolysis of $\beta$ subunits**

The regulated intramembrane proteolysis (RIP) of the  $\beta$  subunits of voltage-gated sodium channels was first described in 2005 (Wong et al., 2005). The proteolysis mechanism is the same as that of the formation of A $\beta$  plaques through the sequential cleavage of the amyloid precursor protein (APP) by  $\beta$ - and  $\gamma$ - secretases (Chen et al., 2017). The process for  $\beta 1$  involves two sequential cleavage steps. First, the extracellular domain is cleaved off by BACE1 resulting in a c-terminal fragment (CTF) containing the transmembrane domain and the intracellular domain (ICD). The second cleavage is performed by  $\gamma$ -secretase resulting in the ICD being released from the transmembrane domain and translocating to the nucleus where it affects transcription (Bouza et al., 2021; Wong et al., 2005).

More recently, the RIP of  $\beta 1$  has been looked at in more detail. The Isom group examined the effects of post-translational modification on RIP in CHL cells, including phosphorylation and palmitoylation (Bouza et al., 2020). They found that phosphorylation at Tyr-181 has no effect on RIP, but that lack of palmitoylation at Cys-162 results in an 80% decreased level of RIP (Bouza et

al., 2020). However, a palmitoylation-null mutant  $\beta 1$ -p.C162A-V5 also had a 77% decrease in the plasma membrane compared to WT  $\beta 1$  suggesting that RIP of the mutant that reached the membrane still occurred, meaning RIP occurs in the plasma membrane and S-palmitoylation is required for  $\beta 1$  to reach the membrane (Bouza et al., 2020). These conclusions were partially supported in MDA-MB-231 breast cancer cells where it was shown that although most  $\beta 1$ -GFP exogenously expressed was retained intracellularly, inhibition of  $\beta 1$  RIP resulted in decreased levels of  $\beta 1$ -GFP at the endosome, suggesting RIP occurs in the endosome or the preceding plasma membrane (Haworth et al., 2022).

Of particular interest in these recent publications is the role of the  $\beta 1$ -ICD. The  $\beta 1$ -ICD translocates to the nucleus and alters transcription of various genes in CHL cells, including sodium channels (upregulation of SCN4A and SCN5A and downregulation of SCN3A), potassium channels (upregulation of KCNS3 and KCNK2 and downregulation of KCNK3) and calcium channels (downregulation of CACNB4) (Bouza et al., 2021). In HEK-hNav1.5 cells transiently transfected with  $\beta 1$ -ICD-V5-2A-eGFP there was no change in sodium current density (Bouza et al., 2021). However, in MDA-MB-231 cells, overexpression of the  $\beta 1$ -ICD resulted in greater sodium current and a less tetrodotoxin resistant sodium current, suggesting the population of active sodium channels is significantly altered by expression of the  $\beta 1$ -ICD (Haworth et al., 2022). Our lab has recently shown that treating 1610 CHL cells stably expressing  $\beta 1$  with a  $\beta 1$  mimetic peptide,  $\beta$ adp1, results in increased RIP of  $\beta 1$  and increased trans-homophilic adhesion after 24 hours. These results together suggest that transcriptional regulation by the  $\beta 1$ -ICD depends on sodium channel population and cell type and has potential as a therapeutic target.

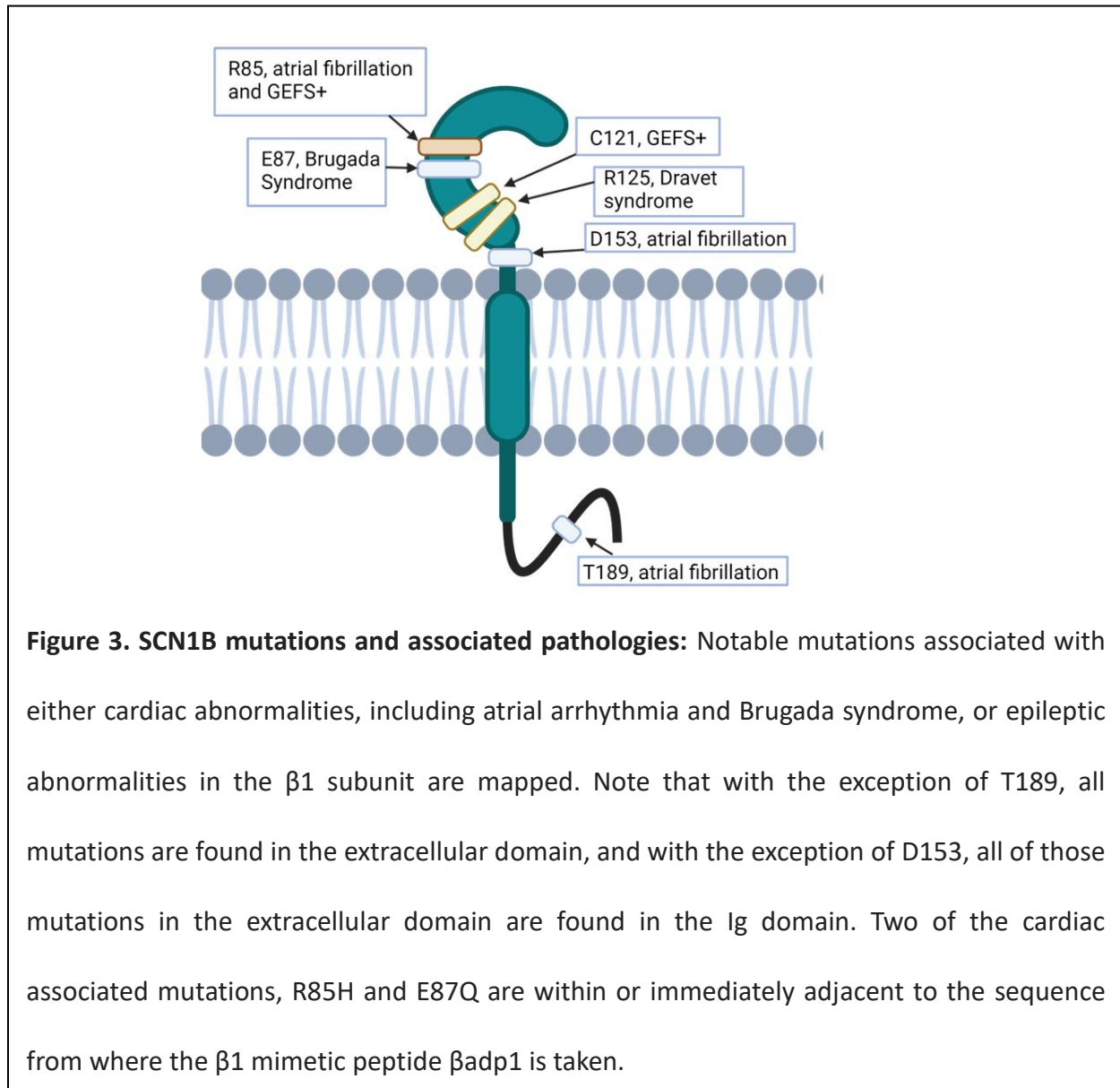
## 5. $\beta$ subunit associated pathologies

The variety of functions the  $\beta$  subunits are responsible for as well as their widespread expression through both excitable and non-excitable tissues means that there are multiple and various pathologies associated with them.  $\beta$  subunit pathology has been studied extensively in cardiac and neuronal contexts, and because of the important functions and new insights into these functions detailed above,  $\beta$  subunits have become prime therapeutic targets.

**5.1  $\beta$  subunit cardiac pathologies:** There have been many  $\beta$  subunit variants associated with cardiac arrhythmias.  $\beta 1/\beta 1B$  variants have been associated with atrial fibrillation (Olesen et al., 2012; Watanabe et al., 2009), Long-QT Syndrome (Riuró et al., 2014), and Brugada Syndrome (Hu et al., 2012; Peeters et al., 2015; Ricci et al., 2014; Watanabe et al., 2008).  $\beta 2$  is associated with atrial fibrillation and Brugada Syndrome (Riuró et al., 2013; Watanabe et al., 2009).  $\beta 3$  has also been associated with atrial fibrillation (Lin et al., 2022; Olesen et al., 2010; Wang et al., 2010) and Brugada syndrome (Hu et al., 2009). As expected,  $\beta 4$  has also been linked to atrial fibrillation (Li et al., 2013) as well as ventricular tachycardia (Yang et al., 2019) and Long-QT Syndrome (Medeiros-Domingo et al., 2007).

Recently, the Silva group investigated 8 variants in  $\beta 1$  or  $\beta 3$  linked to either atrial fibrillation or Brugada Syndrome to learn more about the underlying mechanisms leading to arrhythmia (Angsutararux et al., 2021). Of the variants investigated, the majority were found in the extracellular domain of  $\beta 1/\beta 3$ , including R85H, E87Q, and D153N in  $\beta 1$  and R6K, L10P, and

V110I in  $\beta 3$ . Some important known mutations in  $\beta 1$  associated with arrhythmia or Brugada syndrome are shown in figure 3.



Interestingly, all these variants are associated not with  $\alpha$  subunit interaction, but rather integrity of the Ig domain, or in the case of D153N, located in the linker region between the Ig domain and the transmembrane domain, with the orientation of the Ig domain. The results of the study showed a variety of effects of  $\beta 1$  and  $\beta 3$  variants, including altering levels of  $\text{Na}_v$  at the cell

surface, regulation of Na<sub>v</sub> channel activation and inactivation gating, and direct effects on VSD-III activation, which has been shown to affect the response of the sodium channel to anti-arrhythmic drugs (Angsutararux et al., 2021; Zhu et al., 2021). This study reiterates the importance of the extracellular domain of  $\beta$  subunits, especially the putative adhesion domain of  $\beta 1/\beta 1B$  (aa 66-86).

Aside from variants, there is other clear evidence that the  $\beta 1$  subunit is vital to normal cardiac conduction and that disruption of its function results in conduction abnormalities. A SCN1B null mouse line that knocks out both  $\beta 1$  and  $\beta 1B$  generated by the Isom group generally does not live past three weeks of age (Chen et al., 2004). These mice have been shown to exhibit prolonged RR and QT intervals, and isolated null myocytes show slowed repolarization, suggesting a link to long-QT syndrome and the importance of SCN1B to normal cardiac conduction (Lopez-Santiago et al., 2007). Additionally, these mice have atrial dysfunction, including sinoatrial node dysfunction, increased atrial collagen, and atrial fibrillation (Ramos-Mondragon et al., 2022). SCN1B null mice also have widened perinexii, supporting the hypothesis that  $\beta 1$  is vital to maintaining perinexal width (Veeraraghavan et al., 2018). In human with atrial fibrillation, perinexal width in atrial appendages has been shown to be approximately 3nm wider than controls without atrial fibrillation, and SCN1B ( $\beta 1/\beta 1B$ ) was confirmed to be located in human perinexii, supporting the hypothesis that  $\beta 1$  is vital to normal cardiac conduction in mammals (Raisch et al., 2018).

$\beta$ 2 null mice also have conduction abnormalities (Bao et al., 2016). These mice are reported to have both atrial and ventricular arrhythmias, with the sodium current in atrial myocytes being normal, but reduced total sodium current in ventricular myocytes (Bao et al., 2016). SCN3B knock-out mice have abnormal ventricular and atrial electrophysiology, with reduced peak sodium current densities in ventricular myocytes and susceptibility to ventricular tachycardia when stimulated or atrial tachycardias or fibrillation with burst pacing, and a disconnect between atrial and ventricular activity, indicating sinoatrial node dysfunction (Hakim et al., 2010; Hakim et al., 2008). Interestingly, it appeared that there was a compensatory increase in SCN1B mRNA levels in the ventricles in the absence of SCN3B (Hakim et al., 2008). A thorough search of the current literature does not produce any studies that have looked at the effects of global SCN4B KO on the heart.

Multiple groups have indicated the importance of targeting  $\beta$  subunits to treat or prevent arrhythmias, whether through direct interaction with the adhesion function of the Ig domain, by targeting the interaction of the  $\beta$  and  $\alpha$  subunits and effects on drug efficacy, or through downstream effects of  $\beta$  subunit RIP (Bouza and Isom, 2018; Hodges et al., 2022; O'Malley and Isom, 2015; Veeraraghavan et al., 2018; Zhu et al., 2021). Currently, there are no  $\beta$  subunit targeting drugs, but our lab has synthesized the first  $\beta$ 1 specific targeting mimetic peptides, setting the precedent for a method of targeting  $\beta$  subunits that may be applied in the future to other  $\beta$  subunit pathologies.



**5.2  $\beta$  subunit brain pathologies:** While the importance of the  $\beta$  subunits in the heart is known and has gained much more attention in the literature recently, the majority of  $\beta$  subunit research has been done in the brain. A variant in the SCN1B subunit has been associated with Dravet Syndrome, a severe genetic epilepsy where symptoms typically start showing in the first year of life (Patino et al., 2009), although other studies have stated that SCN1B variants are not common causes of Dravet Syndrome (Gong et al., 2019; Kim et al., 2013). Other SCN1B variants have been associated with genetic epilepsy with febrile seizures (GEFS+) (Audenaert et al., 2003; Fendri-Kriaa et al., 2011; Scheffer et al., 2007; Wallace et al., 2002; Wallace et al., 1998) and with early myoclonic encephalopathy (Zhu et al., 2022). Important known  $\beta$ 1 mutations in epilepsies are indicated in figure 3. There has been evidence of isolated variants in other  $\beta$  subunits associated with various epilepsies (Baum et al., 2014), but the majority of the literature seems to agree that  $\beta$  subunits other than SCN1B in general are likely not causative in leading to epilepsies (Gong et al., 2019; Lu et al., 2010; Wallace et al., 2002).

Genetically modified mouse models indicate the importance of the  $\beta$  subunits in regulating normal action potential conduction in the brain. The SCN1B null mouse generated by the Isom lab has also been extensively studied in a neuronal context. The SCN1B null mouse has a severe phenotype, with ataxia and spontaneous seizures, and has an average lifespan of 19.9 days post-natal (Chen et al., 2004). The Isom lab has shown that these mice have reduced neuronal proliferation and migration, as well as hindered pathfinding during development (Brackenbury et al., 2013). Two other recent mouse studies by the Isom lab have shed more light on the vital nature of SCN1B in developing and adult mice. Deletion of SCN1B in adult mice results in

epilepsy and sudden unexplained death in epilepsy (SUDEP), so  $\beta 1$  is important in the developing mouse and into adulthood in the brain (O'Malley et al., 2019). Another mouse line generated had a human SCN1B variant (R89C) associated with epilepsy introduced with CRISPR/Cas9 to produce both heterozygous  $Scn1b^{(R89/C89)}$  and homozygous  $Scn1b^{(C89/C89)}$  for the variant (Chen et al., 2023). The  $Scn1b^{(C89/C89)}$  mouse did display convulsive seizures that corresponded to measured epileptic discharges in young adult mice (Chen et al., 2023), but they survived to adulthood and do not model complete SCN1B loss-of-function, as  $Scn1b^{(-/-)}$  do.

SCN2B null mice displayed a tendency for seizures, but overall brain development was normal and they do not die in the first three weeks of life (Chen et al., 2002). SCN3B null mice do not display a tendency for seizures or other brain pathologies associated with SCN1B and SCN2B KO mice (O'Malley and Isom, 2015). SCN4B null mice show decreased sodium current and decreased firing frequency of medium spiny neurons, and they did show sudden unexplained death without seizures (Miyazaki et al., 2014).

It is clear from the heart and brain effects and overall phenotype of various  $\beta$  subunit variants and  $\beta$  subunit KO mice that the  $\beta$  subunits are vital players in function of the  $\alpha$  subunits and in roles attributed solely to the  $\beta$  subunits, such as adhesion and pathfinding. However, the role and even the distribution of the various  $\beta$  subunits is still not fully understood, and basic questions such as: "Why  $\beta 1$  is virtually undetectable in the heart in a Western blot assay even

though SCN1B null mice have severe cardiac phenotypes?” will have to be answered before the field can push towards introducing  $\beta$ -subunit targeting peptides or drugs as therapeutics.

This dissertation will attempt to add information on the function of SCN1B proteins  $\beta 1/\beta 1B$ , as well as presenting the first evidence of potential therapeutic SCN1B targeting peptides. Chapter 2 will show effects of our novel SCN1B peptides on  $\beta 1$  expression, adhesion, and regulated intramembrane proteolysis. Chapter 3 will attempt to translate some of our findings in Chapter 2 to cardiomyocytes, resulting in the surprising finding that the distribution of SCN1B proteins  $\beta 1/\beta 1B$  may be much different than what is currently understood in the field.

## REFERENCES

- Adams, W.P., Raisch, T.B., Zhao, Y., Davalos, R., Barrett, S., King, D.R., Bain, C.B., Colucci-Chang, K., Blair, G.A., Hanlon, A., *et al.* (2023). Extracellular Perinexal Separation Is a Principal Determinant of Cardiac Conduction. *Circ Res* *133*, 658-673.
- Angsutararux, P., Zhu, W., Voelker, T.L., and Silva, J.R. (2021). Molecular Pathology of Sodium Channel Beta-Subunit Variants. *Front Pharmacol* *12*, 761275.
- Audenaert, D., Claes, L., Ceulemans, B., Löfgren, A., Broeckhoven, C.V., and Jonghe, P.D. (2003). A deletion in *SCN1B* is associated with febrile seizures and early-onset absence epilepsy. *Neurology* *61*, 854-856.
- Bao, Y., Willis, B.C., Frasier, C.R., Lopez-Santiago, L.F., Lin, X., Ramos-Mondragón, R., Auerbach, D.S., Chen, C., Wang, Z., Anumonwo, J., *et al.* (2016). *Scn2b* Deletion in Mice Results in Ventricular and Atrial Arrhythmias. *Circulation: Arrhythmia and Electrophysiology* *9*, e003923.
- Baum, L., Haerian, B.S., Ng, H.-K., Wong, V.C.N., Ng, P.W., Lui, C.H.T., Sin, N.C., Zhang, C., Tomlinson, B., Wong, G.W.-K., *et al.* (2014). Case-control association study of polymorphisms in the voltage-gated sodium channel genes *SCN1A*, *SCN2A*, *SCN3A*, *SCN1B*, and *SCN2B* and epilepsy. *Human Genetics* *133*, 651-659.
- Beneski, D.A., and Catterall, W.A. (1980). Covalent labeling of protein components of the sodium channel with a photoactivable derivative of scorpion toxin. *Proceedings of the National Academy of Sciences* *77*, 639-643.
- Bouza, A.A., Edokobi, N., Hodges, S.L., Pinsky, A.M., Offord, J., Piao, L., Zhao, Y.-T., Lopatin, A.N., Lopez-Santiago, L.F., and Isom, L.L. (2021). Sodium channel  $\beta$ 1 subunits participate in regulated intramembrane proteolysis-excitation coupling. *JCI Insight* *6*.

Bouza, A.A., and Isom, L.L. (2018). Voltage-Gated Sodium Channel  $\beta$  Subunits and Their Related Diseases. *Handb Exp Pharmacol* 246, 423-450.

Bouza, A.A., Philippe, J.M., Edokobi, N., Pinsky, A.M., Offord, J., Calhoun, J.D., Lopez-Florán, M., Lopez-Santiago, L.F., Jenkins, P.M., and Isom, L.L. (2020). Sodium channel  $\beta$ 1 subunits are post-translationally modified by tyrosine phosphorylation, S-palmitoylation, and regulated intramembrane proteolysis. *Journal of Biological Chemistry* 295, 10380-10393.

Brackenbury, W., and Isom, L. (2011). Na<sup>+</sup> Channel  $\beta$  Subunits: Overachievers of the Ion Channel Family. *Front Pharmacol* 2.

Brackenbury, W.J., Yuan, Y., O'Malley, H.A., Parent, J.M., and Isom, L.L. (2013). Abnormal neuronal patterning occurs during early postnatal brain development of *Scn1b*-null mice and precedes hyperexcitability. *Proceedings of the National Academy of Sciences* 110, 1089-1094.

Buffington, S.A., and Rasband, M.N. (2013). Na<sup>+</sup> channel-dependent recruitment of Nav $\beta$ 4 to axon initial segments and nodes of Ranvier. *J Neurosci* 33, 6191-6202.

Cervantes, D.O., Pizzo, E., Ketkar, H., Parambath, S.P., Tang, S., Cianflone, E., Cannata, A., Vinukonda, G., Jain, S., Jacobson, J.T., *et al.* (2022). *Scn1b* expression in the adult mouse heart modulates Na<sup>+</sup> influx in myocytes and reveals a mechanistic link between Na<sup>+</sup> entry and diastolic function. *American Journal of Physiology-Heart and Circulatory Physiology* 322, H975-H993.

Chen, C., Bharucha, V., Chen, Y., Westenbroek, R.E., Brown, A., Malhotra, J.D., Jones, D., Avery, C., Gillespie, P.J., Kazen-Gillespie, K.A., *et al.* (2002). Reduced sodium channel density, altered voltage dependence of inactivation, and increased susceptibility to seizures in mice lacking

sodium channel  $\beta$ 2-subunits. *Proceedings of the National Academy of Sciences* 99, 17072-17077.

Chen, C., Calhoun, J.D., Zhang, Y., Lopez-Santiago, L., Zhou, N., Davis, T.H., Salzer, J.L., and Isom, L.L. (2012). Identification of the cysteine residue responsible for disulfide linkage of Na<sup>+</sup> channel  $\alpha$  and  $\beta$ 2 subunits. *J Biol Chem* 287, 39061-39069.

Chen, C., Westenbroek, R.E., Xu, X., Edwards, C.A., Sorenson, D.R., Chen, Y., McEwen, D.P., O'Malley, H.A., Bharucha, V., Meadows, L.S., *et al.* (2004). Mice Lacking Sodium Channel  $\beta$ 1 Subunits Display Defects in Neuronal Excitability, Sodium Channel Expression, and Nodal Architecture. *The Journal of Neuroscience* 24, 4030-4042.

Chen, C., Ziobro, J., Robinson-Cooper, L., Hodges, S.L., Chen, Y., Edokobi, N., Lopez-Santiago, L., Habig, K., Moore, C., Minton, J., *et al.* (2023). Epilepsy and sudden unexpected death in epilepsy in a mouse model of human SCN1B-linked developmental and epileptic encephalopathy. *Brain Communications*.

Chen, G.-f., Xu, T.-h., Yan, Y., Zhou, Y.-r., Jiang, Y., Melcher, K., and Xu, H.E. (2017). Amyloid beta: structure, biology and structure-based therapeutic development. *Acta Pharmacologica Sinica* 38, 1205-1235.

Chopra, S.S., Watanabe, H., Zhong, T.P., and Roden, D.M. (2007). Molecular cloning and analysis of zebrafish voltage-gated sodium channel beta subunit genes: implications for the evolution of electrical signaling in vertebrates. *BMC Evol Biol* 7, 113.

Clatot, J., Hoshi, M., Wan, X., Liu, H., Jain, A., Shinlapawittayatorn, K., Marionneau, C., Ficker, E., Ha, T., and Deschênes, I. (2017). Voltage-gated sodium channels assemble and gate as dimers. *Nat Commun* 8, 2077.

Cortada, E., Brugada, R., and Verges, M. (2019). Trafficking and Function of the Voltage-Gated Sodium Channel  $\beta 2$  Subunit. *Biomolecules* 9.

Cusdin, F.S., Clare, J.J., and Jackson, A.P. (2008). Trafficking and Cellular Distribution of Voltage-Gated Sodium Channels. *Traffic* 9, 17-26.

de Lera Ruiz, M., and Kraus, R.L. (2015). Voltage-Gated Sodium Channels: Structure, Function, Pharmacology, and Clinical Indications. *Journal of Medicinal Chemistry* 58, 7093-7118.

Edokobi, N., and Isom, L.L. (2018). Voltage-Gated Sodium Channel  $\beta 1/\beta 1B$  Subunits Regulate Cardiac Physiology and Pathophysiology. *Frontiers in Physiology* 9.

Fendri-Kriaa, N., Kammoun, F., Salem, I.H., Kifagi, C., Mkaouar-Rebai, E., Hsairi, I., Rebai, A., Triki, C., and Fakhfakh, F. (2011). New mutation c.374C>T and a putative disease-associated haplotype within SCN1B gene in Tunisian families with febrile seizures. *European Journal of Neurology* 18, 695-702.

Gaborit, N., Le Bouter, S., Szuts, V., Varro, A., Escande, D., Nattel, S., and Demolombe, S. (2007). Regional and tissue specific transcript signatures of ion channel genes in the non-diseased human heart. *J Physiol* 582, 675-693.

George, S.A., Bonakdar, M., Zeitz, M., Davalos, R.V., Smyth, J.W., and Poelzing, S. (2016). Extracellular sodium dependence of the conduction velocity-calcium relationship: evidence of ephaptic self-attenuation. *Am J Physiol Heart Circ Physiol* 310, H1129-1139.

Glass, W.G., Duncan, A.L., and Biggin, P.C. (2020). Computational Investigation of Voltage-Gated Sodium Channel  $\beta 3$  Subunit Dynamics. *Front Mol Biosci* 7, 40.

Gong, J.E., Liao, H.M., Long, H.Y., Li, X.M., Long, L.L., Zhou, L., Gu, W.P., Lu, S.H., Qu, Q., Yang, L.M., *et al.* (2019). SCN1B and SCN2B gene variants analysis in dravet syndrome patients: Analysis of 22 cases. *Medicine (Baltimore)* 98, e14974.

Greer-Short, A., George, S.A., Poelzing, S., and Weinberg, S.H. (2017). Revealing the Concealed Nature of Long-QT Type 3 Syndrome. *Circ Arrhythm Electrophysiol* 10, e004400.

Hakim, P., Brice, N., Thresher, R., Lawrence, J., Zhang, Y., Jackson, A.P., Grace, A.A., and Huang, C.L. (2010). Scn3b knockout mice exhibit abnormal sino-atrial and cardiac conduction properties. *Acta Physiol (Oxf)* 198, 47-59.

Hakim, P., Gurung, I.S., Pedersen, T.H., Thresher, R., Brice, N., Lawrence, J., Grace, A.A., and Huang, C.L. (2008). Scn3b knockout mice exhibit abnormal ventricular electrophysiological properties. *Prog Biophys Mol Biol* 98, 251-266.

Haworth, A.S., Hodges, S.L., Capatina, A.L., Isom, L.L., Baumann, C.G., and Brackenbury, W.J. (2022). Subcellular dynamics and functional activity of the cleaved intracellular domain of the Na<sup>+</sup> channel  $\beta$ 1 subunit. *Journal of Biological Chemistry* 298, 102174.

Hichri, E., Abriel, H., and Kucera, J.P. (2018). Distribution of cardiac sodium channels in clusters potentiates ephaptic interactions in the intercalated disc. *J Physiol* 596, 563-589.

Hoagland, D.T., Santos, W., Poelzing, S., and Gourdie, R.G. (2019). The role of the gap junction perinexus in cardiac conduction: Potential as a novel anti-arrhythmic drug target. *Prog Biophys Mol Biol* 144, 41-50.

Hodges, S.L., Bouza, A.A., and Isom, L.L. (2022). Therapeutic Potential of Targeting Regulated Intramembrane Proteolysis Mechanisms of Voltage-Gated Ion Channel Subunits and Cell Adhesion Molecules. *Pharmacological Reviews* 74, 1030-1050.



Hu, D., Barajas-Martinez, H., Burashnikov, E., Springer, M., Wu, Y., Varro, A., Pfeiffer, R., Koopmann, T.T., Cordeiro, J.M., Guerchicoff, A., *et al.* (2009). A Mutation in the  $\beta$ 3 Subunit of the Cardiac Sodium Channel Associated With Brugada ECG Phenotype. *Circulation: Cardiovascular Genetics* 2, 270-278.

Hu, D., Barajas-Martínez, H., Medeiros-Domingo, A., Crotti, L., Veltmann, C., Schimpf, R., Urrutia, J., Alday, A., Casis, O., Pfeiffer, R., *et al.* (2012). A novel rare variant in SCN1Bb linked to Brugada syndrome and SIDS by combined modulation of Na(v)1.5 and K(v)4.3 channel currents. *Heart Rhythm* 9, 760-769.

Hull, J.M., and Isom, L.L. (2018). Voltage-gated sodium channel  $\beta$  subunits: The power outside the pore in brain development and disease. *Neuropharmacology* 132, 43-57.

Isom, L.L., and Catterall, W.A. (1996). Na<sup>+</sup> channel subunits and Ig domains. *Nature* 383, 307-308.

Isom, L.L., De Jongh, K.S., and Catterall, W.A. (1994). Auxiliary subunits of voltage-gated ion channels. *Neuron* 12, 1183-1194.

Isom, L.L., De Jongh, K.S., Patton, D.E., Reber, B.F.X., Offord, J., Charbonneau, H., Walsh, K., Goldin, A.L., and Catterall, W.A. (1992). Primary Structure and Functional Expression of the  $\beta$ 2 Subunit of the Rat Brain Sodium Channel. *Science* 256, 839-842.

Isom, L.L., Ragsdale, D.S., De Jongh, K.S., Westenbroek, R.E., Reber, B.F.X., Scheuer, T., and Catterall, W.A. (1995). Structure and function of the  $\beta$ 2 subunit of brain sodium channels, a transmembrane glycoprotein with a CAM motif. *Cell* 83, 433-442.

Kazarinova-Noyes, K., Malhotra, J.D., McEwen, D.P., Mattei, L.N., Berglund, E.O., Ranscht, B., Levinson, S.R., Schachner, M., Shrager, P., Isom, L.L., *et al.* (2001). Contactin Associates with

Na<sup>+</sup> Channels and Increases Their Functional Expression. The Journal of Neuroscience 21, 7517-7525.

Kazen-Gillespie, K.A., Ragsdale, D.S., D'Andrea, M.R., Mattei, L.N., Rogers, K.E., and Isom, L.L. (2000). Cloning, localization, and functional expression of sodium channel beta1A subunits. J Biol Chem 275, 1079-1088.

Kim, Y.O., Dibbens, L., Marini, C., Suls, A., Chemaly, N., Mei, D., McMahon, J.M., Iona, X., Berkovic, S.F., De Jonghe, P., *et al.* (2013). Do mutations in SCN1B cause Dravet syndrome? Epilepsy Research 103, 97-100.

Kucera, J.P., Rohr, S., and Rudy, Y. (2002). Localization of sodium channels in intercalated disks modulates cardiac conduction. Circ Res 91, 1176-1182.

Li, R.G., Wang, Q., Xu, Y.J., Zhang, M., Qu, X.K., Liu, X., Fang, W.Y., and Yang, Y.Q. (2013). Mutations of the SCN4B-encoded sodium channel  $\beta$ 4 subunit in familial atrial fibrillation. Int J Mol Med 32, 144-150.

Li, Y., Yuan, T., Huang, B., Zhou, F., Peng, C., Li, X., Qiu, Y., Yang, B., Zhao, Y., Huang, Z., *et al.* (2023). Structure of human Na(V)1.6 channel reveals Na(+) selectivity and pore blockade by 4,9-anhydro-tetrodotoxin. Nat Commun 14, 1030.

Lin, J., and Keener, J.P. (2010). Modeling electrical activity of myocardial cells incorporating the effects of ephaptic coupling. Proc Natl Acad Sci U S A 107, 20935-20940.

Lin, L., Li, K., Tian, B., Jia, M., Wang, Q., Xu, C., Xiong, L., Wang, Q., Zeng, Y., and Wang, P. (2022). Two Novel Functional Mutations in Promoter Region of SCN3B Gene Associated with Atrial Fibrillation. Life 12, 1794.

Lopez-Santiago, L.F., Meadows, L.S., Ernst, S.J., Chen, C., Malhotra, J.D., McEwen, D.P., Speelman, A., Noebels, J.L., Maier, S.K.G., Lopatin, A.N., *et al.* (2007). Sodium channel *Scn1b* null mice exhibit prolonged QT and RR intervals. *Journal of Molecular and Cellular Cardiology* 43, 636-647.

Lu, Y., Yu, W., Xi, Z., Xiao, Z., Kou, X., and Wang, X.F. (2010). Mutational analysis of *SCN2B*, *SCN3B* and *SCN4B* in a large Chinese Han family with generalized tonic-clonic seizure. *Neurol Sci* 31, 675-677.

Maier, S.K.G., Westenbroek, R.E., McCormick, K.A., Curtis, R., Scheuer, T., and Catterall, W.A. (2004). Distinct Subcellular Localization of Different Sodium Channel  $\alpha$  and  $\beta$  Subunits in Single Ventricular Myocytes From Mouse Heart. *Circulation* 109, 1421-1427.

Malhotra, J.D., Kazen-Gillespie, K., Hortsch, M., and Isom, L.L. (2000). Sodium Channel  $\beta$  Subunits Mediate Homophilic Cell Adhesion and Recruit Ankyrin to Points of Cell-Cell Contact\*. *Journal of Biological Chemistry* 275, 11383-11388.

McEwen, D.P., Chen, C., Meadows, L.S., Lopez-Santiago, L., and Isom, L.L. (2009). The voltage-gated Na<sup>+</sup> channel  $\beta$ 3 subunit does not mediate trans homophilic cell adhesion or associate with the cell adhesion molecule contactin. *Neuroscience Letters* 462, 272-275.

McEwen, D.P., and Isom, L.L. (2004). Heterophilic interactions of sodium channel beta1 subunits with axonal and glial cell adhesion molecules. *J Biol Chem* 279, 52744-52752.

Medeiros-Domingo, A., Kaku, T., Tester, D.J., Iturralde-Torres, P., Itty, A., Ye, B., Valdivia, C., Ueda, K., Canizales-Quinteros, S., Tusié-Luna, M.T., *et al.* (2007). *SCN4B*-Encoded Sodium Channel  $\beta$ 4 Subunit in Congenital Long-QT Syndrome. *Circulation* 116, 134-142.

Miyazaki, H., Oyama, F., Inoue, R., Aosaki, T., Abe, T., Kiyonari, H., Kino, Y., Kurosawa, M., Shimizu, J., Ogiwara, I., *et al.* (2014). Singular localization of sodium channel  $\beta$ 4 subunit in unmyelinated fibres and its role in the striatum. *Nature Communications* 5, 5525.

Morgan, K., Stevens, E.B., Shah, B., Cox, P.J., Dixon, A.K., Lee, K., Pinnock, R.D., Hughes, J., Richardson, P.J., Mizuguchi, K., *et al.* (2000).  $\beta$ 3: An additional auxiliary subunit of the voltage-sensitive sodium channel that modulates channel gating with distinct kinetics. *Proceedings of the National Academy of Sciences* 97, 2308-2313.

Mori, Y., Fishman, G.I., and Peskin, C.S. (2008). Ephaptic conduction in a cardiac strand model with 3D electrodiffusion. *Proc Natl Acad Sci U S A* 105, 6463-6468.

Namadurai, S., Balasuriya, D., Rajappa, R., Wiemhöfer, M., Stott, K., Klingauf, J., Edwardson, J.M., Chirgadze, D.Y., and Jackson, A.P. (2014). Crystal Structure and Molecular Imaging of the Nav Channel  $\beta$ 3 Subunit Indicates a Trimeric Assembly\*. *Journal of Biological Chemistry* 289, 10797-10811.

Namadurai, S., Yereddi, N.R., Cusdin, F.S., Huang, C.L.-H., Chirgadze, D.Y., and Jackson, A.P. (2015). A new look at sodium channel  $\beta$  subunits. *Open Biology* 5, 140192.

Notredame, C., Higgins, D.G., and Heringa, J. (2000). T-Coffee: A novel method for fast and accurate multiple sequence alignment. *J Mol Biol* 302, 205-217.

Nowak, M.B., Greer-Short, A., Wan, X., Wu, X., Deschênes, I., Weinberg, S.H., and Poelzing, S. (2020). Intercellular Sodium Regulates Repolarization in Cardiac Tissue with Sodium Channel Gain of Function. *Biophys J* 118, 2829-2843.

Nowak, M.B., Poelzing, S., and Weinberg, S.H. (2021). Mechanisms underlying age-associated manifestation of cardiac sodium channel gain-of-function. *J Mol Cell Cardiol* 153, 60-71.

O'Malley, H.A., Hull, J.M., Clawson, B.C., Chen, C., Owens-Fiestan, G., Jameson, M.B., Aton, S.J., Parent, J.M., and Isom, L.L. (2019). Scn1b deletion in adult mice results in seizures and SUDEP. *Annals of Clinical and Translational Neurology* 6, 1121-1126.

O'Malley, H.A., and Isom, L.L. (2015). Sodium channel  $\beta$  subunits: emerging targets in channelopathies. *Annu Rev Physiol* 77, 481-504.

Olesen, M.S., Holst, A.G., Svendsen, J.H., Haunsø, S., and Tfelt-Hansen, J. (2012). SCN1Bb R214Q found in 3 patients: 1 with Brugada syndrome and 2 with lone atrial fibrillation. *Heart Rhythm* 9, 770-773.

Olesen, M.S., Jespersen, T., Nielsen, J.B., Liang, B., Møller, D.V., Hedley, P., Christiansen, M., Varró, A., Olesen, S.-P., Haunsø, S., *et al.* (2010). Mutations in sodium channel  $\beta$ -subunit SCN3B are associated with early-onset lone atrial fibrillation. *Cardiovascular Research* 89, 786-793.

Pan, X., Li, Z., Huang, X., Huang, G., Gao, S., Shen, H., Liu, L., Lei, J., and Yan, N. (2019). Molecular basis for pore blockade of human Na(+) channel Na(v)1.2 by the  $\mu$ -conotoxin KIIIA. *Science* 363, 1309-1313.

Pan, X., Li, Z., Zhou, Q., Shen, H., Wu, K., Huang, X., Chen, J., Zhang, J., Zhu, X., Lei, J., *et al.* (2018). Structure of the human voltage-gated sodium channel Na(v)1.4 in complex with  $\beta$ 1. *Science* 362.

Patino, G.A., Brackenbury, W.J., Bao, Y., Lopez-Santiago, L.F., O'Malley, H.A., Chen, C., Calhoun, J.D., Lafrenière, R.G., Cossette, P., Rouleau, G.A., *et al.* (2011). Voltage-gated Na<sup>+</sup> channel  $\beta$ 1B: a secreted cell adhesion molecule involved in human epilepsy. *J Neurosci* 31, 14577-14591.

Patino, G.A., Claes, L.R., Lopez-Santiago, L.F., Slat, E.A., Dondeti, R.S., Chen, C., O'Malley, H.A., Gray, C.B., Miyazaki, H., Nukina, N., *et al.* (2009). A functional null mutation of SCN1B in a patient with Dravet syndrome. *J Neurosci* 29, 10764-10778.

Peeters, U., Scornik, F., Riuró, H., Pérez, G., Komurcu-Bayrak, E., Van Malderen, S., Pappaert, G., Tarradas, A., Pagans, S., Daneels, D., *et al.* (2015). Contribution of Cardiac Sodium Channel  $\beta$ -Subunit Variants to Brugada Syndrome. *Circ J* 79, 2118-2129.

Raisch, T.B., Yanoff, M.S., Larsen, T.R., Farooqui, M.A., King, D.R., Veeraraghavan, R., Gourdie, R.G., Baker, J.W., Arnold, W.S., AlMahameed, S.T., *et al.* (2018). Intercalated Disk Extracellular Nanodomain Expansion in Patients With Atrial Fibrillation. *Front Physiol* 9, 398.

Ramos-Mondragon, R., Edokobi, N., Hodges, S.L., Wang, S., Bouza, A.A., Canugovi, C., Scheuing, C., Juratli, L., Abel, W.R., Noujaim, S.F., *et al.* (2022). Neonatal Scn1b-null mice have sinoatrial node dysfunction, altered atrial structure, and atrial fibrillation. *JCI Insight* 7.

Ratcliffe, C.F., Westenbroek, R.E., Curtis, R., and Catterall, W.A. (2001). Sodium channel  $\beta$ 1 and  $\beta$ 3 subunits associate with neurofascin through their extracellular immunoglobulin-like domain. *Journal of Cell Biology* 154, 427-434.

Rhett, J.M., Jourdan, J., and Gourdie, R.G. (2011). Connexin 43 connexon to gap junction transition is regulated by zonula occludens-1. *Mol Biol Cell* 22, 1516-1528.

Rhett, J.M., Ongstad, E.L., Jourdan, J., and Gourdie, R.G. (2012). Cx43 associates with Na(v)1.5 in the cardiomyocyte perinexus. *J Membr Biol* 245, 411-422.

Ricci, M.T., Menegon, S., Vatrano, S., Mandrile, G., Cerrato, N., Carvalho, P., De Marchi, M., Gaita, F., Giustetto, C., and Giachino, D.F. (2014). SCN1B gene variants in Brugada Syndrome: a study of 145 SCN5A-negative patients. *Sci Rep* 4, 6470.

Riuró, H., Beltran-Alvarez, P., Tarradas, A., Selga, E., Campuzano, O., Vergés, M., Pagans, S., Iglesias, A., Brugada, J., Brugada, P., *et al.* (2013). A Missense Mutation in the Sodium Channel  $\beta$ 2 Subunit Reveals SCN2B as a New Candidate Gene for Brugada Syndrome. *Human Mutation* *34*, 961-966.

Riuró, H., Campuzano, O., Arbelo, E., Iglesias, A., Batlle, M., Pérez-Villa, F., Brugada, J., Pérez, G.J., Scornik, F.S., and Brugada, R. (2014). A missense mutation in the sodium channel  $\beta$ 1b subunit reveals SCN1B as a susceptibility gene underlying long QT syndrome. *Heart Rhythm* *11*, 1202-1209.

Salvage, S.C., Huang, C.L., and Jackson, A.P. (2020a). Cell-Adhesion Properties of  $\beta$ -Subunits in the Regulation of Cardiomyocyte Sodium Channels. *Biomolecules* *10*.

Salvage, S.C., Rees, J.S., McStea, A., Hirsch, M., Wang, L., Tynan, C.J., Reed, M.W., Irons, J.R., Butler, R., Thompson, A.J., *et al.* (2020b). Supramolecular clustering of the cardiac sodium channel Nav1.5 in HEK293F cells, with and without the auxiliary  $\beta$ 3-subunit. *The FASEB Journal* *34*, 3537-3553.

Scheffer, I.E., Harkin, L.A., Grinton, B.E., Dibbens, L.M., Turner, S.J., Zielinski, M.A., Xu, R., Jackson, G., Adams, J., Connellan, M., *et al.* (2007). Temporal lobe epilepsy and GEFS+ phenotypes associated with SCN1B mutations. *Brain* *130*, 100-109.

Shah, B.S., Stevens, E.B., Pinnock, R.D., Dixon, A.K., and Lee, K. (2001). Developmental expression of the novel voltage-gated sodium channel auxiliary subunit  $\beta$ 3, in rat CNS. *J Physiol* *534*, 763-776.

Shen, H., Liu, D., Wu, K., Lei, J., and Yan, N. (2019). Structures of human Na(v)1.7 channel in complex with auxiliary subunits and animal toxins. *Science* *363*, 1303-1308.

Shimizu, H., Tosaki, A., Ohsawa, N., Ishizuka-Katsura, Y., Shoji, S., Miyazaki, H., Oyama, F., Terada, T., Shirouzu, M., Sekine, S.I., *et al.* (2017). Parallel homodimer structures of the extracellular domains of the voltage-gated sodium channel  $\beta$ 4 subunit explain its role in cell-cell adhesion. *J Biol Chem* 292, 13428-13440.

Signore, S., Sorrentino, A., Borghetti, G., Cannata, A., Meo, M., Zhou, Y., Kannappan, R., Pasqualini, F., O'Malley, H., Sundman, M., *et al.* (2015). Late Na(+) current and protracted electrical recovery are critical determinants of the aging myopathy. *Nat Commun* 6, 8803.

Srinivasan, J., Schachner, M., and Catterall, W.A. (1998). Interaction of voltage-gated sodium channels with the extracellular matrix molecules tenascin-C and tenascin-R. *Proc Natl Acad Sci U S A* 95, 15753-15757.

Tsumoto, K., Ashihara, T., Naito, N., Shimamoto, T., Amano, A., Kurata, Y., and Kurachi, Y. (2020). Specific decreasing of Na(+) channel expression on the lateral membrane of cardiomyocytes causes fatal arrhythmias in Brugada syndrome. *Sci Rep* 10, 19964.

Tveito, A., Jæger, K.H., Kuchta, M., Mardal, K.-A., and Rognes, M.E. (2017). A Cell-Based Framework for Numerical Modeling of Electrical Conduction in Cardiac Tissue. *Frontiers in Physics* 5.

Veeraraghavan, R., Hoeker, G.S., Alvarez-Laviada, A., Hoagland, D., Wan, X., King, D.R., Sanchez-Alonso, J., Chen, C., Jourdan, J., Isom, L.L., *et al.* (2018). The adhesion function of the sodium channel beta subunit ( $\beta$ 1) contributes to cardiac action potential propagation. *Elife* 7, e37610.

Veeraraghavan, R., Lin, J., Hoeker, G.S., Keener, J.P., Gourdie, R.G., and Poelzing, S. (2015). Sodium channels in the Cx43 gap junction perinexus may constitute a cardiac ephapse: an experimental and modeling study. *Pflugers Arch* 467, 2093-2105.



Veeraraghavan, R., Lin, J., Keener, J.P., Gourdie, R., and Poelzing, S. (2016). Potassium channels in the Cx43 gap junction perinexus modulate ephaptic coupling: an experimental and modeling study. *Pflugers Arch* 468, 1651-1661.

Wallace, R.H., Scheffer, I.E., Parasivam, G., Barnett, S., Wallace, G.B., Sutherland, G.R., Berkovic, S.F., and Mulley, J.C. (2002). Generalized epilepsy with febrile seizures plus: Mutation of the sodium channel subunit *SCN1B*. *Neurology* 58, 1426-1429.

Wallace, R.H., Wang, D.W., Singh, R., Scheffer, I.E., George, A.L., Jr., Phillips, H.A., Saar, K., Reis, A., Johnson, E.W., Sutherland, G.R., *et al.* (1998). Febrile seizures and generalized epilepsy associated with a mutation in the Na<sup>+</sup>-channel beta1 subunit gene *SCN1B*. *Nat Genet* 19, 366-370.

Wang, P., Yang, Q., Wu, X., Yang, Y., Shi, L., Wang, C., Wu, G., Xia, Y., Yang, B., Zhang, R., *et al.* (2010). Functional dominant-negative mutation of sodium channel subunit gene *SCN3B* associated with atrial fibrillation in a Chinese GeneID population. *Biochem Biophys Res Commun* 398, 98-104.

Watanabe, H., Darbar, D., Kaiser, D.W., Jiramongkolchai, K., Chopra, S., Donahue, B.S., Kannankeril, P.J., and Roden, D.M. (2009). Mutations in sodium channel  $\beta$ 1- and  $\beta$ 2-subunits associated with atrial fibrillation. *Circ Arrhythm Electrophysiol* 2, 268-275.

Watanabe, H., Koopmann, T.T., Le Scouarnec, S., Yang, T., Ingram, C.R., Schott, J.J., Demolombe, S., Probst, V., Anselme, F., Escande, D., *et al.* (2008). Sodium channel  $\beta$ 1 subunit mutations associated with Brugada syndrome and cardiac conduction disease in humans. *J Clin Invest* 118, 2260-2268.

Wei, N., Mori, Y., and Tolkacheva, E.G. (2016). The dual effect of ephaptic coupling on cardiac conduction with heterogeneous expression of connexin 43. *J Theor Biol* 397, 103-114.

Wei, N., and Tolkacheva, E.G. (2020). Interplay between ephaptic coupling and complex geometry of border zone during acute myocardial ischemia: Effect on arrhythmogeneity. *Chaos* 30, 033111.

Weinberg, S.H. (2017). Ephaptic coupling rescues conduction failure in weakly coupled cardiac tissue with voltage-gated gap junctions. *Chaos* 27, 093908.

Wong, H.-K., Sakurai, T., Oyama, F., Kaneko, K., Wada, K., Miyazaki, H., Kurosawa, M., De Strooper, B., Saftig, P., and Nukina, N. (2005).  $\beta$  Subunits of Voltage-gated Sodium Channels Are Novel Substrates of  $\beta$ -Site Amyloid Precursor Protein-cleaving Enzyme (BACE1) and  $\gamma$ -Secretase\*. *Journal of Biological Chemistry* 280, 23009-23017.

Xiao, Z.-C., Ragsdale, D.S., Malhotra, J.D., Mattei, L.N., Braun, P.E., Schachner, M., and Isom, L.L. (1999). Tenascin-R Is a Functional Modulator of Sodium Channel  $\beta$  Subunits\*. *Journal of Biological Chemistry* 274, 26511-26517.

Yan, Z., Zhou, Q., Wang, L., Wu, J., Zhao, Y., Huang, G., Peng, W., Shen, H., Lei, J., and Yan, N. (2017). Structure of the Na(v)1.4- $\beta$ 1 Complex from Electric Eel. *Cell* 170, 470-482.e411.

Yang, Q., Xiong, H., Xu, C., Huang, Y., Tu, X., Wu, G., Fu, F., Wang, Z., Wang, L., Zhao, Y., *et al.* (2019). Identification of rare variants in cardiac sodium channel  $\beta$ 4-subunit gene SCN4B associated with ventricular tachycardia. *Mol Genet Genomics* 294, 1059-1071.

Yereddi, N.R., Cusdin, F.S., Namadurai, S., Packman, L.C., Monie, T.P., Slavny, P., Clare, J.J., Powell, A.J., and Jackson, A.P. (2013). The immunoglobulin domain of the sodium channel  $\beta$ 3 subunit

contains a surface-localized disulfide bond that is required for homophilic binding. The FASEB Journal 27, 568-580.

Yu, F.H., Westenbroek, R.E., Silos-Santiago, I., McCormick, K.A., Lawson, D., Ge, P., Ferriera, H., Lilly, J., DiStefano, P.S., Catterall, W.A., *et al.* (2003). Sodium channel beta4, a new disulfide-linked auxiliary subunit with similarity to beta2. J Neurosci 23, 7577-7585.

Zhu, W., Wang, W., Angsutararux, P., Mellor, R.L., Isom, L.L., Nerbonne, J.M., and Silva, J.R. (2021). Modulation of the effects of class Ib antiarrhythmics on cardiac NaV1.5-encoded channels by accessory NaV $\beta$  subunits. JCI Insight 6.

Zhu, Z., Bolt, E., Newmaster, K., Osei-Bonsu, W., Cohen, S., Cuddapah, V.A., Gupta, S., Paudel, S., Samanta, D., Dang, L.T., *et al.* (2022). SCN1B Genetic Variants: A Review of the Spectrum of Clinical Phenotypes and a Report of Early Myoclonic Encephalopathy. Children 9, 1507.

## **Chapter 2: Development and Characterization of the Mode-of-Action of Inhibitory and Agonist Peptides Targeting the Voltage-Gated Sodium Channel SCN1B/ $\beta$ 1 Subunit**

*Manuscript in submission*

Zachary J. Williams<sup>1</sup>, Anita Alvarez-Laviada<sup>2</sup>, Daniel Hoagland<sup>1</sup>, L. Jane Jourdan<sup>1</sup>, Steven Poelzing<sup>1,3,4</sup>, Julia Gorelik<sup>2</sup>, Robert G. Gourdie<sup>1,3,4†</sup>

<sup>1</sup>Fralin Biomedical Research Institute, Virginia Polytechnic University, Roanoke, VA, United States

<sup>2</sup>Department of Myocardial Function, Imperial College London, London, United Kingdom

<sup>3</sup>School of Medicine, Virginia Polytechnic University, Roanoke, VA, United States

<sup>4</sup>Department of Biomedical Engineering and Mechanics, Virginia Polytechnic University, Roanoke, VA, United States

Running title:  $\beta$ 1 Inhibitory and Agonist Peptides

†Correspondence should be addressed to: Robert G. Gourdie [gourdier@vtc.vt.edu](mailto:gourdier@vtc.vt.edu)

Fralin Biomedical Research Institute at Virginia Tech Carilion,

Center for Vascular and Heart Research,

2 Riverside Circle, Roanoke, VA, 24016, USA

Keywords: Arrhythmia, peptide therapeutic, Voltage-gated sodium channels, SCN1B ( $\beta$ 1/ $\beta$ 1B)

## ABSTRACT

Cardiac arrhythmia treatment is a clinical challenge necessitating safer and more effective therapies. Recent studies have highlighted the role of the perinexus, a nanodomain enriched in voltage-gated sodium channels including both  $\text{Na}_v1.5$  and  $\beta 1$  subunits, adjacent to gap junctions. These findings offer insights into action potential conduction in the heart. A 19-amino acid SCN1B ( $\beta 1/\beta 1B$ ) mimetic peptide,  $\beta\text{adp1}$ , disrupts  $\beta 1$ -mediated adhesion in cardiac perinexii, inducing arrhythmogenic changes. We aimed to explore  $\beta\text{adp1}$ 's mechanism and develop novel SCN1B mimetic peptides affecting  $\beta 1$ -mediated adhesion. Using patch clamp assays in neonatal rat cardiomyocytes and electric cell substrate impedance sensing (ECIS) in  $\beta 1$ -expressing cells, we observed  $\beta\text{adp1}$  maintained inhibitory effects for up to 5 hours. A shorter peptide (LQLEED) based on the carboxyl-terminus of  $\beta\text{adp1}$  mimicked this inhibitory effect, while dimeric peptides containing repeated LQLEED sequences paradoxically promoted intercellular adhesion over longer time courses. Moreover, we found a link between these peptides and  $\beta 1$  regulated intramembrane proteolysis (RIP) - a signaling pathway effecting gene transcription including that of VGSC subunits.  $\beta\text{adp1}$  increased RIP continuously over 48 hours, while dimeric agonists acutely boosted RIP for up to 6 hours. In the presence of DAPT, an RIP inhibitor,  $\beta\text{adp1}$ 's effects on ECIS-measured intercellular adhesion was reduced, suggesting a relationship between RIP and the peptide's inhibitory action. In conclusion, novel SCN1B ( $\beta 1/\beta 1B$ ) mimetic peptides are reported with the potential to modulate intercellular  $\beta 1$ -mediated adhesion, potentially through  $\beta 1$  RIP. These findings suggest a path towards the development of anti-arrhythmic drugs targeting the perinexus.

## **1. INTRODUCTION**

The United States experiences between 180,000 and 450,000 sudden cardiac deaths annually, with cardiac arrhythmias playing a significant role (Deo and Albert, 2012; Garcia-Elias and Benito, 2018; Khurshid et al., 2018). Many drugs aimed at preventing arrhythmias target ion channels, including the sodium channel Nav1.5, but often have severe side effects (Vidhya Rao, 2015). For example, the Cardiac Arrhythmia Suppression Trial (CAST) was successful in reducing arrhythmogenic triggers, but unfortunately the therapies tested were also found to result in an increase in total deaths (1992; Echt et al., 1991). This problematic clinical trial record, together with high costs, and the inherent deadly risks associated with targeting heart rhythm disorders, has slowed the development of anti-arrhythmic drugs. While there are new and growing methods of treating arrhythmias, such as catheter ablation (Ajijola et al., 2015; Kim et al., 2023) neuroscientific therapies (Hanna et al., 2021), or even optogenetic methods (Müllenbroich et al., 2021), there remains considerable academic and clinical interest in new mechanistic targets to address the growing unmet clinical need for safe and effective pharmacologic treatment of disorders of cardiac electrical rhythm (Moreno et al., 2019; Nguyen et al., 2019).

The voltage-gated sodium channel (VGSC) incorporates both alpha( $\alpha$ )- (e.g. Nav1.5) and beta ( $\beta$ )-subunits. VGSC  $\beta$  subunits are encoded by SCN1B-SCN4B ( $\beta$ 1- $\beta$ 4) and an alternatively spliced variant of SCN1B ( $\beta$ 1B) (Beneski and Catterall, 1980; Brackenbury and Isom, 2011; Isom et al., 1994; Isom et al., 1992; Isom et al., 1995a; Morgan et al., 2000; Patino et al., 2011; Yu et al., 2003). VGSC  $\beta$ -subunits have been reported to regulate channel excitability by altering channel gating, voltage-dependence of activation and inactivation, and inactivation speed. Additionally,

$\beta$  subunits have assignments in cell adhesion - mediated by an extracellular immunoglobulin (Ig) domain that shares homology with other adhesion molecules (Brackenbury and Isom, 2011). Consistent with adhesive function, SCN1B ( $\beta 1/\beta 1B$ ) is prominently localized at zones of electro-mechanical contact between cardiomyocytes (Rhett et al., 2012; Veeraraghavan et al., 2018), in particular at the perinexus, an intercalated disc nanodomain adjacent to the gap junction (GJ), co-locating with Nav1.5 (Rhett et al., 2012; Veeraraghavan et al., 2018), other ion channels and scaffolding proteins (Deschênes et al., 2008; Malhotra et al., 2000; Teng et al., 2022).

A growing body of modeling and experimental data indicate that the perinexus has roles in normal and arrhythmogenic conduction of cardiac electrical excitation (Adams et al., 2023; Hoeker et al., 2020; Ivanovic and Kucera, 2021; Lin et al., 2022; Mezache et al., 2020; Moise et al., 2021; Veeraraghavan et al., 2018; Veeraraghavan et al., 2016). The VGSC-rich perinexal domain at the GJ edge forms a 20-30 nm wide cleft of extracellular space. Adhesive interactions between Ig domains of SCN1B molecules on cells apposed at the GJ-adjacent cleft have been suggested to contribute to perinexal stability (Veeraraghavan et al., 2018). Two recent studies have provided further insights. First, modeling work by Ivanovic and Kucera showed that the narrow intercellular spacing maintained at the perinexus, together with its adjacency to GJs, profoundly affected extracellular potential dynamics and local patterns of current flow, orchestrating propagation of action potentials via an ephaptic mechanism (Ivanovic and Kucera, 2021). Second, Adams et al. demonstrated that the width of the perinexus, and its effect on the ephaptic mechanism, is a key determinant of normal cardiac conduction and not just a phenomenon of pathological states, as had been proposed by some (Adams et al., 2023). Consistent with roles in health and disease, increases in cell-cell spacing at the perinexus has

been linked to atrial arrhythmia in humans, suggesting that regulation of perinexal width and/or SCN1B ( $\beta 1/\beta 1B$ )-mediated adhesion may be targets for treating electrical disturbance to the heart (Raisch et al., 2018; Veeraraghavan et al., 2018). Further supporting this hypothesis, SCN1B KO mice show widened perinexii. Mutations in SCN1B in humans, including in the Ig domain, have been implicated in several arrhythmia-associated pathologies, including Brugada syndrome and Long QT syndrome (Veeraraghavan et al., 2018; Watanabe et al., 2009; Watanabe et al., 2008).

In a previous report, we showed that a SCN1B ( $\beta 1/\beta 1B$ ) mimetic peptide derived from its immunoglobulin (Ig) domain called  $\beta adp1$  acutely disrupted  $\beta 1$ -mediated function. Over time courses of an hour or less,  $\beta adp1$  reduced adhesion in cells expressing SCN1B ( $\beta 1$ ), caused de-adhesion and expansion of perinexii in isolated guinea pig hearts and prompted arrhythmogenic changes in cardiomyocytes and hearts, including loss of sodium channel activity and conduction slowing (Veeraraghavan et al., 2018). In the present study, we investigated short- and long-term effects of  $\beta adp1$  and related peptides – including novel  $\beta 1$ -targeting inhibitory and agonist peptides. We find that the acute effects of  $\beta 1$ -targeting peptides, including loss of junctional sodium currents in cardiomyocytes and reductions in adhesion between  $\beta 1$ -expressing cells, are maintained for up to 5 hours. It was further determined that over longer periods the response of cells to the peptide altered, with treatment being associated with increased adhesion. Moreover, we show that this increase correlates with up-regulation of Regulated Intramembrane Proteolysis (RIP) of  $\beta 1$ .  $\beta 1$  was shown to be modified through RIP almost two decades ago (Wong et al., 2005). Recent studies have solidified the importance of  $\beta 1$  RIP by showing that the intracellular domain of  $\beta 1$  translocates to the nucleus



and alters transcription of various genes involved in the propagation of electrical activity in the heart, including VGSC complex proteins (Bouza et al., 2021; Bouza et al., 2020). The results described herein suggest novel pro-drugs and paths to pharmacologically addressing the VGSC complex, with relevance to potential targeting of the perinexus and its assignments in cardiac conduction.

## **2. RESULTS**

### **2.1. $\beta$ adp1 Reduces Junctional Sodium Channel Activity, $\beta$ 1 Levels and Adhesion Over an**

**Acute Time-Course:** We have previously shown that a 30 minute treatment with  $\beta$ adp1, a 19 amino acid peptide mimetic of the SCN1B/  $\beta$ 1/ $\beta$ 1B immunoglobulin (Ig) domain, reduces peak sodium channel current ( $I_{Na}$ ) at cell-to-cell junctional contacts between neonatal rat ventricular myocytes (NRVMs) (Fig. 1A) (Veeraraghavan et al., 2018).  $\beta$ adp1 had no effect on sodium channel activity in non-junctional membranes distal from cell-cell contacts, or on whole cell  $I_{Na}$ , over similar time courses. We used scanning ion conductance microscopy (SICM) –guided smart patch clamp in NRVM cultures to investigate junctional sodium currents over a longer period (Fig. 1A). Similar to what was observed in the earlier study, 50  $\mu$ M  $\beta$ adp1 reduced junctional  $I_{Na}$  significantly after 30 minutes (Fig 1B). However, longer exposure to  $\beta$ adp1 prompted further reductions of junctional  $I_{Na}$ , reaching levels  $\sim$  1/3 that of untreated cells after 60 minutes, thereafter leveling off to similar reductions in activity at 90 and 120 minutes (Fig 1B). No change in  $I_{Na}$  occurred at junctional contacts in response to scrambled control peptide or in non-junctional membranes in response to  $\beta$ adp1 or control peptide (Fig. 1C). The level of sodium

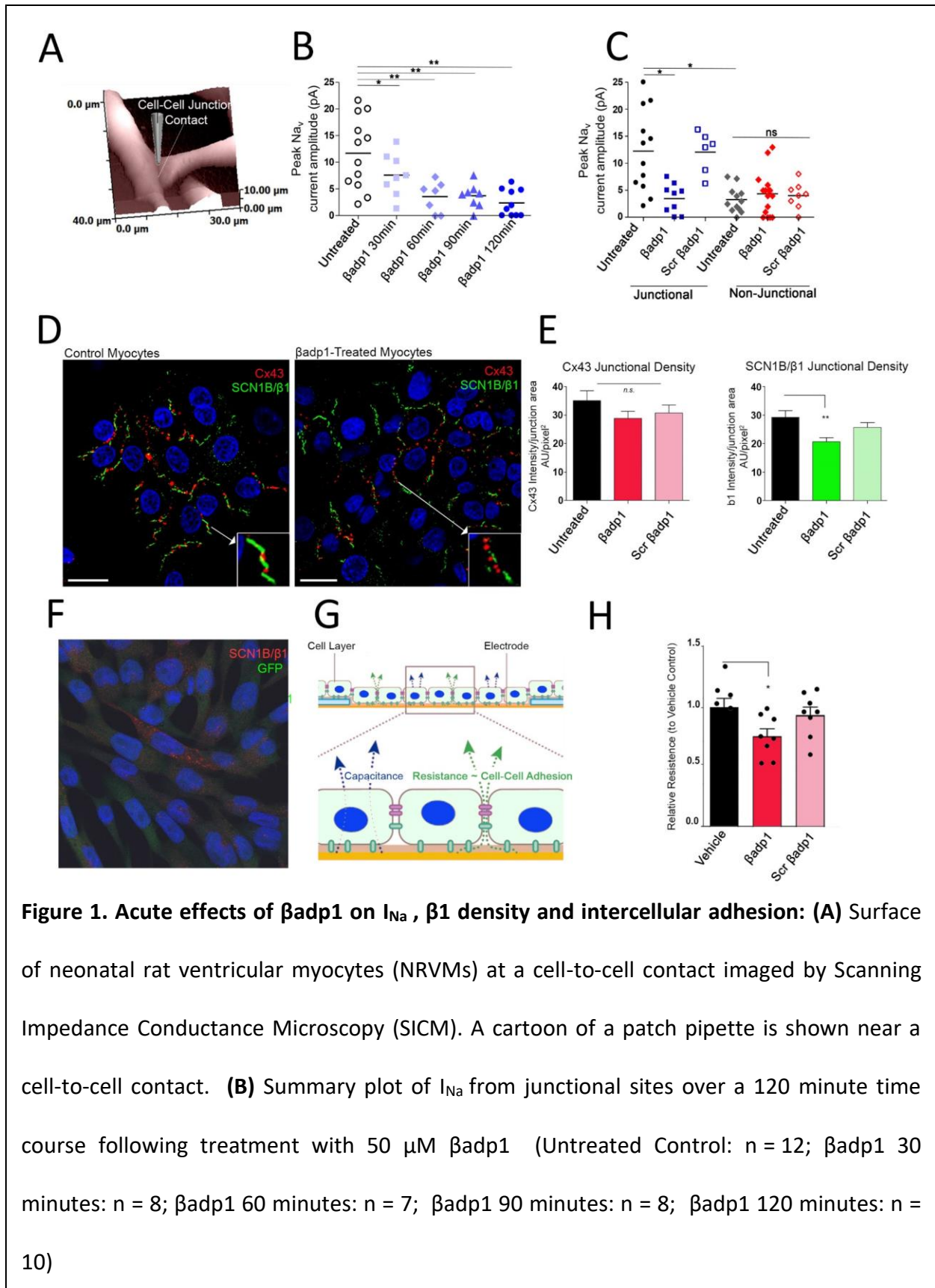


**Figure 1 Cont. (C)** Summary plot of  $I_{Na}$  from junctional and non-junctional sites in presence or absence  $\beta$ adp1 or scrambled  $\beta$ adp1 control peptide (50 mM) after 60 minutes (Junctional untreated Control: n = 12; Junctional  $\beta$ adp1: n = 8; Junctional scrambled  $\beta$ adp1: n = 6; Non-Junctional untreated Control: n = 10; Non-Junctional  $\beta$ adp1: n = 12; Non-Junctional scrambled  $\beta$ adp1: n= 6) **(D)** Representative confocal images of NRVMs immunolabeled for Cx43 (red) and  $\beta$ 1 (green) of control NRVMs or after treatment with  $\beta$ adp1 50  $\mu$ M for 60 minutes. Insets show magnified views of junctional Cx43 (red) and  $\beta$ 1 (green) signals. **(E)** Quantification of immunolabeling density of Cx43 (left hand bar chart) and  $\beta$ 1 (right hand bar chart) in untreated NRVMs and cells treated with  $\beta$ adp1 or scrambled  $\beta$ adp1 control peptide at 50  $\mu$ M for 60 minutes n $\geq$ 3 images per group. **(F)** Representative confocal image of 1610 cells expressing  $\beta$ 1 and GFP (green) immunolabeled for  $\beta$ 1 (red). **(G)** Diagram illustrating Electric Cell-Substrate Impedance Sensing (ECIS) and measurement parameters derived, including relative resistance of the monolayer overlying the electrode, which provides an assay of intercellular adhesion levels. **(H)** ECIS comparison of effects on relative resistance in monolayers of 1610 cells expressing  $\beta$ 1, at 5 hours following treatment with vehicle control solution (n=6) or  $\beta$ adp1 or scrambled control  $\beta$ adp1 at 10  $\mu$ M. \*p<0.05, \*\*p<0.01.

channel activity in non-junctional NRVM membranes was similar to the suppressed levels of  $I_{Na}$  measured after 60 minutes or more of exposure to  $\beta$ adp1 in junctional contacts (Fig 1C).

Confocal immunolabeling of NRVMs revealed  $\beta$ 1 signals juxtaposed with Cx43 GJs at cell-to-cell contact sites in untreated cells (Fig. 1D) or cells treated with control peptide for 60 minutes consistent with localization at perinexal domains (Supplemental Fig. 1).

This labeling occurred as sequential punctate domains of Cx43 and  $\beta$ 1 signal at junctional contacts, which though intense and side-by-side, did not appear to directly co-localize or overlap. By contrast, following treatment of NRVMs with 50  $\mu$ M  $\beta$ adp1 for 60 minutes, dissociation of juxtaposed side-by-side Cx43 and  $\beta$ 1 signals was observed at junctional contacts (compare insets Fig 1D), together with qualitatively lower amounts of  $\beta$ 1 immunolabeling. This reduction was confirmed by image quantification, which indicated that the density and counts of immunolabeled  $\beta$ 1 at junctional contacts were significantly reduced in NRVMs exposed to  $\beta$ adp1 (Fig 1E). Junctional Cx43 immunolabeling density or counts did not show any significant change in response to  $\beta$ adp1 over 60 minutes, relative to controls. Similarly, and in line with whole cell sodium channel activity measurements, the total % areas of Cx43 and  $\beta$ 1 immunolabeling normalized to cell area did not vary significantly between untreated cells, and NRVMs treated with 50  $\mu$ M  $\beta$ adp1 or control peptide for 60 minutes (data not shown).

Further characterization of  $\beta$ adp1 over an acute treatment time-course was provided by electric cell substrate impedance sensing (ECIS) of 1610 cells stably transfected with SCN1B ( $\beta$ 1) and GFP (1610 $\beta$ 1 cells; Fig 1F). In ECIS, changes in relative resistance enable assay of levels of intercellular adhesion (Fig. 1G). Extending previous work, we confirmed that relative to vehicle and scrambled controls, a relatively low concentration of  $\beta$ adp1 (10  $\mu$ M) was sufficient to prompt reductions in relative resistance/intercellular adhesion in 1610 $\beta$ 1cells following 5 hours of exposure of the cells to the peptide (Fig 1H).

In sum, the results shown in Figure 1 indicate that disruption of  $\beta$ 1-adhesion mediated by treatment with  $\beta$ adp1 over acute time courses of up to 5 hours is associated with reductions in

junctional  $I_{Na}$  density and SCN1B ( $\beta 1$ ) immunolabeling levels, with global  $I_{Na}$  and SCN1B ( $\beta 1$ ) levels across the entire cell membrane remaining unaffected.

## 2.2. Identification of Novel SCN1B Mimetic Inhibitory and Monomeric Agonist Peptides:

Modeling *in silico* indicates that  $\beta adp1$  likely mediates its effects over 30 to 60 minute time courses by selectively binding to the  $\beta 1$  extracellular Ig domain (Figure 2A, B). Experimental and modeling data further suggests that this interaction inhibits trans-adherent interactions between apposed  $\beta 1$  molecules on neighboring cell membranes (Hoagland et al., 2019; Salvage et al., 2020; Veeraraghavan et al., 2018). Our approach to design of  $\beta adp1$  as an inhibitor of  $\beta 1$ -mediated adhesion was motivated in part by a strategy reported by groups working on two other cell adhesion molecules; N-cadherin (Williams et al., 2002) and desmosglein-2 (Schlipp et al., 2014). These groups identified peptides in the Ig domain of these molecules that when provided in isolation inhibited adhesive interactions, but also described an approach to promoting adhesion based on dimerization of inhibitory monomers.

Name	Molecular Mass	Sequence	Design
SCN1B	37 kDa	...QKGTEEFVKILRYENEVLQLEEDERFEGRV...	
$\beta adp1$	2610.97 Da	FVKILRYENEVLQLEEDERF	Derived directly from SCN1B
Scr $\beta adp1$	2610.97 Da	EVEQRDILEFYLLFNVNRKE	Scrambled negative control
Scr1	2610.97 Da	FEELELLKVVNFQRDEIYER	Scrambled negative control
R85D	2569.83 Da	FVKILRYENEVLQLEEDDF	Negative control
LQLEED	786.82 Da	LQLEED	Short CT sequence from $\beta adp1$
PS2L	2436.62 Da	LQLEEDERFGLQLEEDERF	Dimerized fragment containing LQLEED repeats
PS2C	2642.91 Da	CLQLEEDERFGLQLEEDERFC	Dimerized and cyclized fragment with a disulfide bond between cysteine residues on either end

A second consideration of our approach to  $\beta 1$  drug design stemmed from data we obtained that molecules of greater than 3 kD do not efficiently penetrate the extracellular space of IDs in

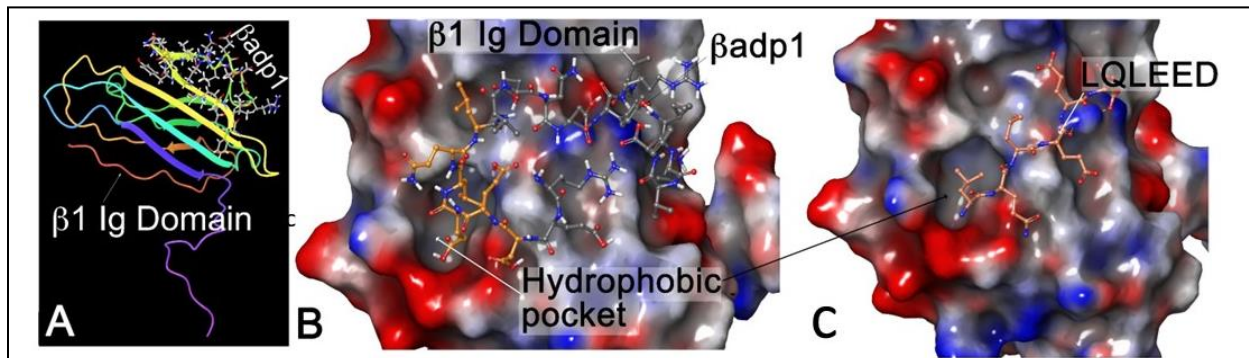


**Figure 2. In silico modeling of binding of  $\beta$ adp1 and LQLEED monomeric inhibitory peptides to the  $\beta$ 1 Immunoglobulin domain. (A)** Homology model of the  $\beta$ 1 extracellular domain based on the SCN3B/ $\beta$ 3 crystal structure (Veeraraghavan et al., 2018), with  $\beta$ adp1 (stick model) docked *in silico* in a low-energy conformation with the adhesion surface of the  $\beta$ 1 Immunoglobulin (Ig) loop. **(B)** Rendering of  $\beta$ adp1 (ball and stick model) docked to the predicted Ig adhesion surface of a  $\beta$ 1 homology model. This perspective of the  $\beta$ 1 Ig domain adhesion surface reveals a hydrophobic pocket, within which hydrophobic amino acids towards the C-terminus of  $\beta$ adp1 (e.g., LQL) are predicted to interact with  $\beta$ 1. Positive and negatively charged moieties on the adhesion surface of the  $\beta$ 1 Ig loop are shown in red and blue, respectively. **(C)** Docking of CT sequence LQLEED from  $\beta$ adp1 with the  $\beta$ 1 homology model in a low-energy conformation. The hydrophobic LQL sequence of peptide in this pose also embeds in the aforementioned hydrophobic pocket of the  $\beta$ 1 Ig domain.

vivo (Adams et al., 2023). The  $\beta$ adp1 monomer has a molecular mass of 2.6 kD and so does not exceed this threshold (Table 1). Thus, consistent with  $\beta$ adp1 having potential to target ID-localized  $\beta$ 1 we found that the peptide had quantifiable effects on perinexus structure in Langendorf-perfused guinea pig hearts (Veeraraghavan et al., 2018). A dimeric peptide comprising  $\beta$ adp1 repeats exceeds the 3kD threshold, likely negating its ability to act as an ID-localized  $\beta$ 1 agonist in the heart in vivo. As a first step in the generation of  $\beta$ 1 agonist that could

penetrate IDs, we used *in silico* modeling and ECIS to identify short peptides within  $\beta$ adp1 that had potential to interact with  $\beta$ 1 and inhibit  $\beta$ 1-mediated adhesion (Supplemental Fig. 2). Based on this approach we found that short peptides near the CT of  $\beta$ adp1 maintained propensity to interact with the  $\beta$ 1 Ig domain and disrupt adhesion. Figure 2C shows one of these peptides, the 6mer LQLEED (Molecular mass  $\sim$  746 daltons), organized in a low energy pose with  $\beta$ 1, with its NT leucine residues in a hydrophobic pocket on the Ig domain adhesion surface, within which portions of  $\beta$ adp1 also appear to embed (compare Figs. 2B and C).

Next, we synthesized LQLEED, and applied the peptide at a 10  $\mu$ M concentration in ECIS on 1610 $\beta$ 1 cell monolayers (Figure 3). Similar to when low concentrations of  $\beta$ adp1 are used, we found that LQLEED caused a reduction in relative resistance like that observed for the larger 19 aa peptide – consistent with the peptide inhibiting intercellular adhesion between 1610 $\beta$ 1 cells. By contrast, short peptides from nearer the  $\beta$ adp1 NT showed no evidence of similar inhibitory activity. (Supplemental Fig 2). The inhibitory effect of LQLEED is further illustrated in Figure 3A, where it is shown to reduce in relative resistance in 1610 monolayers following 5 hours of exposure of the cells to the peptide.

To investigate whether dimerization of short CT inhibitory monomers could generate dimeric agonists, we synthesized LQLEEDERF-G-LQLEEDERF (Table 1). This dimeric peptide, which is called PS2L, is a sequential repeat of the CT-most 9 amino acids of  $\beta$ adp1 including the LQLEED sequence spaced by a glycine (G) linker. We also synthesized a dimeric peptide of identical sequence, except that it had cysteine residues at its NT and CT. This novel peptide, called PS2C (CLQLEEDERF-G-LQLEEDERFC), was designed to be cyclizable via disulfide bonding between its cysteines (Table 1). Importantly, the molecular mass of the PS2L and PS2C dimers are

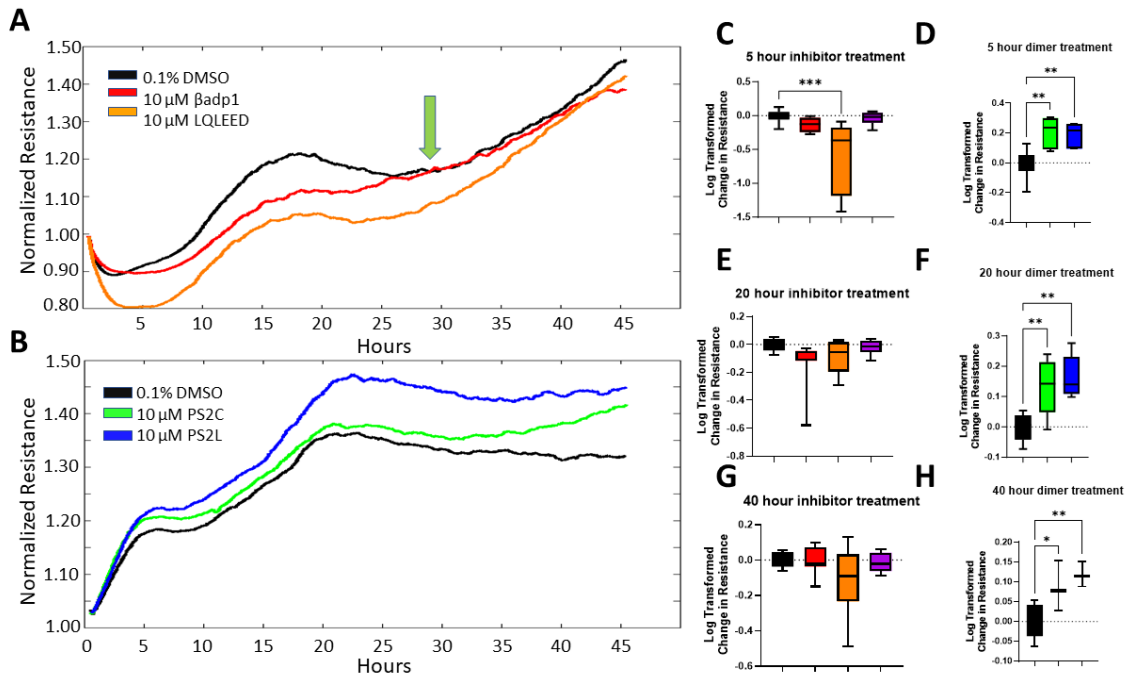


**Figure 3.  $\beta$ adp1 decreases intercellular adhesion in 1610 $\beta$ 1 cells, whereas  $\beta$ adp1-related dimeric peptides PS2C and PS2L increase adhesion. (A)** Multi-well ECIS showing effects of  $\beta$ adp1 (red) and the  $\beta$ adp1-derived peptide monomer LQLEED (orange) on intercellular adhesion as assayed by relative resistance in ECIS compared to vehicle (DMEM/F12 culture media with 0.1% DMSO) control treated (black) cells over 48 hours. Both  $\beta$ adp1 and LQLEED decrease adhesion compared to control at 5 and 20 hours of treatment. There is a shift in the curve of  $\beta$ adp1 at approximately 30 hours indicating increased adhesion is likely occurring beyond this timepoint (green arrow). As a result, at 40 hours there is no significant difference between  $\beta$ adp1 or LQLEED compared to the control. **(B)** Multi-well ECIS demonstrating effects of  $\beta$ adp1-derived dimers, PS2C (green) and PS2L (blue) on intercellular adhesion compared to vehicle control treated (black) cells over 48 hours. Both PS2C and PS2L increase relative resistance/adhesion compared to controls at 5 and 20 hours. At 40 hours, PS2L continues to significantly increase adhesion.



**Figure 3 Cont. (C-H)** Quantification of ECIS relative resistance as compared to vehicle control following treatment with 10  $\mu$ M  $\beta$ adp1 and 10  $\mu$ M LQLEED inhibitory monomers at 5 **(C)**, 20 **(E)**, and 40 **(G)** hours after treatment or PS2C and PS2L agonizing dimers at 5 **(D)**, 20 **(F)**, and 40 **(H)** hours after treatment.  $n \geq 3$  experimental replicates for each treatment, \* $p < .05$ , \*\* $p < .01$ .

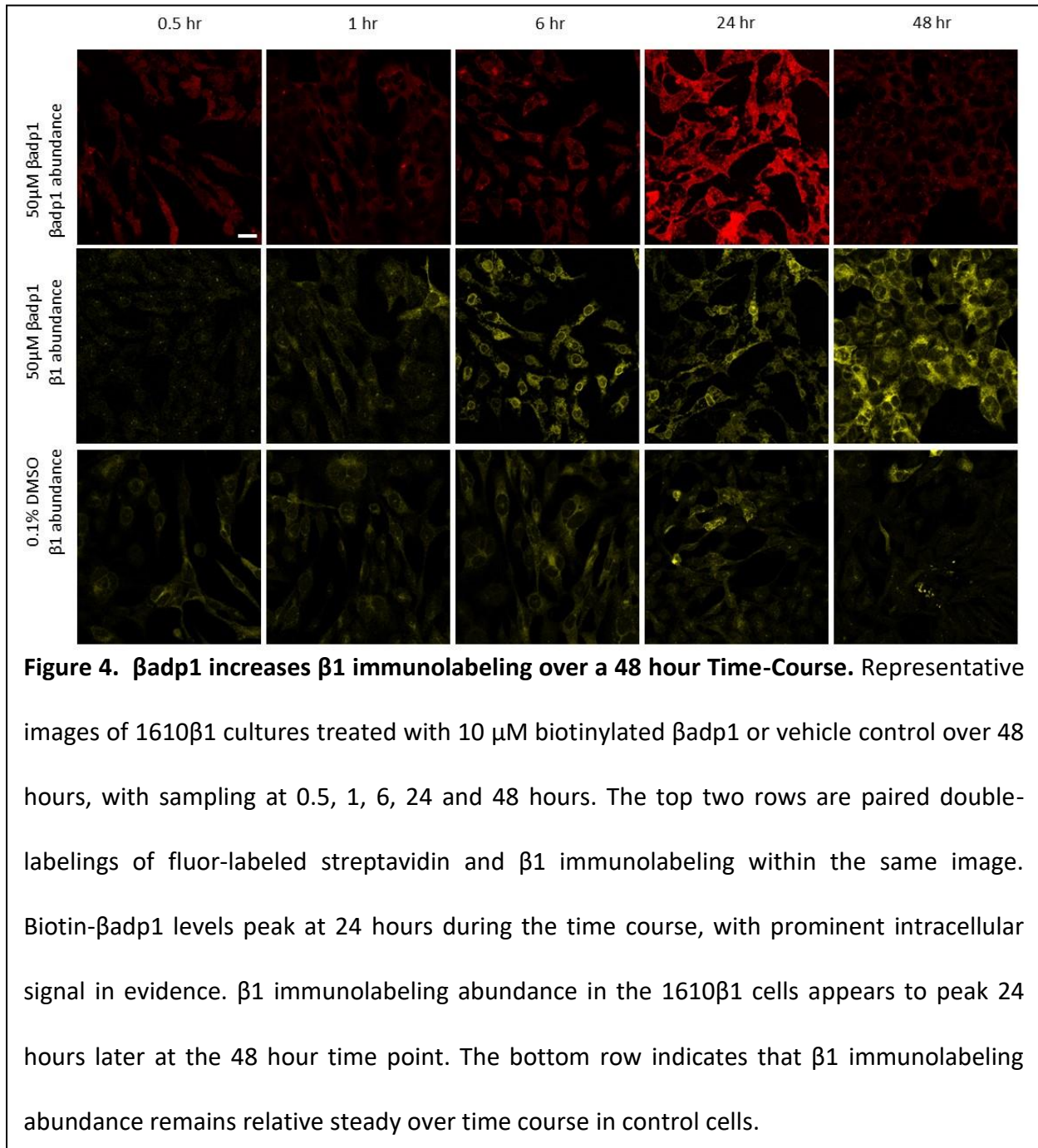
approximately 2395 and 2602 daltons, which like  $\beta$ adp1 and LQLEED falls below the 3 kD threshold for ID-penetration. Results from PS2L and PS2C will be described in detail in the following section – but to summarize in ECIS assays, resistance levels induced by these dimeric peptides in 1610 $\beta$ 1 cells were notably elevated over controls (Figs. 3B).

### **2.3. Differential Effects of Monomeric and Dimeric Mimetic Peptides Targeting $\beta$ 1 on Cell**

#### **Adhesion and $\beta$ 1 Immunolabeling over Prolonged Time-courses:**

Whilst  $\beta$ adp1 and LQLEED reduced intercellular adhesion over courses of 5 hours or less, we found differential effects of the monomers on cellular adhesion over longer times periods. Up to 20-hours, the effects of monomers on cell adhesion were similar to that at 5 hours, with decreases in resistance, compared to controls (Figure 3A, C, E). However, after 24-30 hours a shift occurred, wherein resistance appeared to increase from the lower levels induced by the peptides acutely - as indicated by the green arrow in Figure 3A. In some ECIS runs, the rise in resistance in monomer-treated cells eventually exceeded that of control cells – as shown for  $\beta$ adp1 in Figure 3A. Whilst this increase did not always go above control levels, it was sufficient on average that by 40 hours post-treatment, effects of  $\beta$ adp1 and LQLEED on cellular resistance were no longer significantly below those of controls (Compare Figs. 3C and 3G). We performed similar long-term ECIS assays on the PS2L and PS2C dimeric peptides. Paradoxically with respect to the

monomeric peptides, linear PS2L and cyclized PS2C dimers both significantly increased



resistance in 1610 $\beta$ 1 cells (Figs. 3D, F and H). The agonistic effects of the dimers were notably more potent than those elicited by the monomers, reaching both higher levels of significance and persisting over the entire 40 hour time course of the experiment.

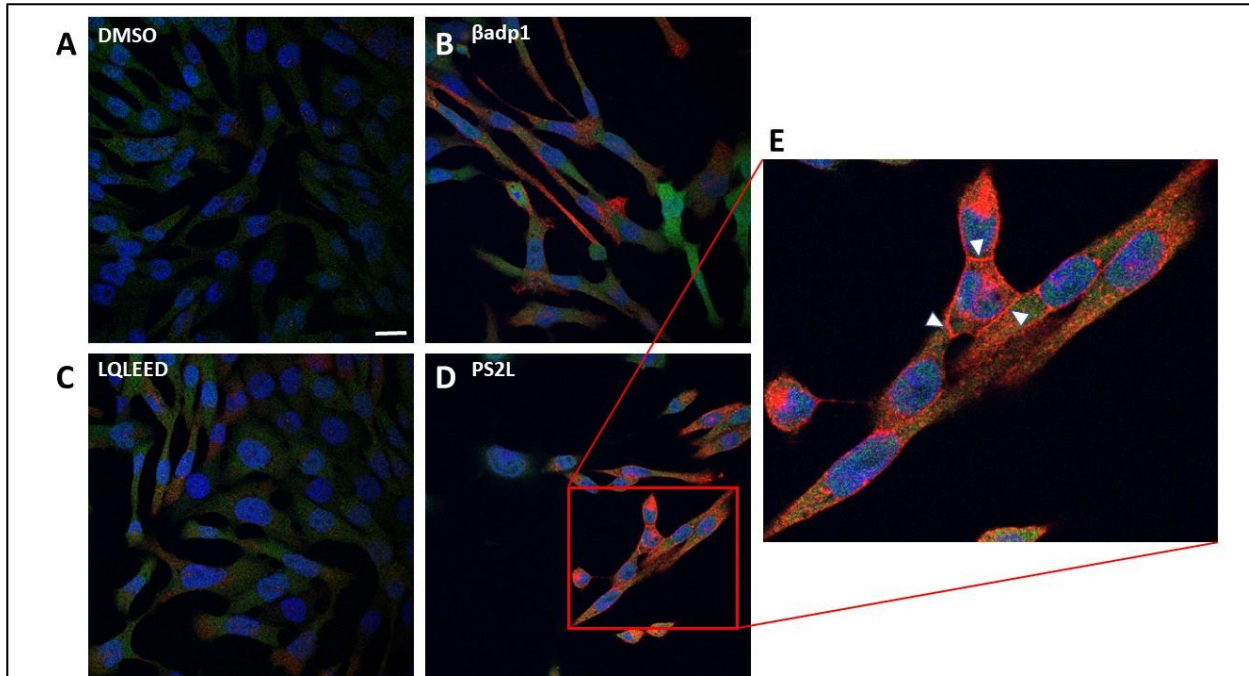


**Figure 5.  $\beta$ adp1 and  $\beta$ adp1-derived monomeric and dimeric peptides increase  $\beta$ 1 immunolabeling at 48 hours of treatment.** 1610 $\beta$ 1 cells treated for 48 hours with vehicle control solution (**A**) or 10  $\mu$ M  $\beta$ adp1 (**B**) or the  $\beta$ adp1-derived peptides LQLEED at 10  $\mu$ M (**C**) or PS2L at 10  $\mu$ M (**D**). Each peptide shows an increase in  $\beta$ 1 immunolabeling abundance (red) compared to vehicle control cells at 48 hours. (**E**) Magnified view of indicated portion of PS2L-treated cells. PS2L increased overall  $\beta$ 1 abundance in 1610 $\beta$ 1 cells, but unlike the other  $\beta$ adp1-derived peptides, it also increased the  $\beta$ 1 abundance at cell-cell borders (white arrows). Scale bar: 10  $\mu$ M.

Immunolabeling was undertaken to probe the effect of the mimetic peptides on 1610 $\beta$ 1 cells over a 48 hour time course using an antibody to the NT Ig domain of  $\beta$ 1 (Fig. 4). 1610 $\beta$ 1 cells incubated with 50  $\mu$ M Biotin- $\beta$ adp1 showed accumulation of the peptide, which peaked at around 24 hours, declining at 48 hours. Interestingly, immunolabeling for the  $\beta$ 1 protein itself indicated a steady increase in abundance in 1610 $\beta$ 1 cells in response to  $\beta$ adp1, which reached

maximal levels at 48 hours, relative to control cells (Fig. 4). Prompted by this observation we examined what effects that LQLEED and PS2L had on  $\beta$ 1 immunolabeling at 48 hours (Fig. 5A-E). As was the case for  $\beta$ adp1, in response to LQLEED  $\beta$ 1 immunolabeling in 1610 $\beta$ 1 cells appeared to be increased at 48 hours (Fig. 5C). High magnification images indicated that this increased immunolabeling was cell-wide, including within the cytoplasm, with occasional evidence of increased intensity of immunolabeling at cell borders. PS2L treatment also led to cell-wide increases in  $\beta$ 1 immunolabeling at 48-hours. Interestingly, we also noted that treatment with PS2L prompted a distinct increase in signal at cell borders, relative to controls and the monomeric peptides (Fig. 5D, E). The increase in cell border localization observed with the dimeric peptide was not seen for the monomers.

#### **2.4. $\beta$ adp1 and PS2L Increase Cleavage of $\beta$ 1 via Regulated Intramembrane Proteolysis (RIP):**

$\beta$ 1 has been reported to undergo a process of sequential intramembrane proteolysis (RIP) by BACE1 and  $\gamma$ -secretase (Bouza et al., 2021; Wong et al., 2005). RIP results in the production of a soluble intracellular domain (ICD) from the CT of full length  $\beta$ 1 that is translocated to the nucleus, with correlated effects on gene expression, including VGSC sub-units. We sought to determine if  $\beta$ 1-targeting peptides effect the RIP process in a manner that may parallel changes in  $\beta$ 1-mediated intercellular adhesion and immunolabeling. First, to confirm that  $\beta$ 1 underwent RIP in 1610 $\beta$ 1 cells, we treated cells with the  $\gamma$ -secretase inhibitor DAPT. In the presence of DAPT, together with an antibody against the CT of  $\beta$ 1, it was found that the 19 kD Carboxyl-Terminal Fragment (CTF) accumulated in Western blots from cells sampled at 6, 24 and 48 hours following initiation of treatment (Fig. 6A). Without DAPT treatment the 19 kD CTF was typically undetectable. Next, we co-treated cells with DAPT in the presence of  $\beta$ adp1 (Fig. 6). As

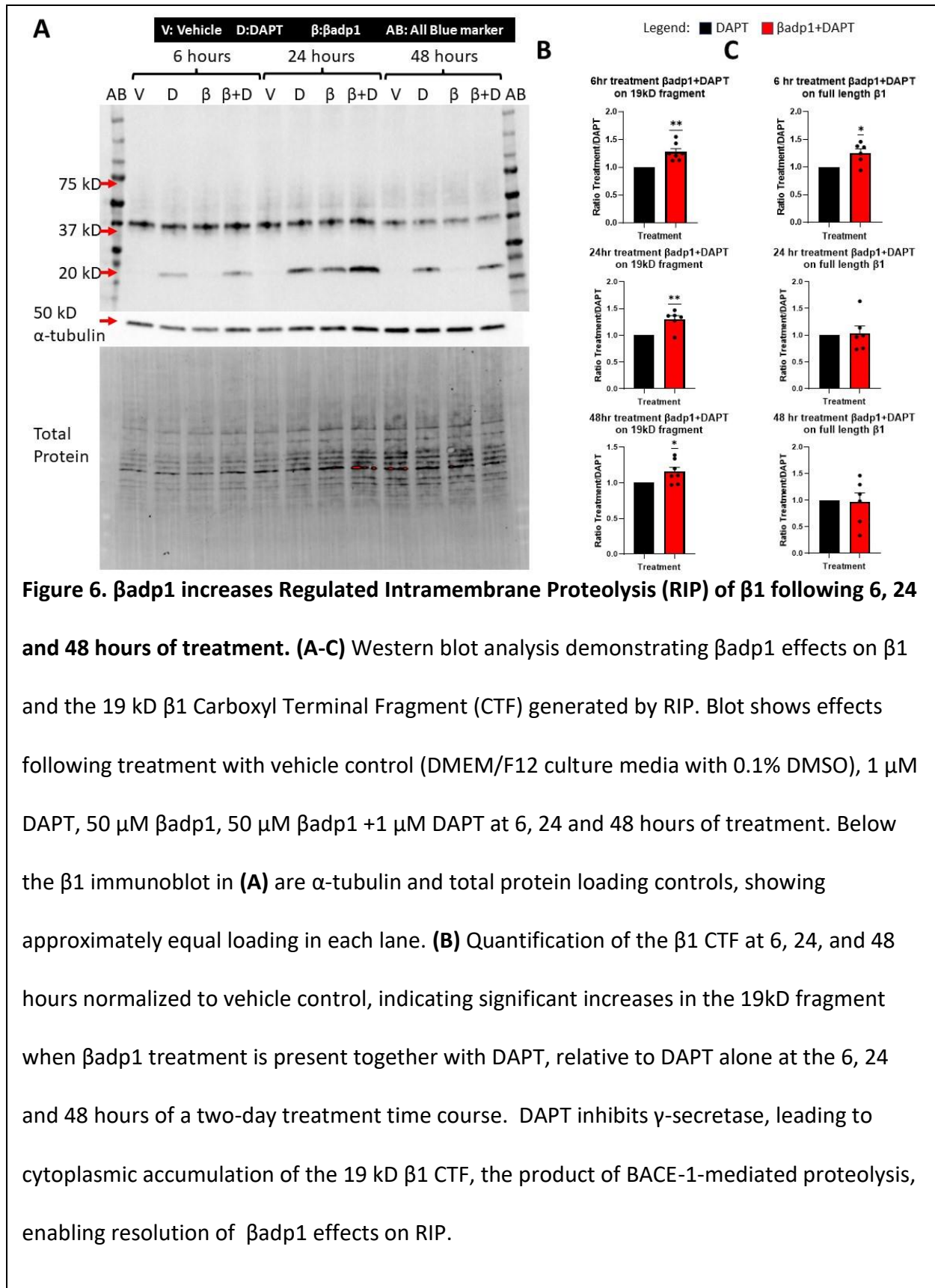


**Figure 6 Cont. (C)** Quantification of full-length  $\beta 1$  normalized to vehicle control in the presence of DAPT or  $\beta adp1$  plus DAPT over the same time course. There is a significant increase in full-length  $\beta 1$  6 hours after co-treatment with  $\beta adp1$  and DAPT, but no significant difference in levels of  $\beta 1$  persist at 24- and 48-hours.  $n \geq 3$  experimental replicates for each treatment, \* $p < .05$ , \*\* $p < .01$ .

expected, all treatments that included DAPT resulted in increased levels of the CTF (Fig. 6A). However, compared to DAPT alone,  $\beta adp1 + DAPT$  significantly increased CTF levels at 6, 24, and 48 hours post treatment (Fig. 6B). Cells treated with a control peptide showed no similar increase in the 19 kD CTF (Supplemental Fig 3). We noted that  $\beta adp1$  alone increased the 19 kD fragment at 24 hours of treatment relative to control levels on occasion (Fig. 6A). However, this was not consistent between experiments and we did not analyze this sporadic effect further. The abundance of the full length  $\beta 1$  (37 kD band) was elevated at 6 hours post-treatment by  $\beta adp1$  in DAPT co-treatments (Fig. 6C), but other than this modest effect, the 37 kD band showed no consistent variation by treatment or time-point on Western blots.

PS2L+DAPT also significantly increased the CTF of  $\beta 1$  at 6 hours post treatment compared to DAPT alone, though not at 24 and 48 hours (Fig. 7). PS2L alone did not appear to have a consistent effect on CTF levels. In response to combinatorial DAPT and PS2L treatments, full length  $\beta 1$  showed no change at the 6 and 24 hour time points, though at 48 hours Western blots revealed a significant reduction of the 37 kD band relative to controls.

To explore whether inhibiting  $\beta 1$  RIP may disrupt the longer term gain-of-function effect of  $\beta adp1$  on intercellular adhesion in 1610 $\beta 1$  cells, we repeated ECIS experiments with  $\beta adp1$

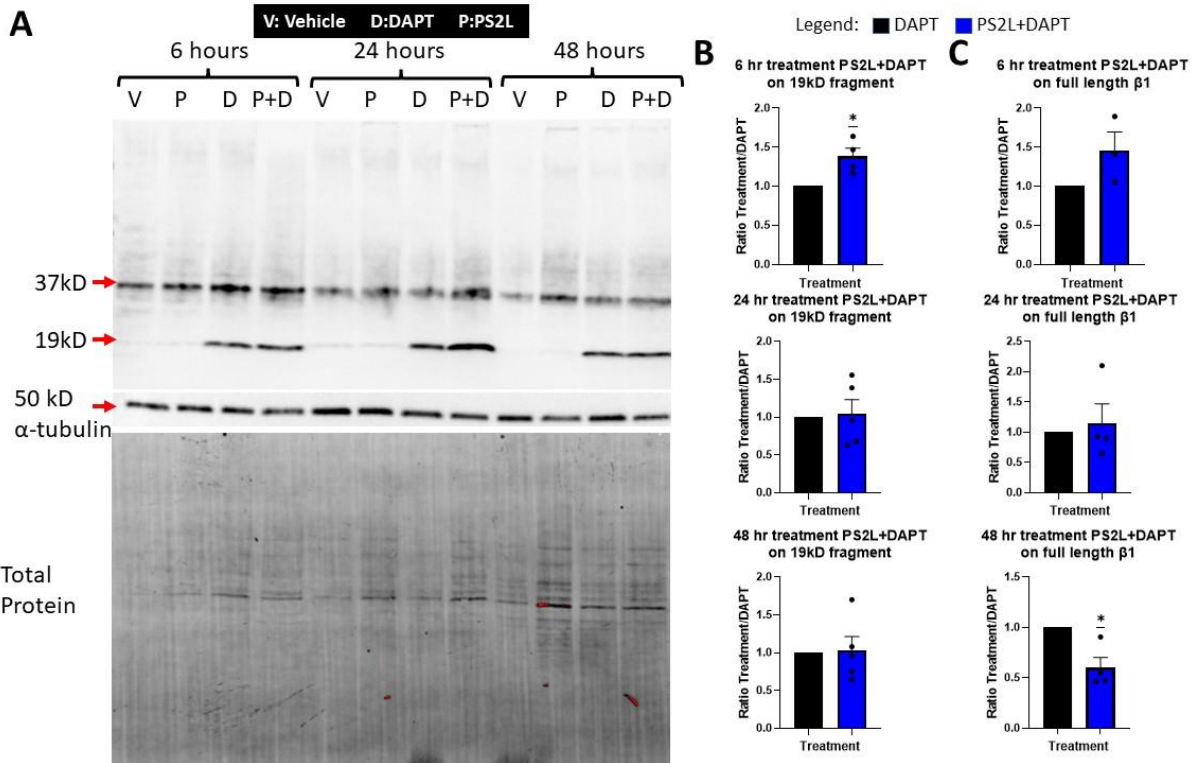
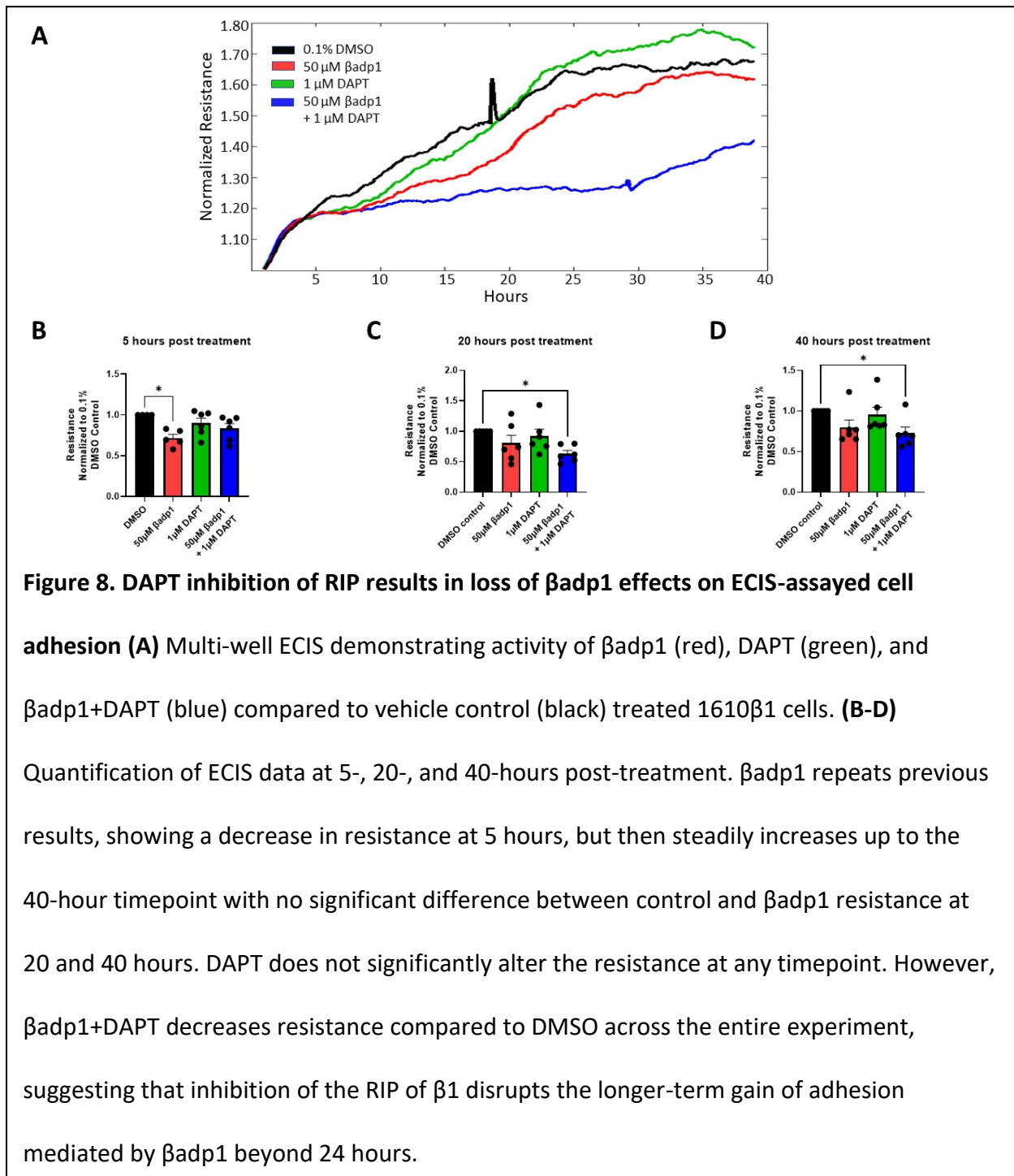


**Figure 7. The PS2L dimer acutely increases the RIP of  $\beta 1$ , but not subsequently. (A-C)**

Western blot analysis showing effects on full-length  $\beta 1$  and the  $\beta 1$  CTF of treatment with vehicle control (DMEM/F12 with 0.1% DMSO), 1  $\mu$ M DAPT, 50  $\mu$ M PS2L, 50  $\mu$ M PS2L +1  $\mu$ M DAPT for 6, 24 and 48 hours. Below the  $\beta 1$  immunoblots in (A) are  $\alpha$ -tubulin and total protein controls, showing approximately equal loading in each lane. (B) Quantification of the  $\beta 1$  CTF at 6, 24, and 48 hours normalized to vehicle control, indicates a significant increase in the 19kD fragment occurs at the 6 hour time-point of a two-day treatment time course in response PS2L treatment in the presence of DAPT, but not at 24 and . (C) Quantification of full-length  $\beta 1$  normalized to vehicle control in the presence of DAPT or PS2L plus DAPT over the same time course. There is a significant decrease in full-length  $\beta 1$  following 48 hours of co-treatment with  $\beta$ adp1 and DAPT.  $n \geq 3$  experimental replicates for each treatment, \* $p < .05$ , \*\* $p < .01$ .



treatment over 48 hours, including a  $\beta$ adp1 + DAPT treatment (Fig. 8C). We found that a co-treatment of  $\beta$ adp1 and DAPT resulted in prolongation of the inhibitory effect, with relative resistance significantly decreased across the entire length of the experiment (Fig. 8D-F). These



results would be consistent with contribution of RIP to the longer term gain-of-function effect on intercellular adhesion observed with treatment with  $\beta$ adp1 over periods of greater than 24 hours.

### **3. DISCUSSION**

In the present study, the effects of targeting VGSC  $\beta 1$  with amino acid sequences mimicking its extracellular immunoglobulin (Ig) domain were investigated. A short sequence (LQLEED) was characterized at the C-terminus of  $\beta adp1$  - a previously reported 19 amino acid mimetic of the SCN1B Ig domain (Veeraraghavan et al., 2018). LQLEED inhibited cell-to-cell adhesion in 1610  $\beta 1$ -expressing cells in a manner comparable to  $\beta adp1$ . Dimeric peptides incorporating repeats of LQLEED were found to demonstrate agonist-like activity, paradoxically increasing adhesion in 1610  $\beta 1$  monolayers in contrast to the inhibitory effects of monomeric peptides. New insights into the activity of SCN1B mimetic peptides over time courses longer than previously reported were provided, including that: 1) The  $\beta adp1$  monomer reduced peak sodium current at intercellular contacts between cardiomyocytes, associated with reductions in  $\beta 1/\beta 1B$  immunolabeling at these junctional regions; 2) The inhibitory effects of monomeric  $\beta adp1$  and LQLEED on cell adhesion in 1610  $\beta 1$  expressing monolayers was biphasic, being sustained for time courses of up to 5 hours, but thereafter blunted; 3) Conversely, the adhesion-promoting effects of dimeric peptides were maintained over 48 hours; 4) The biphasic time course of  $\beta adp1$  on cell adhesion in 1610  $\beta 1$ -expressing cells was correlated with increased levels of a C-terminal fragment (CTF) of  $\beta 1$  – a known intermediate product of the regulated intramembrane proteolysis (RIP) of  $\beta 1$  (Bouza et al., 2021; Wong et al., 2005) and that 5) The second phase of the biphasic effect of  $\beta adp1$  appeared to be prevented by co-treatment with DAPT - an inhibitor of  $\gamma$ -secretase a peptidase involved in the final step of  $\beta 1$  RIP (Bouza et al., 2021; Wong et al., 2005). In sum, our results suggest pathways to pharmacological development of

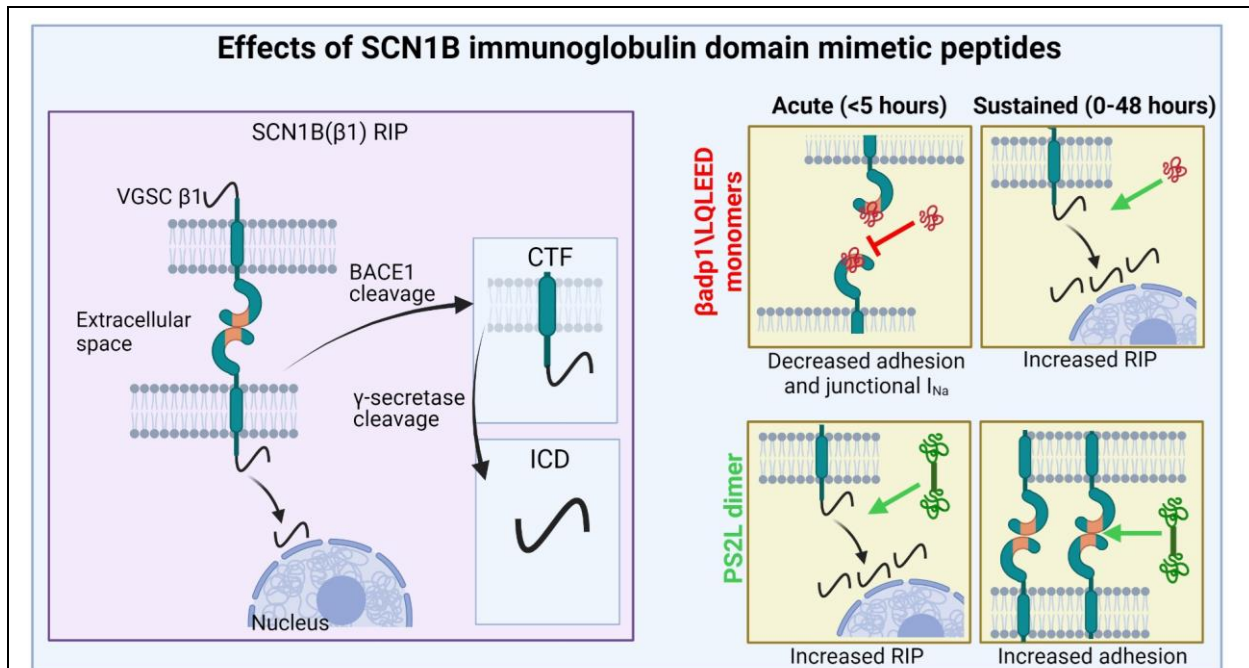


**Figure 9. Model for Effects of SCN1B (β1/β1B) immunoglobulin domain mimetic peptides.**

The left panel illustrates the adhesion function and regulated intramembrane proteolysis (RIP) of SCN1B (β1). Full length β1 is 37kD and is first cleaved by BACE1. This releases the extracellular domain of β1 containing the Ig domain responsible for cell adhesion, resulting in a 19kD fragment simply called the c-terminal fragment (CTF), which is still located in the membrane and is made up of the transmembrane and intracellular portions of β1. The CTF is sequentially cleaved by γ-secretase. This results in the intracellular domain (ICD) being released. The ICD is the final cleavage product and translocates to the nucleus, resulting in transcriptional changes. The 4 yellow panels to the right illustrate the effects of the βadp1/LQLEED monomers and the PS2L dimer on adhesion and RIP during acute and sustained treatments. βadp1/LQLEED decrease adhesion and junctional I<sub>Na</sub> acutely while increasing RIP over sustained treatment. PS2L increases RIP on an acute level and increases adhesion over the sustained treatment timecourses. Figure created with BioRender.com.

agonists and antagonists targeting the main beta subunit (i.e., SCN1B) of the principle sodium channel found in the mammalian ventricle (Brackenbury and Isom, 2011; Isom et al., 1992), as well as complexities in the response of  $\beta$ 1-expressing cells to such pro-drugs. Figure 9 illustrates and summarizes our findings.

When designing the peptides derived from the initial  $\beta$ adp1 sequence, we ensured biologically relevant residues were included. A human population study of SCN1B mutants found an R85H variant in a patient with atrial fibrillation (Watanabe et al., 2009). When the mutant  $\beta$ 1 subunit was expressed in Chinese hamster ovary cells, sodium current via Nav1.5 was reduced (Watanabe et al., 2009). Interestingly, this mutation is also associated with epilepsy (Patino et al., 2011; Scheffer et al., 2007). The full  $\beta$ adp1 sequence is derived from residues 67-86 of  $\beta$ 1, which includes amino acid R85. Another mutation one residue removed from the  $\beta$ adp1 sequence, E87Q, has been associated with Brugada syndrome (Watanabe et al., 2008). Thus, combined with our *in silico* modeling and experimental ECIS results (Supplemental Fig. 2) we focused on the carboxyl-terminus (CT) of  $\beta$ adp1 when developing short dimeric and monomeric mimetic sequences of the  $\beta$ 1/ $\beta$ 1B Ig domain. Interestingly, the control peptide  $\beta$ adp1-R85D, does not appear to cause significant changes in accumulation of the CTF compared to DMSO, unlike  $\beta$ adp1 – again reinforcing the concept that bioactivity resides in the CT region of the sequence (Supplemental Fig. 3).

Although the focus is on  $\beta$ 1 in this study, there is an alternatively spliced variant of SCN1B named  $\beta$ 1B.  $\beta$ 1B is formed by retention of an intron that results in a novel CT that lacks the transmembrane domain of  $\beta$ 1 (Kazen-Gillespie et al., 2000; Qin et al., 2003). Thus,  $\beta$ 1B is not thought to be anchored in the cell membrane and is widely held to be secreted, except in one

report where  $\beta 1B$  was found to be retained in the cell membrane when co-expressed with  $Nav1.5$  in HEK cells (Patino et al., 2011). Since  $\beta 1B$  is exclusively retained at the membrane in the presence of  $Nav1.5$ , the predominant cardiac VGSC isoform, this suggests a unique role for  $\beta 1B$  in the heart, including potential to act as an adhesive substrate. Although  $\beta 1B$  differs at the CT from  $\beta 1$ , it does contain the same Ig domain that appears to be necessary for adhesive interactions mediated by the canonical (i.e. the non-alternatively transcribed)  $\beta 1$  isoform. This leads to the question of whether  $\beta adp1$  could mimic a natural function of  $\beta 1B$  in regulating  $\beta 1$ -mediated cell adhesion, as well as modulating  $\beta 1$  RIP, since  $\beta adp1$  is a sequence common to both  $\beta 1B$  and  $\beta 1$ . Interestingly,  $\beta 1B$  loss of function mutations are implicated in various cardiac and neural pathologies (Baroni and Moran, 2015), including Long QT-Syndrome (Giudicessi and Ackerman, 2013), epilepsy (Wallace et al., 2002; Wallace et al., 1998), Dravet syndromes (Ogiwara et al., 2012; Patino et al., 2009), Brugada syndrome (Martinez-Moreno et al., 2020; Watanabe et al., 2008), and atrial fibrillation (Angsutararux et al., 2021; Watanabe et al., 2009). Importantly, the R85D and E87Q mutations near or within the  $\beta adp1$  sequence can occur in both  $\beta 1$  and  $\beta 1B$ . Further work is needed to determine the differing roles of  $\beta 1$  and  $\beta 1B$  and in regard to the SCN1B ( $\beta 1/\beta 1B$ ) peptides studied herein.

To further understand how short peptides mimicking the  $\beta 1/\beta 1B$  Ig domain prompt changes to  $\beta 1$ -mediated adhesion, we investigated effects of our peptides on RIP of  $\beta 1$ .  $\beta 1$  RIP occurs in two steps. First, BACE1 cleaves the extracellular Ig domain, leaving the 19kD CTF composed of the transmembrane and intracellular domains (Bouza et al., 2021; Wong et al., 2005). Under normal conditions, the 19kD CTF is subsequently cleaved by  $\gamma$ -secretase to produce an intracellular domain (ICD) that translocates to the nucleus and results in transcriptional

changes, including differential changes in gene expression of VGSC genes, as well as genes responsible for cell adhesion, immune response, cellular proliferation, and calcium ion binding (Bouza et al., 2021). It has been shown in MDA-MB-231 cells, a breast cancer cell line, that overexpression of full length  $\beta 1$ -GFP or ICD-GFP alone is sufficient to increase sodium currents, whereas expression of  $\beta 1$ STOP-GFP, which does not include the ICD, does not increase sodium current (Haworth et al., 2022). This indicates that the SCN1B mimetic peptides that are the focus of the present study may be capable of modulating transcriptional effects mediated by the ICD, as well as causing changes to sodium currents. Whether or not peptides such as  $\beta$ adp1 and LQLEED have this potential represents a fruitful line of inquiry for ongoing study.

Aside from  $\beta 1$ , there are multiple other substrates of similar RIP processes, including the  $\beta$ -amyloid precursor protein (APP) implicated in Alzheimer's disease and Notch. The cleavage process of APP that produces  $A\beta$  plaques involves sequential activity of  $\beta$ -secretase and  $\gamma$ -secretase. The resulting intracellular domain (AICD) also shows nuclear signaling activity, including effects such as endogenous defense against Alzheimer's disease (Liu et al., 2021) and regulating neurogenesis (Shu et al., 2015). Notch is a transmembrane protein that is sequentially cleaved by ADAM10 then  $\gamma$ -secretase once it is in the membrane (van Tetering and Vooijs, 2011). Comprehending the much larger body of work surrounding RIP of both APP and Notch, as well as other voltage gated ion channel subunits and cell adhesion molecules, appears to offer the prospect of further progress on understanding the  $\beta 1$  RIP process and targeting it for therapeutic purposes (Hodges et al., 2022).

One potential downstream method by which increasing  $\beta 1$  RIP results in increases in cellular adhesion as seen in our various ECIS assays, may be via increased abundance of the  $\beta 1$  subunit

itself. The literature has not shown whether the  $\beta 1$  ICD affects levels of VGSC  $\beta$  subunit transcription, but it does upregulate VGSC  $\alpha$  subunit transcription (Bouza et al., 2021; Wong et al., 2005). Localization of  $\alpha$  and  $\beta$  subunits are closely related, with  $\beta$  subunits usually found in regions of high  $\alpha$  subunit density (O'Malley and Isom, 2015). Our immunofluorescent data also indicates an increase in  $\beta 1$  abundance in the 1610 $\beta 1$  cells after treatment with SCN1B ( $\beta 1/\beta 1B$ ) mimetic peptides. Previously, we have shown that  $\beta 1$  is important in maintaining inter-membrane adhesion at the perinexus, a specialized nanodomain directly adjacent to gap junctions in the intercalated disc that is the proposed region where ephaptic coupling takes place in cardiac tissues (Veeraraghavan et al., 2018). Knockout of the  $\beta 1$  protein in mice is fatal by postnatal day 21 (Chen et al., 2004) and disrupting  $\beta 1$  trans-adhesion in the perinexus *ex vivo* results in loss of GJ-associated VGSCs, conduction slowing and arrhythmias (Veeraraghavan et al., 2018). By instead increasing the levels of  $\beta 1$ , these rationally designed peptides may thus have antiarrhythmic treatment or prevention abilities, albeit that our present data suggests that there may be acute pro-arrhythmic effects of such approach to therapy. Ongoing studies may well address the latter issue, but until such time it is probably best that assessments of the potential long-term clinical benefits of such strategies be taken with caution.

One question raised by our studies, and by others, is whether or not RIP of  $\beta 1$  takes place at the cell membrane or subcellularly. Our immunofluorescent data indicates that  $\beta 1$  heterologously expressed in 1610 cells is mainly cytoplasmic. This observation is similar to those made by others in the MDA-MB-231  $\beta 1$  expressing cells (Haworth et al., 2022) and Madin-Darby canine kidney cells (Dulsat et al., 2017). In the MDA-MB-231 cells  $\beta 1$  has been shown to colocalize with the endoplasmic reticulum, the endolysosomal pathway and the nucleus (Haworth et al., 2022).

From our immunofluorescence experiments we find that there is a significant uptake of  $\beta$ adp1 into the cells at 24 hours post-treatment. The greatest increase in  $\beta$ 1 abundance occurs at 48 hours post-treatment, which aligns with the increase we see in resistance in ECIS. There is little difference in  $\beta$ 1 levels between DMSO and  $\beta$ adp1-treated cells up to this point. We also see the greatest increase of CTF with  $\beta$ adp1+DAPT at 24 hours post-treatment, corresponding to the timing of maximal uptake of the peptide by cells. This suggests that the internalization of the peptide is important in causing the observed increase in RIP. Thus, the literature, together with data presented here, suggests that a considerable fraction of  $\beta$ 1 RIP may occur intracellularly, so  $\beta$ adp1 may affect the process to a greater extent once it has been taken up by the cells. This indicates potential for delivery systems such as small extracellular vesicles loaded with SCN1B ( $\beta$ 1/ $\beta$ 1B) mimetic peptides that can be directly delivered inside the cells. Previous work has shown potential for drug delivery with bovine milk derived extracellular vesicles, and our lab has optimized a protocol for isolating large quantities of small extracellular vesicles to allow for loading and treatment of the vesicles (Marsh et al., 2021; Munagala et al., 2016; Pieters et al., 2022). This being said, evidence remains that the majority of  $\beta$ 1 RIP can and does occur at the plasma membrane (Bouza et al., 2020; Haworth et al., 2022).  $\beta$ 1 is S-palmitoylated, and when palmitoylation is inhibited by a C162A mutation in  $\beta$ 1, this results in decreased  $\beta$ 1 in the plasma membrane and decreased RIP (Bouza et al., 2020). Therefore, ongoing work is needed to establish the location of  $\beta$ 1 RIP in different biological settings, both in health and disease and to compare efficacy of extracellular versus intracellular delivery systems for peptides targeting SCN1B.



We have previously hypothesized the function of  $\beta 1$  in the perinexus is to regulate intermembrane spacing via trans-adhesion and our peptides were initially designed with perinexal trans-interaction in mind (Veeraraghavan et al., 2018). While the initial and late effects of the  $\beta adp1$  monomer may be respectively explained by an acute disruption of trans-adhesion among  $\beta$  subunits, and possibly a subsequent increase in SCN1B level via downstream effects on RIP, the basis for the sustained increase in resistance (and thus intercellular adhesion) in ECIS after treatment with dimeric PS2L awaits mechanistic explanation. Other groups have demonstrated that dimer mimetics of adhesion molecules result in increased adhesion, namely in desmoglein-2 and N-cadherin (Schlipp et al., 2014; Williams et al., 2002). However, if PS2L increased adhesion by facilitating trans-adhesion among  $\beta 1$  subunits, this would be at odds with how the increased RIP of  $\beta 1$  is triggered by both  $\beta adp1$  and PS2L, with one inhibiting and one facilitating trans-adhesion. Therefore, more work is required to determine how PS2L facilitates adhesion while simultaneously increasing the rate of  $\beta 1$  RIP at early timepoints.

In summary, we show that  $\beta 1$  mimetic peptides increase the amount of regulated intramembrane proteolysis that  $\beta 1$  undergoes in 1610 $\beta 1$  cells. Although we do not provide evidence that the  $\beta 1$  mimetics studied herein directly affect transcription of  $\beta$  subunits of VGSCs, we see evidence that  $\beta 1$  abundance is increased in treated cells and previous work has shown changes to VGSC  $\alpha$  subunit transcription in response to  $\beta 1$  ICD increase (Bouza et al., 2021). We also as yet have no direct evidence that increased resistance in ECIS corresponds to decreased perinexal width and changes to heart rhythm, so these are next steps. To conclude, we have identified novel SCN1B ( $\beta 1/\beta 1B$ ) mimetic peptides with potential to inhibit or promote

intercellular  $\beta$ 1-mediated adhesion, possibly including by effects on  $\beta$ 1 RIP, suggesting paths to development of anti-arrhythmic drugs targeting the perinexus.

## **4. MATERIALS AND METHODS**

### **4.1. Peptide synthesis**

Peptides used in the study are summarized in Table 1. Peptides were synthesized by and obtained from LifeTein (Somerset, NJ) modified by N-terminal acetylation, C-terminal amidation, and TFA removal. Peptides were solubilized in DMSO to the concentration shown by experiment, ranging from 10  $\mu$ M-100  $\mu$ M.

### **4.2. Neonatal rat ventricular myocyte (NRVM) isolation**

NRVM isolation was performed as previously described (Veeraraghavan et al., 2018). NRVM isolation procedures conformed to the UK Animal Scientific Procedures Act 1986. In brief, isolated ventricles were taken from one-day-old rat pups anesthetized with a lethal dose of isoflurane. The ventricles were sectioned into small cubes and processed using mechanical dissociation (gentleMACS) and enzymatic degradation (neonatal heart dissection kit; Miltenyi Biotec, Bergisch Gladbach, Germany). The cell suspension was then filtered and the cells were plated onto glass-bottom dishes (MatTek Corp., Ashland, MA) in M199 media supplemented with newborn calf serum (10%), vitamin B12, glutamate and penicillin/streptomycin (1%). Myocytes were allowed to grow and establish connections for 3–4 days *in vitro*. Peptide treatments were applied to cell monolayers the specified amount of time (Fig. 1) prior to  $I_{Na}$  measurements.

### **4.3. Scanning ion conductance microscopy (SICM) guided smart patch clamp**

A type of SICM, called hopping probe ion conductance microscopy, was combined with cell-attached recordings of cardiac sodium channels from NRVM monolayers, as previously described (Veeraraghavan et al., 2018), to assess  $I_{Na}$  at cell-to-cell contact sites. Currents were recorded in cell-attached mode using an Axopatch 200A/B patch-clamp amplifier (Molecular Devices, Sunnyvale, CA), and digitized using a Digidata 1200B data acquisition system and pClamp 10 software (Axon Instruments; Molecular Devices, Sunnyvale, CA). Cell-to-cell junctional sites were identified using a sharp scanning nano-probe (40–50 M $\Omega$ ), followed by controlled increase of pipette diameter (20–25 M $\Omega$ ) for capture of active sodium channel clusters. The external solution contained (in mM): KCl 145, Glucose 10, HEPES 10, EGTA 2, MgCl<sub>2</sub> 1, and, CaCl<sub>2</sub> 1 (300 mOsm and pH 7.4). The internal (pipette) solution contained (in mM) NaCl 135, TEA-Cl 20, CsCl 10, 4AP 10, Glucose 5.5, KCl 5.4, HEPES 5, MgCl<sub>2</sub> 1, CaCl<sub>2</sub> 1, NaH<sub>2</sub>PO<sub>4</sub> 0.4 and CdCl<sub>2</sub> 0.2 (pH 7.4). The voltage-clamp protocol was made up of sweeps testing potentials from –70 to +30 mV from a holding potential of –120 mV.

#### **4.4. Molecular modeling**

Molecular modeling was used as described previously to simulate the docking of  $\beta$ adp1 and LQLEED with the homology model of  $\beta$ 1 using Maestro (Maestro, Schrödinger, LLC, New York, NY) (Veeraraghavan et al., 2018).

#### **4.5. Whole-cell $I_{Na}$ recordings in NRVMs**

Whole cell sodium current recordings were collected as previously described (Veeraraghavan et al., 2018). Whole-cell  $I_{Na}$  was recorded from NRVMs in low-sodium extracellular solution containing the following (in mM): CsCl 130, NaCl 11, Glucose 10, HEPES 10, MgCl<sub>2</sub> 2, CaCl<sub>2</sub> 0.5,

CdCl<sub>2</sub> 0.3, adjusted to 7.4 with CsOH. The intracellular (pipette) solution contained (in mM): Cesium methanesulfonate (CsMeS) 100, CsCl 40, HEPES 10, EGTA 5, MgATP 5, MgCl<sub>2</sub> 0.75, adjusted to pH 7.3 with CsOH. Pipettes were pulled from the borosilicate glass microelectrodes and had a resistance of 3–4 MΩ. Sweeps were initiated from the holding potential of –100 mV to test potentials ranging from –75 to + 20 mV in 5 mV increments. Peak current was measured between –30 and –40 mV. Whole cell capacitance ranged between 9 and 16 pF. Current density (in pA/pF) was calculated as the ratio of the peak current to cell capacitance.

#### **4.6. Heterologous expression of β1 in 1610 cells**

We have previously described how Chinese hamster lung 1610 cells have been used as a heterologous expression system (Veeraraghavan et al., 2018). These cells were used to measure SCN1B/β1 mediated adhesion and the regulated intramembrane proteolysis of SCN1B/β1 and they do not endogenously express SCN1B/β1 (Isom et al., 1995b).

#### **4.7. Electric cell-substrate impedance sensing (ECIS)**

Resistance of adherent monolayers of 1610 cells expressing SCN1B/β1 was measured using an ECIS Zθ system (Applied Biophysics) over the entire range possible, (62.5-64000 Hz). For analysis, we used the resistance calculated from the 4000 Hz measurement as previously shown (Veeraraghavan et al., 2018). Cells were plated on 8-well dishes (8W10E+, 40 electrodes per well, Applied Biophysics) at a concentration of 500,000cells/mL, 300 μL per well. Impedance was measured continuously over the treatment time courses, and resistance is calculated as the real component of impedance.

#### **4.8. Fluorescent Immunolabeling**

Fluorescent immunolabeling was performed on adherent monolayers of 1610 cells expressing SCN1B/ $\beta$ 1 fixed with 4% paraformaldehyde for 10 minutes. Samples were labeled with a rabbit polyclonal antibody against an amino-terminal region of  $\beta$ 1 (Epitope: <sub>44</sub>KRRSETTAETFTIEWTFR<sub>60</sub>). We have previously published validation results for this antibody (Veeraraghavan et al., 2018). Samples were then labeled with goat anti-rabbit AlexaFluor 568 (1:2000, ThermoFisher Scientific) secondary antibodies for confocal microscopy. Nuclei were stained with Hoescht 33342 for 10 minutes (1:30,000, Invitrogen).

#### **4.9. Confocal microscopy**

Confocal microscopy was done with a TCS SP8 laser scanning confocal microscope equipped with a Plan Aplanachromat 63x/1.4 numerical aperture oil immersion objective and a Leica HyD hybrid detector (Leica) using approach reported previously (Veeraraghavan et al., 2018). Imaging of each fluorophore was performed sequentially, and the excitation wavelength was switched at the end of each frame.

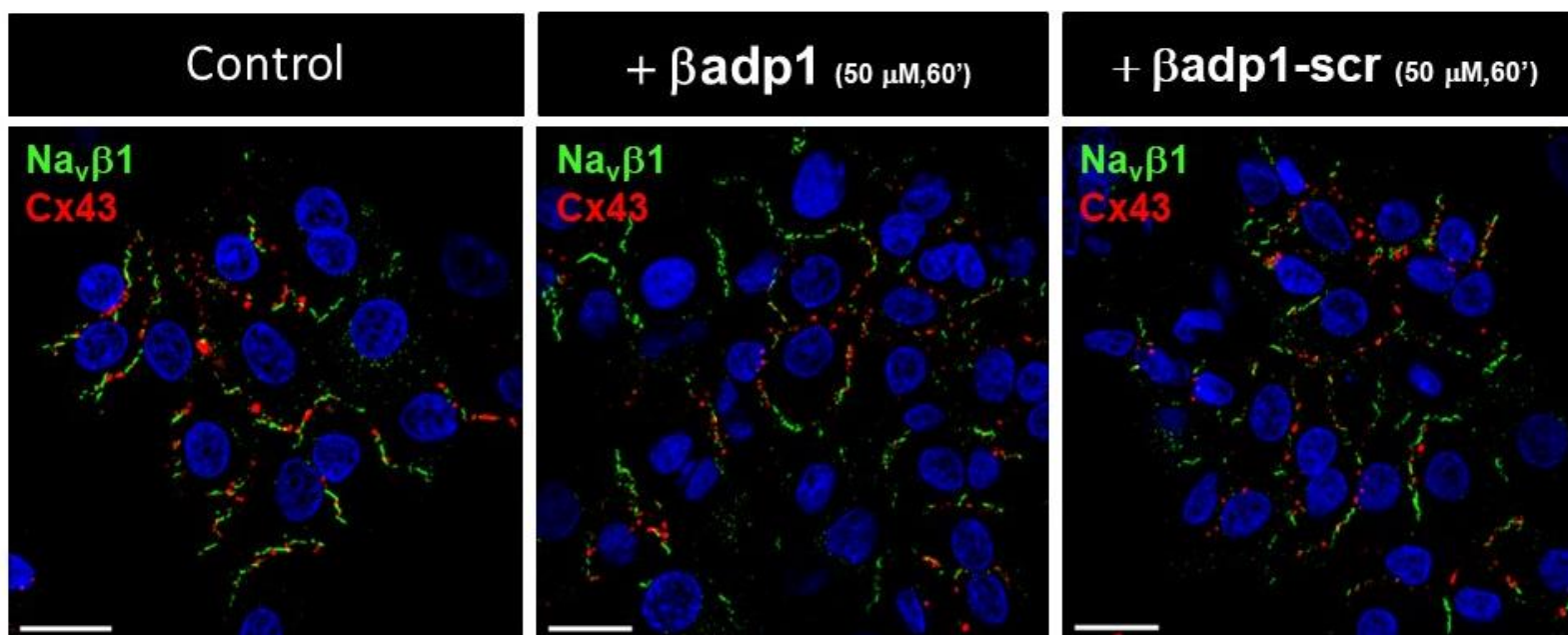
#### **4.10. Western blotting**

Whole cell lysates were collected from 1610 cells expressing SCN1B/ $\beta$ 1 using RIPA buffer on ice while being agitated on a platform rocker. Lysates were then pulled through 22 gauge and 17 gauge syringes 5 times each, vortexed, and spun for 30 minutes at 10,000g at 4°C before being snap-frozen in liquid nitrogen. Lysates were electrophoresed on 4-20% TGX Stain-free gels (BioRad) and were then transferred to polyvinylidene difluoride (PVDF) membrane using a semi-dry method with a Trans-Blot Turbo system for 7 minutes at 25V (BioRad). The membranes were probed with the rabbit polyclonal antibody against an amino-terminal region

of  $\beta 1$  (Veeraraghavan et al., 2018), or a rabbit polyclonal antibody against the carboxy-terminal of  $\beta 1$  (Cell Signaling Technology, D4Z2N) each diluted at 1:1000. These were followed by a goat anti-rabbit HRP-conjugated secondary antibody (JacksonImmuno). Signals were then detected using SuperSignal West Femto Maximum Sensitivity Substrate (ThermoFisher Scientific) and imaged with a ChemiDoc MP imager (BioRad).

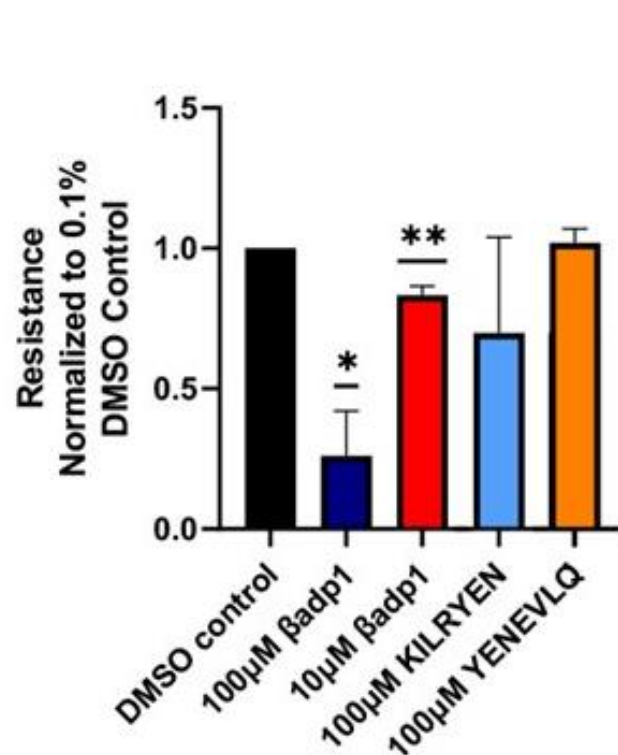
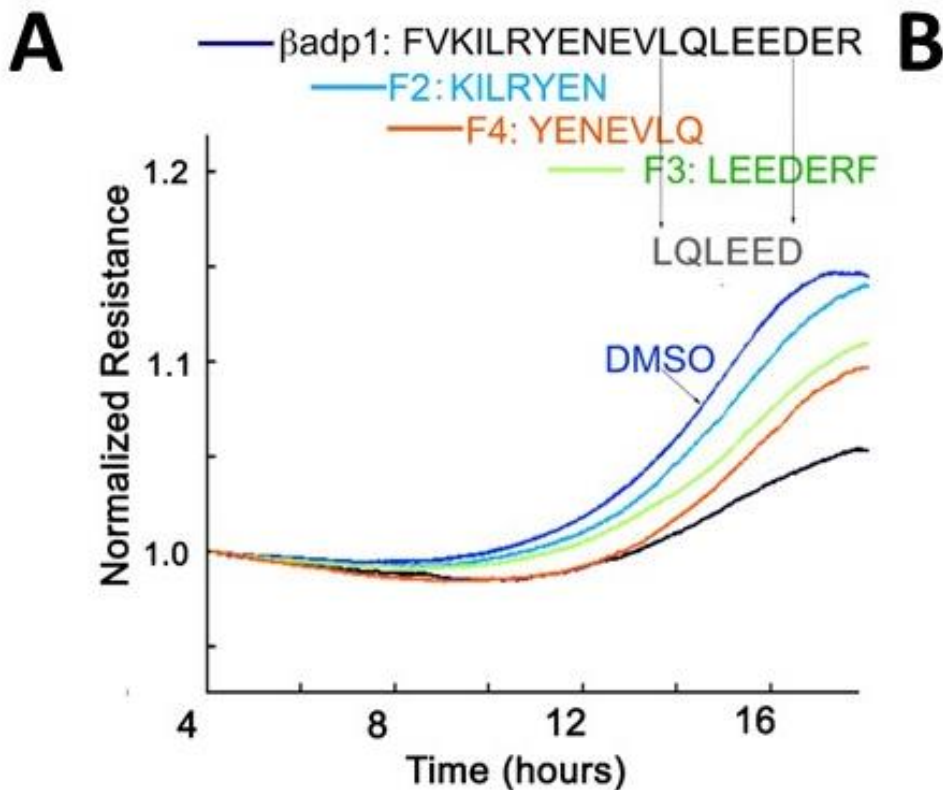
#### **4.11. Statistical analysis**

Data is presented as mean  $\pm$  SEM unless specified. Statistical analysis was performed using one-way ANOVA with Dunnett's multiple comparisons test or one-sample students t-test with a theoretical mean of 1 in the case of the Western Blot data. All statistical analysis was performed using GraphPad Prism v.10.0.2. A  $p < 0.05$  was considered statistically significant.

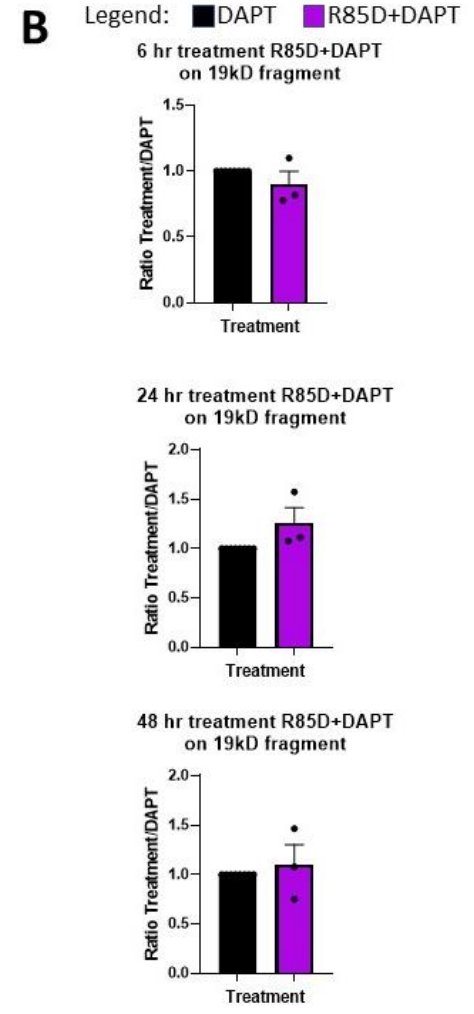
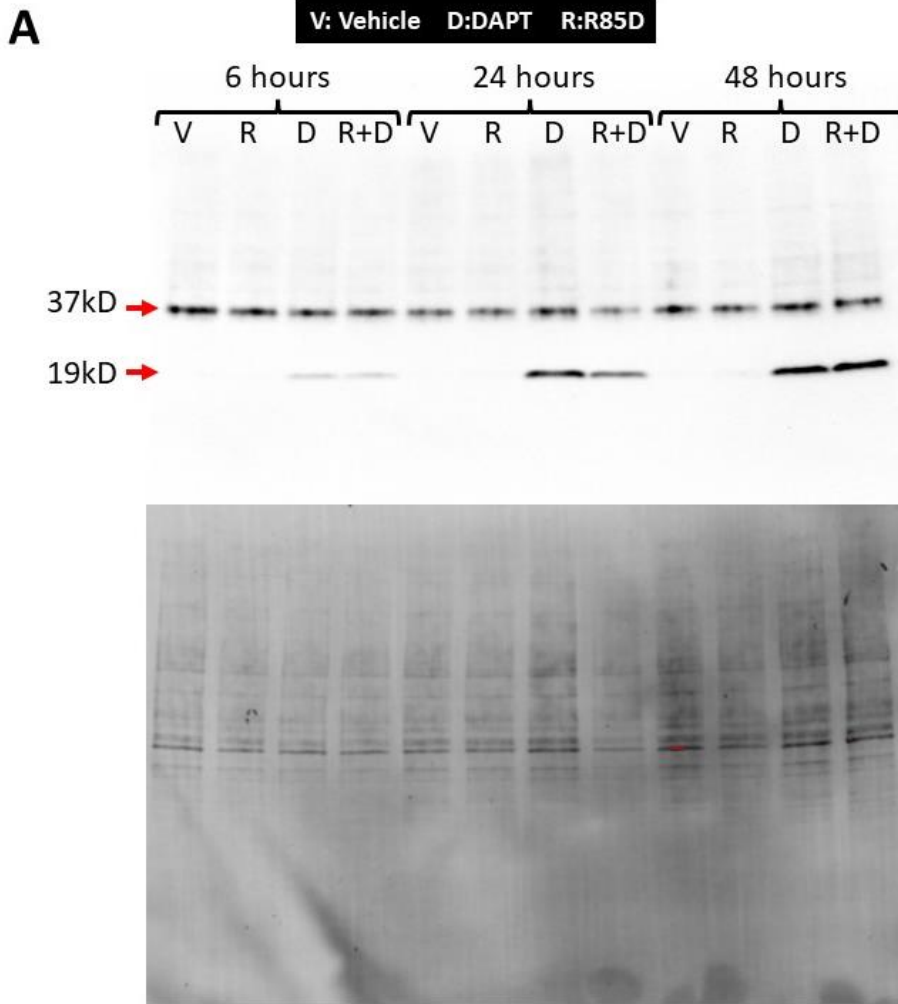


**Supplemental Figure 1. Confocal immunolabeling of NRVMs treated with scrambled control peptide for 60 minutes and immunolabeled for  $\beta$ 1 Cx43:** Representative confocal images of NRVMs immunolabeled for Cx43 (red) and  $\beta$ 1 (green) of control NRVMs or after treatment with  $\beta$ adp1 or scrambled  $\beta$ adp1 control peptide at 50  $\mu$ M for 60 minutes. Quantification of scrambled  $\beta$ adp1 control peptide is included in Fig 1. and shows no significant differences in junctional density of SCN1B ( $\beta$ 1/ $\beta$ 1B) compared to control NRVMs.





**Supplemental Figure 2. Effects of  $\beta$ adp1 and short  $\beta$ adp1-based monomeric sequences on relative resistance in 1610 $\beta$ 1 cells  $\beta$ adp1: A and B)** Multi-well ECIS demonstrating activity of  $\beta$ adp1 and short 6-8 amino acid N-terminal truncation variant peptides of  $\beta$ adp1.  $\beta$ adp1 (black) reduces normalized resistance in these cells relative to vehicle control (blue) over 20 hours. Peptides towards the carboxyl terminus of  $\beta$ adp1, especially those incorporating hydrophobic leucine residues, show the most adhesion reducing activity. Based on the ECIS time course data, and predictions from molecular modeling of likely binding in the hydrophobic pocket  $\beta$ 1/SCN1B Ig domain binding surface, the sequence LQLEED was selected as the most effective short peptide candidate drug molecule. n=3 per peptide, \*p<0.05, \*\*p<0.01.



**Supplemental Figure 3.  $\beta$ adp1 control peptide R85D shows no effects on  $\beta$ 1 RIP: A and B)**

Western blot analysis demonstrating R85D effects on the 19 kD  $\beta$ 1 CTF generated by RIP. Blot shows effects following treatment with vehicle control (DMEM/F12 culture media with 0.1% DMSO), 1  $\mu$ M DAPT, 50  $\mu$ M R85D, 50  $\mu$ M R85D +1  $\mu$ M DAPT at 6, 24 and 48 hours of treatment. Below the blot in (A) is the total protein control blot. (B) Quantification of the  $\beta$ 1 CTF at 6, 24, and 48 hours normalized to vehicle control, indicating no significant difference in the 19kD fragment when Scr1 treatment is present together with DAPT, relative to DAPT alone at the 6, 24 and 48 hours of a two-day treatment time course. n=3 experimental replicates for each treatment.

## **REFERENCES**

- (1992). Effect of the antiarrhythmic agent moricizine on survival after myocardial infarction. *N Engl J Med* 327, 227-233.
- Adams, W.P., Raisch, T.B., Zhao, Y., Davalos, R., Barrett, S., King, D.R., Bain, C.B., Colucci-Chang, K., Blair, G.A., Hanlon, A., *et al.* (2023). Extracellular Perinexal Separation Is a Principal Determinant of Cardiac Conduction. *Circ Res* 133, 658-673.
- Ajijola, O.A., Boyle, N.G., and Shivkumar, K. (2015). Detecting and monitoring arrhythmia recurrence following catheter ablation of atrial fibrillation. *Front Physiol* 6, 90.
- Angsutararux, P., Zhu, W., Voelker, T.L., and Silva, J.R. (2021). Molecular Pathology of Sodium Channel Beta-Subunit Variants. *Front Pharmacol* 12, 761275.
- Baroni, D., and Moran, O. (2015). On the multiple roles of the voltage gated sodium channel  $\beta$ 1 subunit in genetic diseases. *Front Pharmacol* 6, 108-108.
- Beneski, D.A., and Catterall, W.A. (1980). Covalent labeling of protein components of the sodium channel with a photoactivable derivative of scorpion toxin. *Proceedings of the National Academy of Sciences* 77, 639-643.
- Bouza, A.A., Edokobi, N., Hodges, S.L., Pinsky, A.M., Offord, J., Piao, L., Zhao, Y.-T., Lopatin, A.N., Lopez-Santiago, L.F., and Isom, L.L. (2021). Sodium channel  $\beta$ 1 subunits participate in regulated intramembrane proteolysis-excitation coupling. *JCI Insight* 6.
- Bouza, A.A., Philippe, J.M., Edokobi, N., Pinsky, A.M., Offord, J., Calhoun, J.D., Lopez-Florán, M., Lopez-Santiago, L.F., Jenkins, P.M., and Isom, L.L. (2020). Sodium channel  $\beta$ 1 subunits are post-translationally modified by tyrosine phosphorylation, S-palmitoylation, and regulated intramembrane proteolysis. *J Biol Chem* 295, 10380-10393.

Brackenbury, W., and Isom, L. (2011). Na<sup>+</sup> Channel  $\beta$  Subunits: Overachievers of the Ion Channel Family. *Front Pharmacol* 2.

Chen, C., Westenbroek, R.E., Xu, X., Edwards, C.A., Sorenson, D.R., Chen, Y., McEwen, D.P., O'Malley, H.A., Bharucha, V., Meadows, L.S., *et al.* (2004). Mice Lacking Sodium Channel  $\beta$ 1 Subunits Display Defects in Neuronal Excitability, Sodium Channel Expression, and Nodal Architecture. *The Journal of Neuroscience* 24, 4030-4042.

Deo, R., and Albert, C.M. (2012). Epidemiology and genetics of sudden cardiac death. *Circulation* 125, 620-637.

Deschênes, I., Armoundas, A.A., Jones, S.P., and Tomaselli, G.F. (2008). Post-transcriptional gene silencing of KCHIP2 and Navbeta1 in neonatal rat cardiac myocytes reveals a functional association between Na and Ito currents. *J Mol Cell Cardiol* 45, 336-346.

Dulsat, G., Palomeras, S., Cortada, E., Riuró, H., Brugada, R., and Vergés, M. (2017). Trafficking and localisation to the plasma membrane of Na(v) 1.5 promoted by the  $\beta$ 2 subunit is defective due to a  $\beta$ 2 mutation associated with Brugada syndrome. *Biol Cell* 109, 273-291.

Echt, D.S., Liebson, P.R., Mitchell, L.B., Peters, R.W., Obias-Manno, D., Barker, A.H., Arensberg, D., Baker, A., Friedman, L., Greene, H.L., *et al.* (1991). Mortality and Morbidity in Patients Receiving Encainide, Flecainide, or Placebo. *New England Journal of Medicine* 324, 781-788.

Garcia-Elias, A., and Benito, B. (2018). Ion Channel Disorders and Sudden Cardiac Death. *Int J Mol Sci* 19, 692.

Giudicessi, J.R., and Ackerman, M.J. (2013). Determinants of incomplete penetrance and variable expressivity in heritable cardiac arrhythmia syndromes. *Transl Res* 161, 1-14.

Hanna, P., Buch, E., Stavrakis, S., Meyer, C., Tompkins, J.D., Ardell, J.L., and Shivkumar, K. (2021). Neuroscientific therapies for atrial fibrillation. *Cardiovasc Res* 117, 1732-1745.

Haworth, A.S., Hodges, S.L., Capatina, A.L., Isom, L.L., Baumann, C.G., and Brackenbury, W.J. (2022). Subcellular dynamics and functional activity of the cleaved intracellular domain of the Na<sup>+</sup> channel  $\beta$ 1 subunit. *Journal of Biological Chemistry*, 102174.

Hoagland, D.T., Santos, W., Poelzing, S., and Gourdie, R.G. (2019). The role of the gap junction perinexus in cardiac conduction: Potential as a novel anti-arrhythmic drug target. *Prog Biophys Mol Biol* 144, 41-50.

Hodges, S.L., Bouza, A.A., and Isom, L.L. (2022). Therapeutic Potential of Targeting Regulated Intramembrane Proteolysis Mechanisms of Voltage-Gated Ion Channel Subunits and Cell Adhesion Molecules. *Pharmacol Rev* 74, 1028-1048.

Hoeker, G.S., James, C.C., Tegge, A.N., Gourdie, R.G., Smyth, J.W., and Poelzing, S. (2020). Attenuating loss of cardiac conduction during no-flow ischemia through changes in perfusate sodium and calcium. *American Journal of Physiology-Heart and Circulatory Physiology* 319, H396-H409.

Isom, L.L., De Jongh, K.S., and Catterall, W.A. (1994). Auxiliary subunits of voltage-gated ion channels. *Neuron* 12, 1183-1194.

Isom, L.L., De Jongh, K.S., Patton, D.E., Reber, B.F.X., Offord, J., Charbonneau, H., Walsh, K., Goldin, A.L., and Catterall, W.A. (1992). Primary Structure and Functional Expression of the  $\alpha$  Subunit of the Rat Brain Sodium Channel. *Science* 256, 839-842.

Isom, L.L., Ragsdale, D.S., De Jongh, K.S., Westenbroek, R.E., Reber, B.F.X., Scheuer, T., and Catterall, W.A. (1995a). Structure and function of the  $\beta 2$  subunit of brain sodium channels, a transmembrane glycoprotein with a CAM motif. *Cell* *83*, 433-442.

Isom, L.L., Scheuer, T., Brownstein, A.B., Ragsdale, D.S., Murphy, B.J., and Catterall, W.A. (1995b). Functional co-expression of the beta 1 and type IIA alpha subunits of sodium channels in a mammalian cell line. *J Biol Chem* *270*, 3306-3312.

Ivanovic, E., and Kucera, J.P. (2021). Localization of Na(+) channel clusters in narrowed perinexi of gap junctions enhances cardiac impulse transmission via ephaptic coupling: a model study. *J Physiol* *599*, 4779-4811.

Kazen-Gillespie, K.A., Ragsdale, D.S., D'Andrea, M.R., Mattei, L.N., Rogers, K.E., and Isom, L.L. (2000). Cloning, localization, and functional expression of sodium channel beta1A subunits. *J Biol Chem* *275*, 1079-1088.

Khurshid, S., Choi, S.H., Weng, L.-C., Wang, E.Y., Trinquart, L., Benjamin, E.J., Ellinor, P.T., and Lubitz, S.A. (2018). Frequency of Cardiac Rhythm Abnormalities in a Half Million Adults. *Circulation: Arrhythmia and Electrophysiology* *11*, e006273.

Kim, J.A., Khan, K., Kherallah, R., Khan, S., Kamat, I., Ulhaq, O., Marashly, Q., and Chelu, M.G. (2023). Innovations in atrial fibrillation ablation. *J Interv Card Electrophysiol* *66*, 737-756.

Lin, J., Abraham, A., George, S.A., Greer-Short, A., Blair, G.A., Moreno, A., Alber, B.R., Kay, M.W., and Poelzing, S. (2022). Ephaptic Coupling Is a Mechanism of Conduction Reserve During Reduced Gap Junction Coupling. *Frontiers in Physiology* *13*.

Liu, Y.-C., Hsu, W.-L., Ma, Y.-L., and Lee, E.H.Y. (2021). Melatonin Induction of APP Intracellular Domain 50 SUMOylation Alleviates AD through Enhanced Transcriptional Activation and A $\beta$  Degradation. *Molecular Therapy* 29, 376-395.

Malhotra, J.D., Kazen-Gillespie, K., Hortsch, M., and Isom, L.L. (2000). Sodium Channel  $\beta$  Subunits Mediate Homophilic Cell Adhesion and Recruit Ankyrin to Points of Cell-Cell Contact\*. *Journal of Biological Chemistry* 275, 11383-11388.

Marsh, S.R., Pridham, K.J., Jourdan, J., and Gourdie, R.G. (2021). Novel Protocols for Scalable Production of High Quality Purified Small Extracellular Vesicles from Bovine Milk. *Nanotheranostics* 5, 488-498.

Martinez-Moreno, R., Selga, E., Riuró, H., Carreras, D., Parnes, M., Srinivasan, C., Wangler, M.F., Pérez, G.J., Scornik, F.S., and Brugada, R. (2020). An SCN1B Variant Affects Both Cardiac-Type (NaV1.5) and Brain-Type (NaV1.1) Sodium Currents and Contributes to Complex Concomitant Brain and Cardiac Disorders. *Frontiers in Cell and Developmental Biology* 8.

Mezache, L., Struckman, H.L., Greer-Short, A., Baine, S., Györke, S., Radwański, P.B., Hund, T.J., and Veeraraghavan, R. (2020). Vascular endothelial growth factor promotes atrial arrhythmias by inducing acute intercalated disk remodeling. *Sci Rep* 10, 20463.

Moise, N., Struckman, H.L., Dagher, C., Veeraraghavan, R., and Weinberg, S.H. (2021). Intercalated disk nanoscale structure regulates cardiac conduction. *Journal of General Physiology* 153.

Moreno, J.D., Zhu, W., Mangold, K., Chung, W., and Silva, J.R. (2019). A Molecularly Detailed Na(V)1.5 Model Reveals a New Class I Antiarrhythmic Target. *JACC Basic Transl Sci* 4, 736-751.

Morgan, K., Stevens, E.B., Shah, B., Cox, P.J., Dixon, A.K., Lee, K., Pinnock, R.D., Hughes, J., Richardson, P.J., Mizuguchi, K., *et al.* (2000).  $\beta$ 3: An additional auxiliary subunit of the voltage-sensitive sodium channel that modulates channel gating with distinct kinetics. *Proceedings of the National Academy of Sciences* 97, 2308-2313.

Müllenbroich, M.C., Kelly, A., Acker, C., Bub, G., Bruegmann, T., Di Bona, A., Entcheva, E., Ferrantini, C., Kohl, P., Lehnart, S.E., *et al.* (2021). Novel Optics-Based Approaches for Cardiac Electrophysiology: A Review. *Frontiers in Physiology* 12.

Munagala, R., Aqil, F., Jeyabalan, J., and Gupta, R.C. (2016). Bovine milk-derived exosomes for drug delivery. *Cancer Lett* 371, 48-61.

Nguyen, P.T., DeMarco, K.R., Vorobyov, I., Clancy, C.E., and Yarov-Yarovoy, V. (2019). Structural basis for antiarrhythmic drug interactions with the human cardiac sodium channel. *Proc Natl Acad Sci U S A* 116, 2945-2954.

O'Malley, H.A., and Isom, L.L. (2015). Sodium channel  $\beta$  subunits: emerging targets in channelopathies. *Annu Rev Physiol* 77, 481-504.

Ogiwara, I., Nakayama, T., Yamagata, T., Ohtani, H., Mazaki, E., Tsuchiya, S., Inoue, Y., and Yamakawa, K. (2012). A homozygous mutation of voltage-gated sodium channel  $\beta$ (I) gene SCN1B in a patient with Dravet syndrome. *Epilepsia* 53, e200-203.

Patino, G.A., Brackenbury, W.J., Bao, Y., Lopez-Santiago, L.F., O'Malley, H.A., Chen, C., Calhoun, J.D., Lafrenière, R.G., Cossette, P., Rouleau, G.A., *et al.* (2011). Voltage-gated Na<sup>+</sup> channel  $\beta$ 1B: a secreted cell adhesion molecule involved in human epilepsy. *J Neurosci* 31, 14577-14591.



Patino, G.A., Claes, L.R., Lopez-Santiago, L.F., Slat, E.A., Dondeti, R.S., Chen, C., O'Malley, H.A., Gray, C.B., Miyazaki, H., Nukina, N., *et al.* (2009). A functional null mutation of SCN1B in a patient with Dravet syndrome. *J Neurosci* 29, 10764-10778.

Pieters, B.C.H., Arntz, O.J., Aarts, J., Feitsma, A.L., van Neerven, R.J.J., van der Kraan, P.M., Oliveira, M.C., and van de Loo, F.A.J. (2022). Bovine Milk-Derived Extracellular Vesicles Inhibit Catabolic and Inflammatory Processes in Cartilage from Osteoarthritis Patients. *Mol Nutr Food Res* 66, e2100764.

Qin, N., D'Andrea, M.R., Lubin, M.L., Shafae, N., Codd, E.E., and Correa, A.M. (2003). Molecular cloning and functional expression of the human sodium channel beta1B subunit, a novel splicing variant of the beta1 subunit. *Eur J Biochem* 270, 4762-4770.

Raisch, T.B., Yanoff, M.S., Larsen, T.R., Farooqui, M.A., King, D.R., Veeraraghavan, R., Gourdie, R.G., Baker, J.W., Arnold, W.S., AlMahameed, S.T., *et al.* (2018). Intercalated Disk Extracellular Nanodomain Expansion in Patients With Atrial Fibrillation. *Front Physiol* 9, 398.

Rhett, J.M., Ongstad, E.L., Jourdan, J., and Gourdie, R.G. (2012). Cx43 associates with Na(v)1.5 in the cardiomyocyte perinexus. *J Membr Biol* 245, 411-422.

Salvage, S.C., Huang, C.L., and Jackson, A.P. (2020). Cell-Adhesion Properties of  $\beta$ -Subunits in the Regulation of Cardiomyocyte Sodium Channels. *Biomolecules* 10.

Scheffer, I.E., Harkin, L.A., Grinton, B.E., Dibbens, L.M., Turner, S.J., Zielinski, M.A., Xu, R., Jackson, G., Adams, J., Connellan, M., *et al.* (2007). Temporal lobe epilepsy and GEFS+ phenotypes associated with SCN1B mutations. *Brain* 130, 100-109.

Schlipp, A., Schinner, C., Spindler, V., Vielmuth, F., Gehmlich, K., Syrris, P., McKenna, W.J., Dendorfer, A., Hartlieb, E., and Waschke, J. (2014). Desmoglein-2 interaction is crucial for cardiomyocyte cohesion and function. *Cardiovasc Res* 104, 245-257.

Shu, R., Wong, W., Ma, Q.H., Yang, Z.Z., Zhu, H., Liu, F.J., Wang, P., Ma, J., Yan, S., Polo, J.M., *et al.* (2015). APP intracellular domain acts as a transcriptional regulator of miR-663 suppressing neuronal differentiation. *Cell Death & Disease* 6, e1651-e1651.

Teng, A.C.T., Gu, L., Di Paola, M., Lakin, R., Williams, Z.J., Au, A., Chen, W., Callaghan, N.I., Zadeh, F.H., Zhou, Y.-Q., *et al.* (2022). Tmem65 is critical for the structure and function of the intercalated discs in mouse hearts. *Nature Communications* 13, 6166.

van Tetering, G., and Vooijs, M. (2011). Proteolytic cleavage of Notch: "HIT and RUN". *Curr Mol Med* 11, 255-269.

Veeraraghavan, R., Hoeker, G.S., Alvarez-Laviada, A., Hoagland, D., Wan, X., King, D.R., Sanchez-Alonso, J., Chen, C., Jourdan, J., Isom, L.L., *et al.* (2018). The adhesion function of the sodium channel beta subunit ( $\beta$ 1) contributes to cardiac action potential propagation. *Elife* 7, e37610.

Veeraraghavan, R., Lin, J., Keener, J.P., Gourdie, R., and Poelzing, S. (2016). Potassium channels in the Cx43 gap junction perinexus modulate ephaptic coupling: an experimental and modeling study. *Pflugers Arch* 468, 1651-1661.

Vidhya Rao, M.P.N. (2015). Current and Potential Antiarrhythmic Drugs Targeting Voltage-Gated Cardiac Ion Channels. *Cardiovascular Pharmacology: Open Access* 04.

Wallace, R.H., Scheffer, I.E., Parasivam, G., Barnett, S., Wallace, G.B., Sutherland, G.R., Berkovic, S.F., and Mulley, J.C. (2002). Generalized epilepsy with febrile seizures plus: mutation of the sodium channel subunit SCN1B. *Neurology* 58, 1426-1429.

Wallace, R.H., Wang, D.W., Singh, R., Scheffer, I.E., George, A.L., Jr., Phillips, H.A., Saar, K., Reis, A., Johnson, E.W., Sutherland, G.R., *et al.* (1998). Febrile seizures and generalized epilepsy associated with a mutation in the Na<sup>+</sup>-channel beta1 subunit gene SCN1B. *Nat Genet* *19*, 366-370.

Watanabe, H., Darbar, D., Kaiser, D.W., Jiramongkolchai, K., Chopra, S., Donahue, B.S., Kannankeril, P.J., and Roden, D.M. (2009). Mutations in sodium channel  $\beta$ 1- and  $\beta$ 2-subunits associated with atrial fibrillation. *Circ Arrhythm Electrophysiol* *2*, 268-275.

Watanabe, H., Koopmann, T.T., Le Scouarnec, S., Yang, T., Ingram, C.R., Schott, J.J., Demolombe, S., Probst, V., Anselme, F., Escande, D., *et al.* (2008). Sodium channel  $\beta$ 1 subunit mutations associated with Brugada syndrome and cardiac conduction disease in humans. *J Clin Invest* *118*, 2260-2268.

Williams, G., Williams, E.J., and Doherty, P. (2002). Dimeric versions of two short N-cadherin binding motifs (HAVDI and INPISG) function as N-cadherin agonists. *J Biol Chem* *277*, 4361-4367.

Wong, H.-K., Sakurai, T., Oyama, F., Kaneko, K., Wada, K., Miyazaki, H., Kurosawa, M., De Strooper, B., Saftig, P., and Nukina, N. (2005).  $\beta$  Subunits of Voltage-gated Sodium Channels Are Novel Substrates of  $\beta$ -Site Amyloid Precursor Protein-cleaving Enzyme (BACE1) and  $\gamma$ -Secretase\*. *Journal of Biological Chemistry* *280*, 23009-23017.

Yu, F.H., Westenbroek, R.E., Silos-Santiago, I., McCormick, K.A., Lawson, D., Ge, P., Ferriera, H., Lilly, J., DiStefano, P.S., Catterall, W.A., *et al.* (2003). Sodium channel beta4, a new disulfide-linked auxiliary subunit with similarity to beta2. *J Neurosci* *23*, 7577-7585.

### **Chapter 3: New insights on the expression of SCN1B splice variants $\beta$ 1 and $\beta$ 1B in cardiac cells**

*Manuscript in preparation*

Zachary Williams<sup>1,2,3</sup>, Mason Wheeler<sup>1,2,3</sup>, Xiaobo Wu<sup>1,2</sup>, Jamie Renick<sup>1,2</sup>, Jane Jourdan<sup>1,2</sup>, Steve Poelzing<sup>1,2,3,4,5</sup>, Jessica Pflieger<sup>1,2,6</sup>, Rob Gourdie<sup>1,2,4,5</sup>

<sup>1</sup>Fralin Biomedical Research Institute at VTC, Virginia Tech, Roanoke, VA 24016, USA

<sup>2</sup>Center for Vascular and Heart Research, Virginia Tech, Roanoke, VA 24016, USA

<sup>3</sup>Translational Biology Medicine and Health Graduate Program, Virginia Tech, Roanoke, VA 24016, USA

<sup>4</sup>Department of Biomedical Engineering and Mechanics, Virginia Tech, Blacksburg, VA 24061, USA

<sup>5</sup>Virginia Tech Carilion School of Medicine, Virginia Tech, Roanoke, VA 24016, USA

<sup>6</sup>Department of Biological Sciences, College of Science, Virginia Tech, Blacksburg, VA 24061, USA

Running Title: Investigating SCN1B expression in cardiac cells

Fralin Biomedical Research Institute at Virginia Tech Carilion,

Center for Vascular and Heart Research,

2 Riverside Circle, Roanoke, VA, 24016, USA

Keywords: Voltage-gated sodium channels, SCN1B ( $\beta$ 1/ $\beta$ 1B), Ig adhesion domain, NRVMs

## ABSTRACT

Voltage gated sodium channels (VGSCs) are responsible for the upstroke of the action potential in ventricular myocytes. VGSCs are typically composed of a single pore-forming  $\alpha$ -subunit and 1 or 2 accessory  $\beta$ -subunits. SCN1B-SCN4B are the genes that encode  $\beta$ 1- $\beta$ 4 respectively, and an alternatively spliced variant,  $\beta$ 1B, is encoded by SCN1B.  $\beta$ 1- $\beta$ 4 all have similar homology, with an extracellular Ig domain, a transmembrane domain, and an intracellular domain.  $\beta$ 1 and  $\beta$ 1B share identical sequences through the Ig domain and a portion of the remaining extracellular domain, but are quite different in their C-terminal sequences. This Ig domain is critical for maintaining normal cardiac conduction and associating with the major cardiac  $\alpha$  isoform,  $\text{Na}_v1.5$ . Although  $\beta$ 1B is thought to be secreted under most conditions, when heterologously co-expressed with  $\text{Na}_v1.5$ , the major  $\alpha$ -subunit of cardiomyocytes, it has been reported to be maintained at the cell membrane, suggesting a unique role for  $\beta$ 1B in the heart. Previous work has shown that mRNA levels of  $\beta$ 1 are ~100 fold greater than those of  $\beta$ 1B in human atria and ventricles. Despite the seemingly high expression of  $\beta$ 1 transcripts, it has been notoriously difficult to detect at the protein level. To further complicate the differentiation of  $\beta$ 1 and  $\beta$ 1B, they can be found at nearly identical masses in immunoblots. Recently, a C-terminal  $\beta$ 1 antibody (D4Z2N, Cell Signaling Technology) was developed commercially and has been used by multiple labs to study  $\beta$ 1. Using this  $\beta$ 1 CT antibody, together with a well characterized  $\beta$ 1 NT antibody developed by our lab, we explored the profiles of SCN1B in multiple cardiac cell types, including neonatal rat ventricular myocytes and fibroblasts (NRVMs and NFs) and isolated adult mouse cardiomyocytes (MCMs). The CT  $\beta$ 1 antibody failed to detect any bands in these 3 cardiac cell

types. By contrast, the NT  $\beta 1$  antibody did detect a band at 37kD, consistent with the expected size of SCN1B gene products. Thus, we hypothesized that we may be detecting  $\beta 1B$  rather than  $\beta 1$  with the NT antibody. To further test our hypothesis, we carried out immunofluorescence (IF) experiments in NRVMs with both antibodies. The NT  $\beta 1$  antibody showed high expression of SCN1B at cell-cell contacts in NRVM cultures where it has previously been shown to localize, while CT  $\beta 1$  antibody showed little evidence of localization in cardiac cells. Lastly, we developed a custom antibody with ThermoFisher against a unique peptide within the CT of  $\beta 1B$ , predicted not to cross-react with the canonical  $\beta 1$  polypeptide. In WB with NRVMs using the raw sera containing the  $\beta 1B$  antibody, we identified a band at approximately 37kD consistent with a SCN1B gene product. Taking together results of each antibody in both WB and IF, there is evidence that the major  $\beta$  subunit found in rat and mouse ventricular myocytes may be the alternatively spliced variant of SCN1B,  $\beta 1B$ . This could have significant implications in the role of  $\beta 1$  and  $\beta 1B$  in the heart. Although initial experiments have supported our hypothesis, further work is necessary to characterize the  $\beta$  subunits in cardiac cells.

## **1. INTRODUCTION**

The field of cardiac electrophysiology has recently had a major breakthrough with the discovery that gap junctional coupling may not be the only mechanism supporting electrical conduction between cardiomyocytes. A parallel mechanism to gap junctional coupling has been proposed, termed ephaptic coupling, with the requirements for such coupling including a concentration of VGSCs associated with a narrow domain of extracellular space between two closely apposed cells, with models indicating the width of that space being no more than 30nm (Adams et al., 2023; Hoeker et al., 2020; Ivanovic and Kucera, 2021; Lin et al., 2022; Lin and Keener, 2010; Moise et al., 2021; Mori et al., 2008; Veeraraghavan et al., 2015; Veeraraghavan et al., 2016; Wei et al., 2016). In the intercalated disc, the specialized junctional region that forms between cardiomyocytes, underpinning intercellular electrical and mechanical connectivity, such a space has been discovered and investigated extensively over the last decade or so and is named the perinexus (Adams et al., 2023; Hoagland et al., 2019; Raisch et al., 2018; Rhett and Gourdie, 2012; Rhett et al., 2012; Veeraraghavan et al., 2015; Veeraraghavan et al., 2016). The perinexus has been shown to have dense sodium channel populations and a width less than 30 nm (Rhett et al., 2012; Veeraraghavan et al., 2018). It has been proposed that the width of the perinexus is modulated by SCN1B/ $\beta$ 1, a non-pore-forming VGSC subunit involved in trafficking of the  $\alpha$  subunit, modulating kinetics and gating properties of the  $\alpha$  subunit, and participating in a variety of adhesion interactions via its extracellular Ig domain (Veeraraghavan et al., 2018). In Langendorff perfused guinea pig hearts, disruption of trans-homophilic SCN1B $\beta$ 1 adhesion using a SCN1B/ $\beta$ 1 mimetic peptide,  $\beta$ adp1, resulted in widened perinexii and decreased

conduction velocity, as well as increased spontaneous incidences of arrhythmia (Veeraraghavan et al., 2018). Furthermore, as indicated in the second chapter of this thesis,  $\beta$ adp1 has been shown to increase the regulated intramembrane proteolysis (RIP) of SCN1B/ $\beta$ 1 in a heterologous expression system, a process through which a cleaved intracellular fragment (CTF) of  $\beta$ 1 translocates to the nucleus and alters transcription of multiple genes, including VGSC  $\alpha$  subunits and other ion channels [Chapter 2]. Together, these results suggest a major role for SCN1B/ $\beta$ 1 adhesion and downstream effects of RIP of  $\beta$ 1 in endogenous systems, such as neonatal rat cardiomyocytes, that need further investigation.

VGSCs are responsible for the upstroke of the action potential in cardiac cells and are typically composed of a single pore-forming  $\alpha$ -subunit and 1 or 2 accessory  $\beta$ -subunits (Bouza and Isom, 2018; O'Malley and Isom, 2015). SCN1B-SCN4B are the genes that encode  $\beta$ 1- $\beta$ 4 respectively, while SCN1B also encodes a splice variant,  $\beta$ 1B (Beneski and Catterall, 1980; Isom et al., 1992; Isom et al., 1995; Morgan et al., 2000; Qin et al., 2003; Yu et al., 2003).  $\beta$ 1- $\beta$ 4 have similar homology, composed of an extracellular Ig domain, a transmembrane domain, and an intracellular domain.  $\beta$ 1B is oft reported to be a secreted isoform given that it is thought to lack a C-terminal transmembrane domain (Patino et al., 2011). This being said, when initially reported in the literature, a putative transmembrane domain was identified by hydrophobicity plots (Qin et al., 2003). Whilst,  $\beta$ 1 and  $\beta$ 1B share identical sequences through their N-terminal Ig domain and a portion of the remaining extracellular domain, alternate splicing results in a completely non-homologous C-terminal sequence for the two SCN1B gene products (Qin et al., 2003). The  $\beta$ 1/ $\beta$ 1B Ig domain is critical for maintaining normal cardiac conduction and associating with the major cardiac  $\alpha$  isoform,  $\text{Na}_v1.5$  (McCormick et al., 1999). When  $\beta$ 1B is

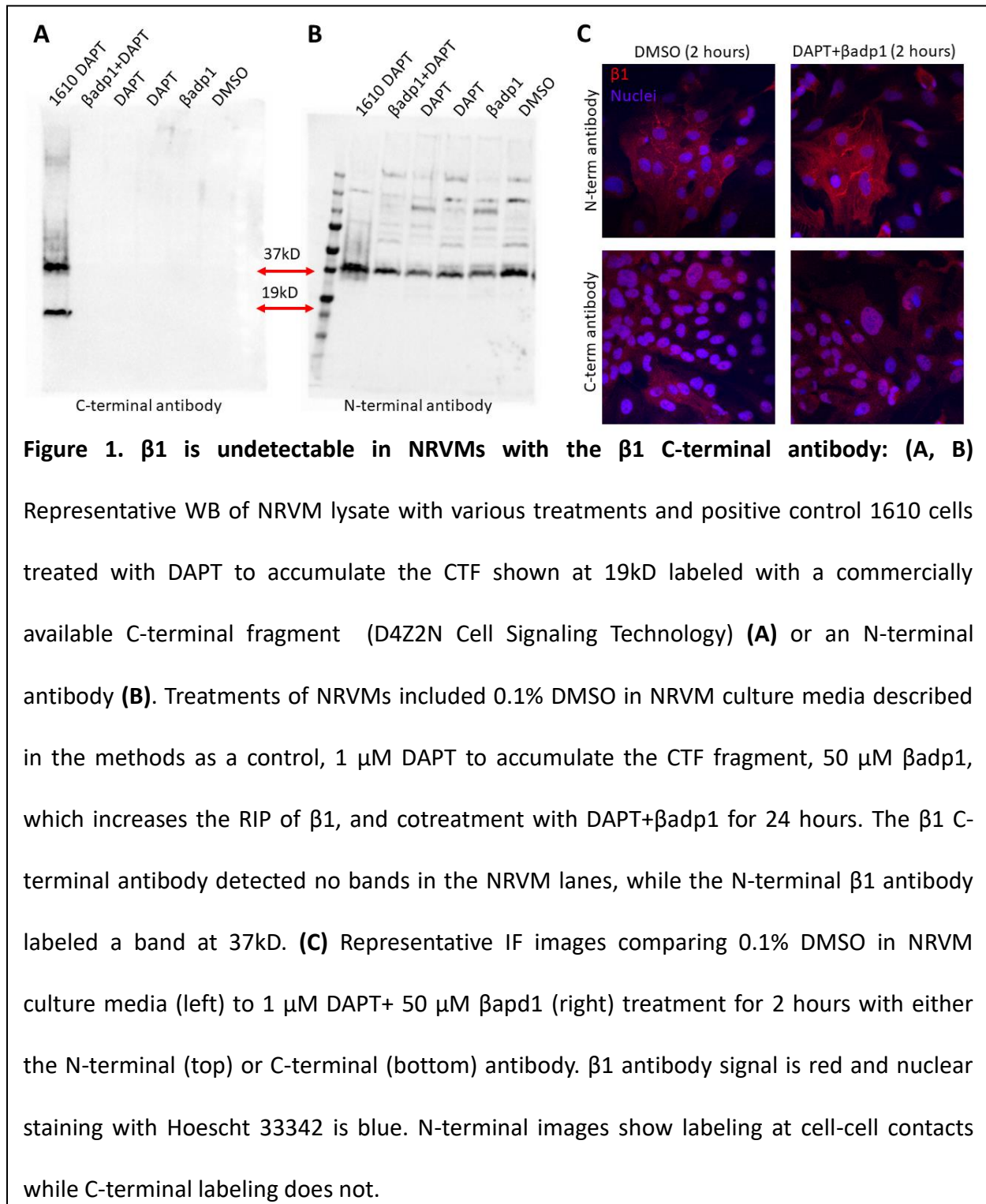


heterologously co-expressed with  $\text{Na}_v1.5$ , it is maintained at the membrane, whereas  $\beta1B$  is not maintained at the membrane if  $\text{Nav}1.5$  is not expressed, suggesting a unique role for  $\beta1B$  in VGSC complexes present in the heart (Patino et al., 2011). Previous work has shown that mRNA levels of  $\beta1$  are ~100 fold greater than those of  $\beta1B$  in human atria and ventricles, with about twice to three times as much expression for both variants in the atria than the ventricles (Ramos-Mondragon et al., 2022; Zhu et al., 2021). Despite the seemingly high expression of  $\beta1$  transcripts, it has been notoriously difficult to detect the protein via Western blot (WB) (Cervantes et al., 2022; Zhu et al., 2021). Detection of  $\beta1$  protein is complicated by sequence homology with  $\beta1B$ , especially since many of the most commonly used and best characterized SCN1B antibodies are against an epitope in the Ig domain common to both isoforms variants. To further complicate the differentiation of  $\beta1$  and  $\beta1B$ , they can be found at nearly identical masses in WB despite the expected mass of  $\beta1B$  being much higher than the expected mass of  $\beta1$ . Recently, a C-terminal  $\beta1$  specific antibody (D4Z2N, Cell Signaling Technology) was developed commercially and has been used by multiple labs to study  $\beta1$ , and the RIP of  $\beta1$ , because the antibody also detects the CTF (Bouza et al., 2021; Haworth et al., 2022). To expand our knowledge of the RIP of  $\beta1$  and its function in a cardiac context, as well as the seemingly unique role for  $\beta1B$  in a cardiac context, we sought to characterize the expression at the protein level of each variant. Using antibodies against the  $\beta1$  NT and CT (i.e. D4Z2N), we explored the profiles of SCN1B in multiple cardiac cell types, including neonatal rat ventricular myocytes (NRVMs), neonatal rat cardiac fibroblasts (NRFs) and isolated adult mouse cardiomyocytes (MCMs). We also developed a custom antibody with ThermoFisher specific to the CT of  $\beta1B$ . Our findings described herein could have major implications in the roles of  $\beta1$  and  $\beta1B$  and

which functional effects have previously been attributed to either, including the role of  $\beta 1/\beta 1B$  on regulation of perinexal width and ephaptic coupling in the heart.

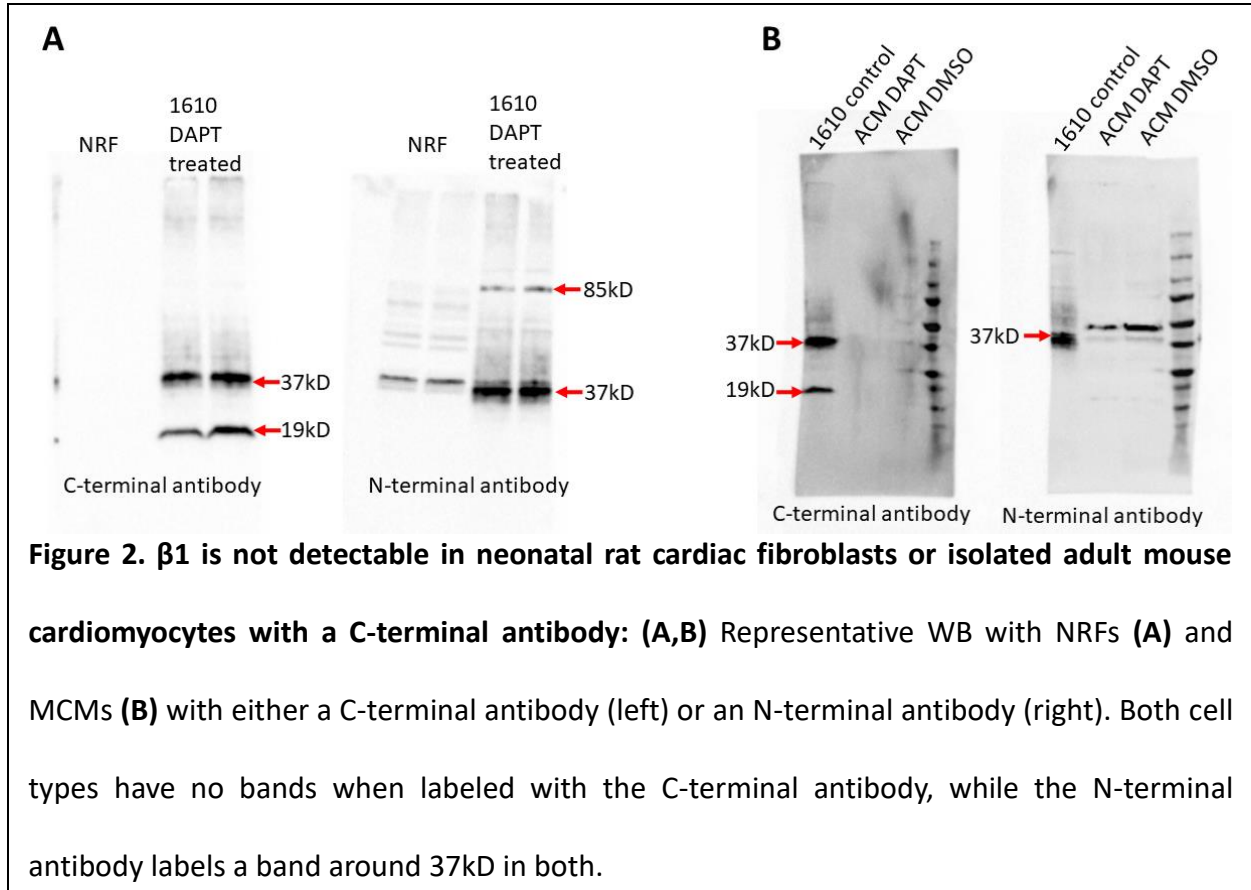
## **2. RESULTS**

**2.1 WB and IF assays show lack of  $\beta 1$  RIP occurring in NRVMs, NRFs, and MCMs:** We and others have previously shown that  $\beta 1$  undergoes a sequential two-step (BACE1 cleavage followed by  $\gamma$ -secretase cleavage) regulated intramembrane proteolysis (RIP) (Bouza et al., 2021; Wong et al., 2005)[Chapter 2].  $\beta 1$  RIP results in a cleaved intracellular C-terminal fragment (CTF) that translocates to the nucleus and alters transcription of various genes. The presence of the CTF in cells confirms the RIP process and allows for investigation into effects on the RIP process as a whole. The CTF is detectable via Western blot (WB) with a commercially available C-terminal antibody (D4Z2N Cell Signaling Technology). Importantly, our lab has only confirmed the RIP of  $\beta 1$  in 1610 Chinese Hamster lung fibroblasts stably heterologously expressing  $\beta 1$  (1610 $\beta 1$ ) [Chapter 2]. We sought to investigate  $\beta 1$  RIP in neonatal rat ventricular myocytes (NRVMs) with the  $\beta 1$  C-terminal antibody. We treated NRVMs for 24 hours with either DMSO as a control, DAPT to inhibit the second cleavage step of the RIP of  $\beta 1$  and cause an accumulation of the CTF,  $\beta adp1$ , a  $\beta 1$  mimetic peptide which has previously been shown to increase the RIP of  $\beta 1$ , or a cotreatment with  $\beta adp1$  and DAPT. Surprisingly, the  $\beta 1$  C-terminal antibody showed no evidence of  $\beta 1$  in NRVMs regardless of treatment (Fig. 1A), compared to the positive control with 1610 $\beta 1$  cells, which showed the expected full-length  $\beta 1$  band at 37kD and the CTF band at 19kD after DAPT treatment. However, an N-terminal  $\beta 1/\beta 1B$  antibody did show a band at 37kD in both NRVMs and 1610 $\beta 1$  cells (Fig. 1B). To further characterize the expression of  $\beta 1$  protein in NRVMs, we again used both antibodies in confocal immunofluorescence imaging (IF) after 2



hours of treatment with the same 4 treatments. Previous work has shown the localization of signal with an N-terminal  $\beta 1/\beta 1B$  antibody to cell-cell contacts between NRVMs and alterations

to that localization after treatment with  $\beta$ adp1 on a similar time scale (Domínguez et al., 2005; Veeraraghavan et al., 2018)[Chapter 2]. We confirmed this result with the N-terminal  $\beta$ 1/ $\beta$ 1B



antibody (Fig 1C, top row). However, the C-terminal antibody showed little evidence of specific staining and no localization of signal to intracellular organelles or cell-cell contacts (Fig 1C, bottom row). Since  $\beta$ 1 is considered by most to be present in the heart, we reasoned that alternative explanations for our results could be that other cardiac cell types may express  $\beta$ 1,

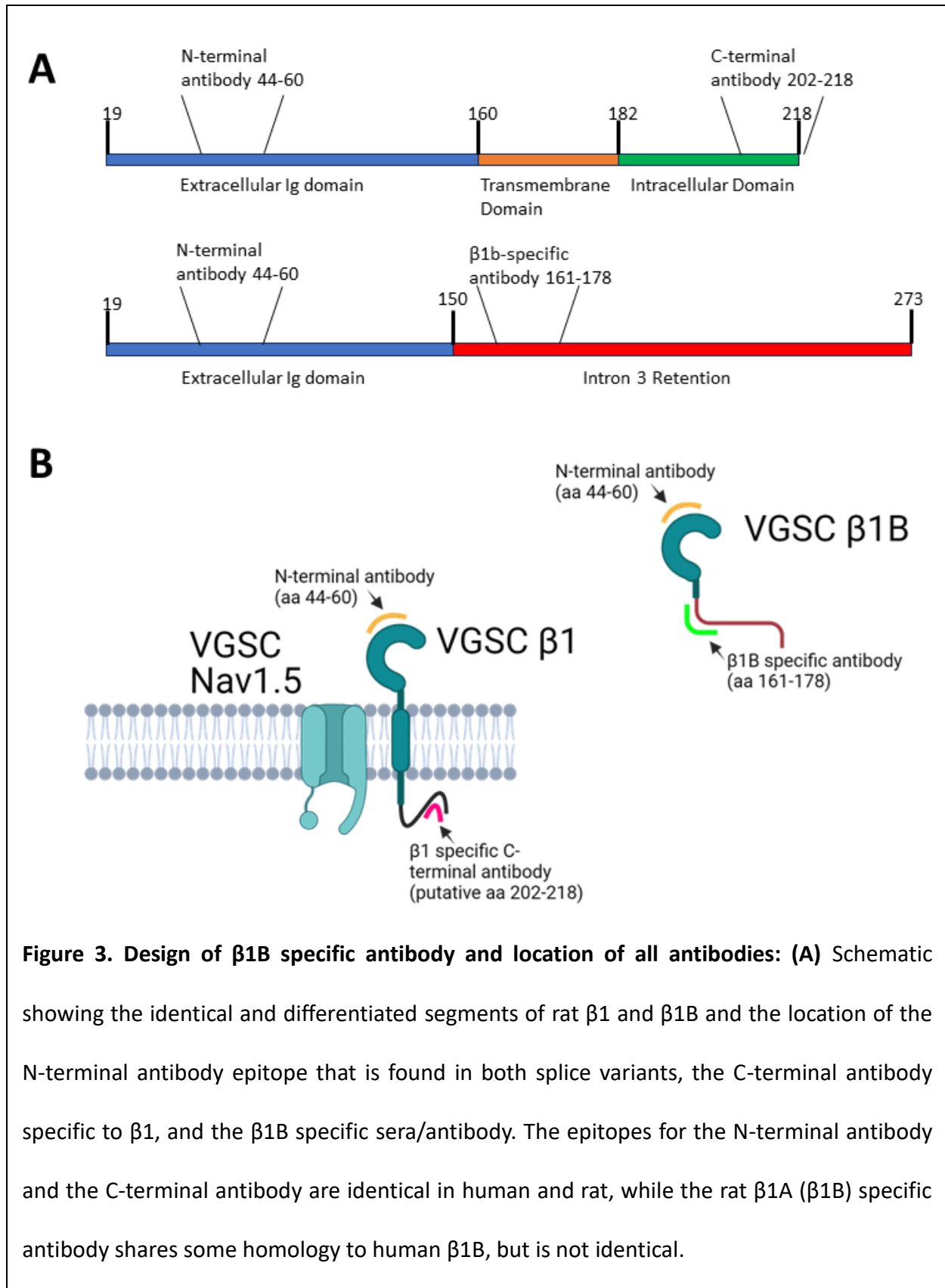


**Figure 3 Cont. (B)** Cartoon indicating where each antibody falls in the primary sequence of  $\beta 1$  and  $\beta 1B$ . Figure 3B was created with BioRender.com.

and also that NRVMs may be not sufficiently mature to express  $\beta 1$ . Thus, we also investigated the protein expression of  $\beta 1$  in neonatal rat cardiac fibroblasts (NRFs) and in isolated adult mouse cardiomyocytes (MCMs). However, similar to results with NRVMs, we found that the C-terminal antibody did not detect  $\beta 1$  signal in NRFs, whereas the N-terminal  $\beta 1/\beta 1B$  antibody showed a prominent band at 37kD (Fig 2A) in Western blot. In MCMs, we also found that the  $\beta 1$  C-terminal antibody did not detect  $\beta 1$  while an N-terminal  $\beta 1/\beta 1B$  antibody also showed a band at 37kD (Fig 2B). Thus, in 3 different cardiac cell types, we found no evidence of  $\beta 1$  RIP and we also found that the C-terminal  $\beta 1$  antibody does not detect full-length  $\beta 1$ , whilst an N-terminal antibody does. Since the N-terminal antibody detects both  $\beta 1$  and  $\beta 1B$  while the C-terminal antibody detects only  $\beta 1$ , we could not rule out the possibility that in these particular cells, we were solely detecting the alternatively spliced isoform,  $\beta 1B$ .

**2.2 A  $\beta 1B$  specific antibody mirrors result of the N-terminal  $\beta 1/\beta 1B$  antibody in NRVMs:** To address the potential for the N-terminal antibody to detect both  $\beta 1/\beta 1B$ , and the lack of commercially available antibodies specific to  $\beta 1B$ , we developed an antibody with ThermoFisher specific to rat  $\beta 1A$  (homologous to human  $\beta 1B$ ), using a C-terminal epitope reported previously in the literature (Qin et al., 2003). The epitope (amino acids of  $\beta 1B$  161-178) is unique to  $\beta 1B$ , and is not present  $\beta 1$ , being located on the  $\beta 1B$  primary sequence just after where the alternatively spliced isoform diverges from  $\beta 1$  - at  $\sim$  amino acid 150 of  $\beta 1$  (Fig. 3A). The location of the  $\beta 1$  and  $\beta 1B$  epitopes of each antibody used in this study is shown in Fig. 3B. Currently, we

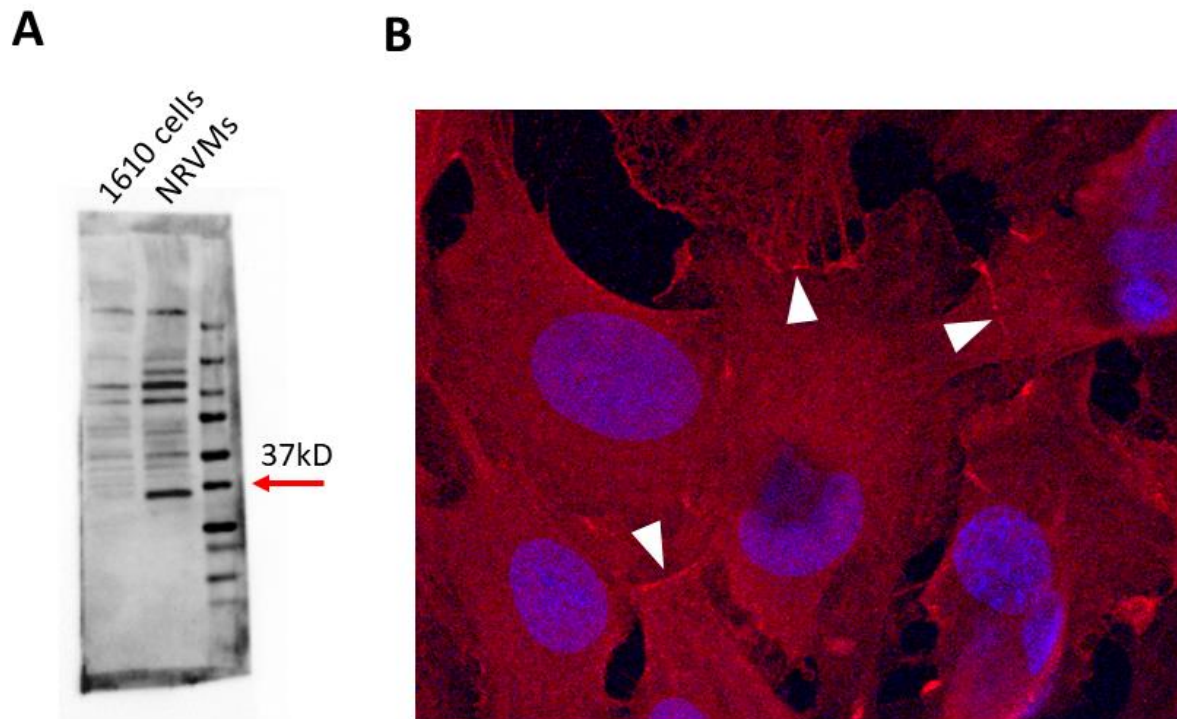


**Figure 4. The  $\beta$ 1B specific antibody mirrors the results in WB and IF with the N-terminal  $\beta$ 1/ $\beta$ 1B antibody: (A)** Representative WB showing negative control 1610 $\beta$ 1 cell lysate compared to NRVM lysate labeled with the  $\beta$ 1B specific antibody raw sera. The 1610 $\beta$ 1 cells are a negative control because they do not endogenously express significant levels of  $\beta$ 1B. The NRVMs show a prominent band at 37kD consistent with  $\beta$ 1b. **(B)** Representative IF image showing NRVMs stained with the  $\beta$ 1B specific antibody sera. White arrows indicate areas of localization of signal to cell-cell contacts, similar to what was observed with the N-terminal  $\beta$ 1/ $\beta$ 1B antibody.

have raw sera containing the  $\beta$ 1B specific antibody, so the results with this probe are preliminary – much further characterization is needed. Nonetheless, in WB, the  $\beta$ 1B specific sera did not show a significant band at 37kD in our 1610 $\beta$ 1 controls as expected, since they do not endogenously express  $\beta$ 1 or  $\beta$ 1B. By contrast in the NRVMs, the  $\beta$ 1B specific sera did

indicate the presence of a significant band at 37kD consistent with an SCN1B gene product, also coinciding with where the N-terminal  $\beta 1/\beta 1B$  antibody detects a band (Fig. 4A). In IF, it was determined that the  $\beta 1B$  specific sera shows evidence of localization of signal at cell-cell contacts (white arrows, Fig. 4B), similar to our results with the N-terminal  $\beta 1/\beta 1B$  antibody. Taken together, the data with the N-terminal  $\beta 1/\beta 1B$  and C-terminal  $\beta 1$  antibodies and  $\beta 1B$  specific sera suggest that in NRVMs,  $\beta 1B$ , and not  $\beta 1$ , may be expressed at the protein level.



### **3. DISCUSSION**

The present study investigated the presence of Scn1b proteins  $\beta 1$  and  $\beta 1B$  in neonatal rat ventricular myocytes (NRVMs), as well as the potential for regulated membrane proteolysis (RIP) of  $\beta 1$  to occur in NRVMs. We have previously shown that in a heterologous expression system (1610 $\beta 1$ cells)  $\beta 1$  undergoes RIP, and that treatment with  $\beta 1$  mimetic monomer  $\beta adp1$ , or dimer PS2L, increases the RIP of  $\beta 1$  [Chapter 2]. Surprisingly, here we found that the C-terminal  $\beta 1$ -specific antibody used to study this process in 1610 $\beta 1$  cells shows no evidence of  $\beta 1$  in NRVMs, or RIP of  $\beta 1$ . An N-terminal SCN1B ( $\beta 1/\beta 1B$ ) antibody does show labeling of a band at 37kD in Western blots with NRVM lysate and signal at cell-cell contacts between NRVMs with IF staining. We further demonstrate that this pattern is repeated in neonatal rat cardiac fibroblasts and isolated adult mouse cardiomyocytes, with the C-terminal antibody showing no evidence of  $\beta 1$ , while the N-terminal antibody showed bands at 37kD in both cell types. Lastly, we designed a  $\beta 1B$ -specific antibody, and in preliminary data, we find the raw sera of this antibody gave similar results to the N-terminal SCN1B ( $\beta 1/\beta 1B$ ) antibody, suggesting the presence of  $\beta 1B$  rather than  $\beta 1$  in NRVMs.

Our findings here, if supported by more rigorous and expanded future work, could have major implications in the field. There is a history of research on SCN1B ( $\beta 1/\beta 1B$ ) going back decades now. Whilst much of that research has carefully considered the differences between  $\beta 1$  and  $\beta 1B$ , and whilst our findings are likely to be tissue specific, there are instances where findings will need to be looked at in a new light without the assumption that  $\beta 1$  is the major expressed SCN1B variant at the protein level, at least in the ventricular myocyte types studied herein. Although we are the first to show direct data that suggests  $\beta 1B$  is a major isoform in

cardiomyocytes, there have been hints in the literature before this point. The Isom group has previously shown that  $\beta 1B$  is a secreted cell adhesion molecule, except when co-expressed with  $Na_v1.5$ , the major cardiac  $\alpha$  isoform (Patino et al., 2011). Other groups have reported difficulties detecting  $\beta 1$  in heart tissue with a C-terminal  $\beta 1$  specific antibody, while this same probe readily detects  $\beta 1$  in whole brain lysate (Cervantes et al., 2022; Zhu et al., 2021). To complicate the data, it has also been reported that the mRNA levels of  $\beta 1$  are much higher than those of  $\beta 1B$  in the heart (Zhu et al., 2021). Some groups have used Myc- or EGFP- tagged  $\beta 1$  subunits to circumvent the detection difficulties (Angsutararux et al., 2021; Haworth et al., 2022). With further testing and confirmation that the new  $\beta 1B$  antibody is specific and reliable, the field can begin to reexamine assumptions of  $\beta 1$  vs  $\beta 1B$  activity in the heart.

One area that could see major changes in assumptions is the role of SCN1B ( $\beta 1/\beta 1B$ ) in the perinexus, a specialized nanodomain in the intercalated disc where ephaptic coupling is proposed to occur. The current hypothesis for  $\beta 1$ 's function in the perinexus is that it regulates the perinexal width via Ig domain mediated trans-homophilic adhesion while anchored in the membrane and likely associated with  $Na_v1.5$ , as well as other intercalated disc localized proteins, such as Tmem65 and ankyrin G (Salvage et al., 2020; Teng et al., 2022; Veeraraghavan et al., 2018). The N-terminal SCN1B ( $\beta 1/\beta 1B$ ) antibody has shown signal in the intercalated disc of guinea pig hearts, but this does not rule out the presence of  $\beta 1B$  instead of  $\beta 1$  (Veeraraghavan et al., 2018). Since  $\beta 1B$  contains an identical Ig domain to  $\beta 1$ , it could still perform a similar function, whether anchored in the membrane or secured in place by  $Na_v1.5$  association. Also once freed from direct association with the membrane  $\beta 1B$  in the perinexus could regulate the perinexus similar to our mimetic peptide  $\beta adp1$ .  $\beta adp1$  is taken from aa 66-

86 of the Ig domain, meaning that region is identical in  $\beta 1$  and  $\beta 1B$ . Results with  $\beta adp1$  show that it can widen the perinexus in Langendorff-perfused guinea pig hearts, resulting in decreased conduction velocity and increased incidences of arrhythmias (Veeraraghavan et al., 2018).

While the initial findings presented here are novel and provocative, there are multiple limitations that will need to be addressed. While the data with the C-terminal antibody is highly replicable and has been repeated multiple times in NRVMs, the data with the new  $\beta 1B$  sera is limited, thus other hypotheses cannot be completely ruled out, such as: 1) There is a conformational change or event that restricts access of the C-terminal antibody to the correct epitope on  $\beta 1$  or 2) The  $\beta 1$  subunit undergoes an as yet unknown C-terminal cleavage that eliminates the epitope the C-terminal antibody recognizes but the resulting fragment is close enough to its initial mass to continue running similarly in Western blot assays. Further controls and testing are necessary with the  $\beta 1B$  specific antibody, such as peptide inhibition, affinity purification, and more positive and negative controls, together with rigorous replication of such studies are required. The results presented here are mainly taken from NRVMs, with some supporting data in neonatal rat cardiac fibroblasts and isolated adult mouse cardiomyocytes, but how the results will translate to human cardiomyocytes is also unknown.

The overall conclusion of this chapter is that canonical  $\beta 1$  is likely not expressed in NRVMs, and raising the hypothesis that  $\beta 1B$  may be expressed instead. While the results presented herein are exciting and novel and have the potential to greatly impact the field of cardiac electrophysiology and study of the intercalated disc and perinexus, there are still many limitations and questions to address.

## **4. MATERIALS AND METHODS**

### **4.1. Peptide synthesis**

The SCN1B ( $\beta 1/\beta 1B$ ) mimetic peptide monomer  $\beta adp1$  (FVKILRYENEVLQLEEDERF) used in this study has been previously reported (Veeraraghavan et al., 2018). Peptides were synthesized by and obtained from LifeTein (Somerset, NJ) modified by N-terminal acetylation, C-terminal amidation, and TFA removal. Peptides were solubilized in DMSO to 50  $\mu M$ .

### **4.2 Neonatal rat ventricular myocyte (NRVM) and cardiac fibroblast isolation**

NRVM isolation procedures were approved by the Virginia Tech Institutional Animal Care and Use Committee. Briefly, hearts were isolated from one- to two-day-old Sprague-Dawley rats. Cells were dissociated with collagenase+DNase, then were subjected to Percoll gradient purification to separate myocytes from fibroblasts followed by differential pre-plating incubated at 37°C 30 min to enrich for cardiac myocytes or fibroblasts. Cardiomyocytes were plated and cultured in DMEM/F-12 supplemented with 10% fetal bovine serum (FBS) and 1% penicillin-streptomycin. Myocytes were allowed to grow and establish connections for 3–4 days *in vitro*. Peptide treatments were applied to cell monolayers for either 24 hours or 2 hours prior to each assay, as listed in the text. Fibroblast lysate was collected 24-48 hours post plating, when cells were mostly confluent and stored at -80°C until used for the Western blotting assay.

### **4.3 Adult mouse cardiomyocyte isolation**

Adult mouse cardiomyocytes were isolated from CD1 mice following a protocol previously described by the Gramolini group (Callaghan et al., 2020). Mice were euthanized by the open

drop exposure to isoflurane method followed by cervical dislocation. Then the chest cavity was opened, and the descending aorta was severed after dissecting through the diaphragm. 7 ml of EDTA buffer with 15  $\mu$ M blebbistatin was injected into the right ventricle. Next the heart was clamped using hemostats at the ascending aorta and excised, then placed into a 10 cm dish with fresh EDTA (3-5mL) with 15  $\mu$ M blebbistatin. At the same time, 9 ml of the EDTA with 15  $\mu$ M blebbistatin was injected slowly into the apex of the heart over approximately 6 min. After clearing the heart of blood, it was moved to a new dish containing the same buffer, and injected with 3 ml of 15  $\mu$ M blebbistatin in the same location over 2 minutes. Then, the heart was placed in another dish with 475 U/ml collagenase type II in the same buffer, and then 20 ml more was injected in the same location over a heating block to maintain temperature. The atria were removed and the ventricles moved to a new dish containing 3 mL of the collagenase buffer. The tissue was finely cut up to 1mm<sup>2</sup> cubes in 3 ml of fresh collagenase buffer with forceps, then triturated with a wide-bore 1 ml pipette. Next, we inhibited collagenase activity by adding 3 ml of perfusion buffer containing blebbistatin and 10% FBS. The isolate was put through a 70  $\mu$ m strainer and rinsed with 3 ml additional stop buffer. The filtrate was then divided between 2 upright 15 mL conical tubes and cells were allowed to settle for 15-20 minutes. The supernatant was removed, and the cells were put through a series of buffers for calcium reintroduction, first with 75:25 perfusion buffer:culture media, then 50:50, 25:75 and finally 100% culture media composed of M199 with 1x lipid supplement (Gibco), Insulin-transferrin-selenium supplement (Gibco), Pencillin/Streptomycin, 5% FBS, and 15  $\mu$ M blebbistatin. Cells were then put directly through the Western blot lysate collection protocol outlined below.

#### **4.4 Heterologous expression of $\beta$ 1 in 1610 cells**

We have previously described how Chinese hamster lung 1610 cells have been used as a heterologous expression system (Veeraraghavan et al., 2018). These cells were used to measure SCN1B/ $\beta$ 1 mediated adhesion and the regulated intramembrane proteolysis of SCN1B/ $\beta$ 1 and they do not endogenously express SCN1B/ $\beta$ 1.

#### **4.5 $\beta$ 1B specific antibody production**

A peptide derived from the rat  $\beta$ 1A ( $\beta$ 1B) c-terminus (Epitope: <sub>161</sub>RWRDRWKEGDRLVSHRGQ<sub>178</sub>) was synthesized by ThermoScientific and used for raising polyclonal antibodies in rabbits. The raw sera from bleeds of these rabbits were used for fluorescent immunolabeling and Western blotting of neonatal rat ventricular myocytes.

#### **4.6 Fluorescent Immunolabeling**

Fluorescent immunolabeling was performed on neonatal rat ventricular myocytes fixed with 4% paraformaldehyde for 10 minutes. Samples were labeled with a rabbit polyclonal antibody against an amino-terminal region of  $\beta$ 1 (Epitope: <sub>44</sub>KRRSETTAETFTEWTFR<sub>60</sub> 1:2000), a carboxy-terminal commercially available antibody (D4Z2N, Cell Signaling Technology 1:2000), or a  $\beta$ 1B specific antibody (Epitope: <sub>161</sub>RWRDRWKEGDRLVSHRGQ<sub>178</sub> 1:50 raw sera). We have previously published validation results for the N-terminal antibody (Veeraraghavan et al., 2018). Samples were then labeled with goat anti-rabbit AlexaFluor 568 (1:2000, ThermoFisher Scientific) secondary antibodies for confocal microscopy. Nuclei were stained with Hoescht 33342 for 10 minutes (1:30,000, Invitrogen).

#### **4.7 Confocal microscopy**

Confocal microscopy was done with a TCS SP8 laser scanning confocal microscope equipped with a Plan Achromat 63x/1.4 numerical aperture oil immersion objective and a Leica HyD hybrid detector (Leica) using an approach reported previously (Veeraraghavan et al., 2018). Imaging of each fluorophore was performed sequentially, and the excitation wavelength was switched at the end of each frame.

#### **4.8 Western blotting**

Whole cell lysates were collected from NRVMs or 1610 $\beta$ 1 cells using RIPA buffer on ice while being agitated on a platform rocker. Adult mouse cardiomyocytes and neonatal rat cardiac fibroblasts from suspension and NRVMs and 1610 $\beta$ 1 cells were then pulled through 22 gauge and 17 gauge syringes 5 times each, vortexed, and spun for 30 minutes at 10,000g at 4°C before being snap-frozen in liquid nitrogen. Lysates were electrophoresed on 4-20% TGX Stain-free gels (BioRad) and were then transferred to a polyvinylidene difluoride (PVDF) membrane using a semi-dry method with a Trans-Blot Turbo system for 7 minutes at 25V (BioRad). The membranes were probed with the rabbit polyclonal antibody against an amino-terminal region of  $\beta$ 1 (Epitope: <sub>44</sub>KRRSETTAETFTEWTFR<sub>60</sub> 1:1000), a rabbit polyclonal antibody against the carboxy-terminal of  $\beta$ 1 (D4Z2N, Cell Signaling Technology 1:1000), or a  $\beta$ 1B specific antibody (Epitope: <sub>161</sub>RWRDRWKEGDRLVSHRGQ<sub>178</sub> 1:250 raw sera). These were followed by a goat anti-rabbit HRP-conjugated secondary antibody (JacksonImmuno, 1:30,000). Signals were then detected using SuperSignal West Femto Maximum Sensitivity Substrate (ThermoFisher Scientific) and imaged with a ChemiDoc MP imager (BioRad).

## REFERENCES

Adams, W.P., Raisch, T.B., Zhao, Y., Davalos, R., Barrett, S., King, D.R., Bain, C.B., Colucci-Chang, K., Blair, G.A., Hanlon, A., *et al.* (2023). Extracellular Perinexal Separation Is a Principal Determinant of Cardiac Conduction. *Circ Res* 133, 658-673.

Angsutararux, P., Zhu, W., Voelker, T.L., and Silva, J.R. (2021). Molecular Pathology of Sodium Channel Beta-Subunit Variants. *Front Pharmacol* 12, 761275.

Beneski, D.A., and Catterall, W.A. (1980). Covalent labeling of protein components of the sodium channel with a photoactivable derivative of scorpion toxin. *Proceedings of the National Academy of Sciences* 77, 639-643.

Bouza, A.A., Edokobi, N., Hodges, S.L., Pinsky, A.M., Offord, J., Piao, L., Zhao, Y.-T., Lopatin, A.N., Lopez-Santiago, L.F., and Isom, L.L. (2021). Sodium channel  $\beta$ 1 subunits participate in regulated intramembrane proteolysis-excitation coupling. *JCI Insight* 6.

Bouza, A.A., and Isom, L.L. (2018). Voltage-Gated Sodium Channel  $\beta$  Subunits and Their Related Diseases. *Handb Exp Pharmacol* 246, 423-450.

Callaghan, N.I., Lee, S.H., Hadipour-Lakmehsari, S., Lee, X.A., Ahsan Siraj, M., Driouchi, A., Yip, C.M., Husain, M., Simmons, C.A., and Gramolini, A.O. (2020). Functional culture and in vitro genetic and small-molecule manipulation of adult mouse cardiomyocytes. *Commun Biol* 3, 229.

Cervantes, D.O., Pizzo, E., Ketkar, H., Parambath, S.P., Tang, S., Cianflone, E., Cannata, A., Vinukonda, G., Jain, S., Jacobson, J.T., *et al.* (2022). *Scn1b* expression in the adult mouse heart modulates  $\text{Na}^+$  influx in myocytes and reveals a mechanistic link between  $\text{Na}^+$  entry and diastolic function. *American Journal of Physiology-Heart and Circulatory Physiology* 322, H975-H993.



Domínguez, J.N., Navarro, F., Franco, D., Thompson, R.P., and Aránega, A.E. (2005). Temporal and spatial expression pattern of  $\beta$ 1 sodium channel subunit during heart development. *Cardiovascular Research* 65, 842-850.

Haworth, A.S., Hodges, S.L., Capatina, A.L., Isom, L.L., Baumann, C.G., and Brackenbury, W.J. (2022). Subcellular dynamics and functional activity of the cleaved intracellular domain of the Na<sup>+</sup> channel  $\beta$ 1 subunit. *Journal of Biological Chemistry*, 102174.

Hoagland, D.T., Santos, W., Poelzing, S., and Gourdie, R.G. (2019). The role of the gap junction perinexus in cardiac conduction: Potential as a novel anti-arrhythmic drug target. *Prog Biophys Mol Biol* 144, 41-50.

Hoeker, G.S., James, C.C., Tegge, A.N., Gourdie, R.G., Smyth, J.W., and Poelzing, S. (2020). Attenuating loss of cardiac conduction during no-flow ischemia through changes in perfusate sodium and calcium. *American Journal of Physiology-Heart and Circulatory Physiology* 319, H396-H409.

Isom, L.L., De Jongh, K.S., Patton, D.E., Reber, B.F.X., Offord, J., Charbonneau, H., Walsh, K., Goldin, A.L., and Catterall, W.A. (1992). Primary Structure and Functional Expression of the  $\beta$ 1 Subunit of the Rat Brain Sodium Channel. *Science* 256, 839-842.

Isom, L.L., Ragsdale, D.S., De Jongh, K.S., Westenbroek, R.E., Reber, B.F.X., Scheuer, T., and Catterall, W.A. (1995). Structure and function of the  $\beta$ 2 subunit of brain sodium channels, a transmembrane glycoprotein with a CAM motif. *Cell* 83, 433-442.

Ivanovic, E., and Kucera, J.P. (2021). Localization of Na<sup>(+)</sup> channel clusters in narrowed perinexi of gap junctions enhances cardiac impulse transmission via ephaptic coupling: a model study. *J Physiol* 599, 4779-4811.

Lin, J., Abraham, A., George, S.A., Greer-Short, A., Blair, G.A., Moreno, A., Alber, B.R., Kay, M.W., and Poelzing, S. (2022). Ephaptic Coupling Is a Mechanism of Conduction Reserve During Reduced Gap Junction Coupling. *Frontiers in Physiology* 13.

Lin, J., and Keener, J.P. (2010). Modeling electrical activity of myocardial cells incorporating the effects of ephaptic coupling. *Proc Natl Acad Sci U S A* 107, 20935-20940.

McCormick, K.A., Srinivasan, J., White, K., Scheuer, T., and Catterall, W.A. (1999). The extracellular domain of the beta1 subunit is both necessary and sufficient for beta1-like modulation of sodium channel gating. *J Biol Chem* 274, 32638-32646.

Moise, N., Struckman, H.L., Dagher, C., Veeraraghavan, R., and Weinberg, S.H. (2021). Intercalated disk nanoscale structure regulates cardiac conduction. *Journal of General Physiology* 153.

Morgan, K., Stevens, E.B., Shah, B., Cox, P.J., Dixon, A.K., Lee, K., Pinnock, R.D., Hughes, J., Richardson, P.J., Mizuguchi, K., *et al.* (2000).  $\beta 3$ : An additional auxiliary subunit of the voltage-sensitive sodium channel that modulates channel gating with distinct kinetics. *Proceedings of the National Academy of Sciences* 97, 2308-2313.

Mori, Y., Fishman, G.I., and Peskin, C.S. (2008). Ephaptic conduction in a cardiac strand model with 3D electrodiffusion. *Proceedings of the National Academy of Sciences of the United States of America* 105, 6463-6468.

O'Malley, H.A., and Isom, L.L. (2015). Sodium channel  $\beta$  subunits: emerging targets in channelopathies. *Annu Rev Physiol* 77, 481-504.

Patino, G.A., Brackenbury, W.J., Bao, Y., Lopez-Santiago, L.F., O'Malley, H.A., Chen, C., Calhoun, J.D., Lafrenière, R.G., Cossette, P., Rouleau, G.A., *et al.* (2011). Voltage-gated Na<sup>+</sup> channel  $\beta$ 1B: a secreted cell adhesion molecule involved in human epilepsy. *J Neurosci* *31*, 14577-14591.

Qin, N., D'Andrea, M.R., Lubin, M.L., Shafae, N., Codd, E.E., and Correa, A.M. (2003). Molecular cloning and functional expression of the human sodium channel beta1B subunit, a novel splicing variant of the beta1 subunit. *Eur J Biochem* *270*, 4762-4770.

Raisch, T.B., Yanoff, M.S., Larsen, T.R., Farooqui, M.A., King, D.R., Veeraraghavan, R., Gourdie, R.G., Baker, J.W., Arnold, W.S., AlMahameed, S.T., *et al.* (2018). Intercalated Disk Extracellular Nanodomain Expansion in Patients With Atrial Fibrillation. *Front Physiol* *9*, 398.

Ramos-Mondragon, R., Edokobi, N., Hodges, S.L., Wang, S., Bouza, A.A., Canugovi, C., Scheuing, C., Juratli, L., Abel, W.R., Noujaim, S.F., *et al.* (2022). Neonatal Scn1b-null mice have sinoatrial node dysfunction, altered atrial structure, and atrial fibrillation. *JCI Insight* *7*.

Rhett, J.M., and Gourdie, R.G. (2012). The perinexus: a new feature of Cx43 gap junction organization. *Heart Rhythm* *9*, 619-623.

Rhett, J.M., Ongstad, E.L., Jourdan, J., and Gourdie, R.G. (2012). Cx43 associates with Na(v)1.5 in the cardiomyocyte perinexus. *J Membr Biol* *245*, 411-422.

Salvage, S.C., Huang, C.L., and Jackson, A.P. (2020). Cell-Adhesion Properties of  $\beta$ -Subunits in the Regulation of Cardiomyocyte Sodium Channels. *Biomolecules* *10*.

Teng, A.C.T., Gu, L., Di Paola, M., Lakin, R., Williams, Z.J., Au, A., Chen, W., Callaghan, N.I., Zadeh, F.H., Zhou, Y.-Q., *et al.* (2022). Tmem65 is critical for the structure and function of the intercalated discs in mouse hearts. *Nature Communications* *13*, 6166.

Veeraraghavan, R., Hoeker, G.S., Alvarez-Laviada, A., Hoagland, D., Wan, X., King, D.R., Sanchez-Alonso, J., Chen, C., Jourdan, J., Isom, L.L., *et al.* (2018). The adhesion function of the sodium channel beta subunit ( $\beta 1$ ) contributes to cardiac action potential propagation. *Elife* 7, e37610.

Veeraraghavan, R., Lin, J., Hoeker, G.S., Keener, J.P., Gourdie, R.G., and Poelzing, S. (2015). Sodium channels in the Cx43 gap junction perinexus may constitute a cardiac ephapse: an experimental and modeling study. *Pflugers Arch* 467, 2093-2105.

Veeraraghavan, R., Lin, J., Keener, J.P., Gourdie, R., and Poelzing, S. (2016). Potassium channels in the Cx43 gap junction perinexus modulate ephaptic coupling: an experimental and modeling study. *Pflugers Arch* 468, 1651-1661.

Wei, N., Mori, Y., and Tolkacheva, E.G. (2016). The dual effect of ephaptic coupling on cardiac conduction with heterogeneous expression of connexin 43. *J Theor Biol* 397, 103-114.

Wong, H.-K., Sakurai, T., Oyama, F., Kaneko, K., Wada, K., Miyazaki, H., Kurosawa, M., De Strooper, B., Saftig, P., and Nukina, N. (2005).  $\beta$  Subunits of Voltage-gated Sodium Channels Are Novel Substrates of  $\beta$ -Site Amyloid Precursor Protein-cleaving Enzyme (BACE1) and  $\gamma$ -Secretase. *Journal of Biological Chemistry* 280, 23009-23017.

Yu, F.H., Westenbroek, R.E., Silos-Santiago, I., McCormick, K.A., Lawson, D., Ge, P., Ferriera, H., Lilly, J., DiStefano, P.S., Catterall, W.A., *et al.* (2003). Sodium channel beta4, a new disulfide-linked auxiliary subunit with similarity to beta2. *J Neurosci* 23, 7577-7585.

Zhu, W., Wang, W., Angsutararux, P., Mellor, R.L., Isom, L.L., Nerbonne, J.M., and Silva, J.R. (2021). Modulation of the effects of class Ib antiarrhythmics on cardiac Nav1.5-encoded channels by accessory Nav $\beta$  subunits. *JCI Insight* 6.

## Chapter 4: Conclusions and Future Directions

**4.1 Summary and discussion:** The VGSC  $\beta$ -subunits have been shown to be vital in both the heart and the brain since they were first discovered and named “auxiliary” in 1980 (Beneski and Catterall, 1980). However, it is clear that they are no longer just auxiliary, with roles that do include trafficking of the  $\alpha$  subunits to the plasma membrane (Cortada et al., 2019; Cusdin et al., 2008) and modulating kinetics and gating of the  $\alpha$  subunits (Brackenbury and Isom, 2011; Edokobi and Isom, 2018), but they also have functions separate from  $\alpha$  subunit modulation, including participating in adhesion interactions in a variety of contexts and with a variety of molecules (Kazarinova-Noyes et al., 2001; Malhotra et al., 2000; McEwen et al., 2009; Namadurai et al., 2015; Ratcliffe et al., 2001; Veeraraghavan et al., 2018; Xiao et al., 1999; Yereddi et al., 2013). It has also emerged that  $\beta$ -subunits have assignments in regulating gene expression of multiple targets, including the VGSC  $\alpha$  subunits as well as other ion channels (Bouza et al., 2021; O'Malley and Isom, 2015; Wong et al., 2005). The SCN1B ( $\beta 1/\beta 1B$ ) proteins are of particular interest in the heart, with past data indicating high concentrations of both  $Na_v1.5$  and  $\beta 1/\beta 1B$  in the intercalated disc adjacent to gap junctions, and the importance of SCN1B in regulating the width of the perinexus and playing a role in maintaining normal cardiac conduction (Rhett et al., 2012; Veeraraghavan et al., 2018). Thus, my project focused on the effects of SCN1B mimetic peptides, including monomers  $\beta adp1$  and LQLEED and dimers PS2C and PS2L, with the goal of synthesizing a peptide that could eventually have therapeutic effects on cardiac arrhythmias.

In a heterologous expression system, we observed the regulated intramembrane proteolysis (RIP) of  $\beta 1$ , as other groups have described (Bouza et al., 2021; Haworth et al., 2022; Wong et al., 2005). We added new and important information to the understanding of  $\beta 1$  RIP by showing that  $\beta 1$  mimetic peptide monomer  $\beta adp1$  and dimer PS2L both increased the RIP of  $\beta 1$ . This suggests an ability for  $\beta 1$  to regulate gene expression in a way related to the adhesion function of the Ig domain, since the ICD of  $\beta 1$  translocates to the nucleus when released after cleavage by  $\gamma$ -secretase. However, looking at this result in the broader context of this dissertation we know that  $\beta 1$  is likely not present at high levels in the heart, at least in the rat and mouse, and that instead  $\beta 1B$  may be expressed. This could have important for our understanding of *Scn1b* function in the heart, routes to therapeutic targeting of  $\beta$ -subunits and also on the time course of translating such insights into the clinic in preventing or treating arrhythmias.

While the RIP effects of our peptides may not translate to cardiac *in vivo* models, that does not rule out the possibility of directly targeting the adhesion function of *SCN1B* in the heart.  $\beta 1$  and  $\beta 1B$  do have an identical Ig domain and putative adhesion domain from amino acids 67-86, where the  $\beta adp1$  sequence is taken from.  $\beta adp1$  treatment in *ex vivo* experiments with Langendorff-perfused guinea pig hearts does appear to cause arrhythmogenic alterations in action potential conduction velocity and increase incidents of spontaneous ventricular tachycardia (Veeraraghavan et al., 2018), regardless of  $\beta 1$  or  $\beta 1B$  is the predominant  $\beta$  subunit present in the guinea pig heart. We also show here that in neonatal rat ventricular myocytes (NRVMs) acute  $\beta adp1$  treatment results in decreased junctional sodium current, even though  $\beta 1$  proved to be undetectable by Western blot and IF with a c-terminal  $\beta 1$ -specific antibody.

Results herein indicate that adhesion of  $\beta 1$  is decreased by  $\beta adp1$  over a longer time course than previously described, and our results shift after approximately 30 hours to increased adhesion after  $\beta adp1$  treatment that we hypothesize may be downstream of  $\beta 1$  RIP. On the other hand, the  $\beta 1$  mimetic peptide dimers PS2C and PS2L described herein both increase  $\beta 1$ -mediated homophilic trans-adhesion for 48 hours post-treatment, seemingly independent of  $\beta 1$  RIP. Thus, we hypothesize that the  $\beta 1$  mimetic dimers may provide the greatest opportunity to translate from *in vitro* assays to experiments *in vivo* on cardiac electrical physiology and pathophysiology. Further such work *in vivo* may shed light on if and how  $\beta 1B$  regulates perinexal dynamics and electrical activity between cardiomyocytes. It will be important in future work to better understand how the dimers increase adhesion, if it is not RIP related.

An important aspect of the design of the  $\beta 1$  mimetic peptides is that they are very near known mutations in  $\beta 1$  (E87Q and R85H), which are linked to Brugada syndrome and atrial fibrillation respectively. While it is unclear whether these mutations are also found to occur in  $\beta 1B$ , it is possible, since they are in the conserved region between the splice variants. Many of the SCN1B variants discussed in this dissertation are found in the Ig or extracellular domain, where our peptides are thought to interact with either  $\beta 1$  or  $\beta 1B$ . Additionally, if  $\beta 1B$  is present and a population of the total  $\beta 1B$  subunits are secreted by the cell, as the field generally understands  $\beta 1B$  to do (Patino et al., 2011), there is potential for secreted  $\beta 1B$  to act as a ligand, as we believe our  $\beta adp1$  peptide does. This adds weight to the importance of understanding  $\beta 1B$  function in the heart because it could already act as a natural modulator of SCN1B adhesion.

**4.2 Limitations:** Outlined in this dissertation is the potential for modulation of the adhesion function and RIP of  $\beta 1$  with SCN1B mimetic peptides, as well as provocative new evidence that  $\beta 1B$  may be the more highly expressed SCN1B splice variant in ventricular cardiomyocytes. While there is evidence to support our claims, there are multiple limitations that need to be addressed.

1. All the work completed investigating the effects of SCN1B mimetic peptides on the RIP of  $\beta 1$  was done in 1610 Chinese hamster lung cells with stable expression of  $\beta 1$ . We were unable to translate our findings into cardiac animal models or primary cells because we found that  $\beta 1$  and its RIP were impossible to detect with our current available methods. Thus, our findings may not be applicable to endogenous SCN1B in the heart, at least in so far it concerns  $\beta 1$ . It may be that  $\beta 1$  RIP is not a significant aspect of signal transduction in myocardial tissues. Although that may be the case for the heart, evidence shows a role in signal transduction in cancer cells, where the  $\beta 1$ -ICD is necessary and sufficient to not only increase sodium current, but to diversify the  $\alpha$  subunit population at the cell surface (Haworth et al., 2022). In MDA-MB-231 cells, a breast cancer cell line, heterologous expression of only the ICD of  $\beta 1$  with a GFP tag resulted in increased mRNA levels of Nav1.7 and Nav1.1 (Haworth et al., 2022). Similarly,  $\beta 1$ -mediated neurite outgrowth in cerebellar granular neurons is dependent on  $\beta 1$  RIP (Brackenbury and Isom, 2011). When plated on a monolayer of Chinese Hamster Lung cells expressing  $\beta 1$ , cerebellar granular generate lengthened neurite outgrowth, which is attenuated by treatment



with DAPT or L685458, both inhibitors of  $\gamma$ -secretase (Brackenbury and Isom, 2011). Future work to address the role of  $\beta$ 1 in various tissues is necessary.

2. It is unclear whether the effects of increased RIP in the 1610 $\beta$ 1 cells include increased translation of the  $\beta$ 1 subunit through upregulation of the ICD translocating to the nucleus, or through another mechanism. While the ICD is known to translocate the nucleus and alter transcription of many VGSC genes, the effect on SCN1B transcription is not known (Bouza et al., 2021), though this could be one mechanism through which  $\beta$ 1 is increased in the 1610 $\beta$ 1 cells. It is also evident from Chapter 3 and other groups, that the ratio of mRNA to translated Scn1b protein may be misleading (Angsutararux et al., 2021). Thus, it will be important in future work to focus on revealing the underlying mechanism by which  $\beta$ 1 and  $\beta$ 1B are translated and their proteolysis regulated.

3. The  $\beta$ 1B specific antibody generated by ThermoFisher Scientific for our lab will need to be validated with more stringent controls and assays, and the results presented in the final figure interpreted with the understanding that raw sera containing the  $\beta$ 1B antibody was used, and not affinity purified antibody. Future work to be completed here includes peptide inhibition in the assays used in Chapter 3, both IF and WB, with the peptide the antibody was raised against. It will also be important to confirm the antibody's specificity in a  $\beta$ 1B positive (potentially HEK cells with  $\beta$ 1B exogenously expressed) and negative control. The antibody will also be affinity purified for higher specificity.

4. While the results presented and discussed here are novel and exciting, it will be more important in the future to apply the findings to humans. The peptides were initially designed with the hypothesis that they could treat arrhythmias by modulating  $\beta$ 1-mediated adhesion in the perinexus. Using heterologous expression systems and isolated cultured primary cells does not allow for observation of a true intercalated disc or perinexus. Thus, in order to translate our findings, it will be necessary to first determine whether human myocytes align with our results here, which indicate that  $\beta$ 1B is present while  $\beta$ 1 is not. Then, animal models can be used to study the effects of Scn1b mimetic peptides on cardiac function and structure.

**4.3 Future Directions:** The first and most obvious future experiments will be rounding out the second chapter into a more polished story. It is clear that our findings indicate a lack of  $\beta$ 1 and its RIP in rodent ventricular myocytes, but we will need to establish more controls and validation of our current  $\beta$ 1B specific antibody. This can be accomplished through peptide inhibition studies, affinity purification of the antibody, and more positive and negative controls containing known quantities of  $\beta$ 1 and  $\beta$ 1B.

Next steps would further entail a broader approach to investigating  $\beta$ 1 vs.  $\beta$ 1B presence in the heart in more species. After validation of our initial results in mice and rats, it will be important to move on to guinea pigs, the species in which  $\beta$ adp1 was first tested *ex vivo* to inform whether

the results of  $\beta$ adp1 treatment are likely on  $\beta$ 1 or  $\beta$ 1B (Veeraraghavan et al., 2018). The ultimate goal would be to determine whether  $\beta$ 1 and its RIP is detectable in human tissue.

Eventually, testing of the novel dimer peptides described in this dissertation *ex vivo* and *in vivo* will give the best indication whether SCN1B mimetic peptides could have anti-arrhythmic tendencies and eventual translatability to humans. The first experiments would be in Langendorff-perfused guinea pig hearts with the SCN1B mimetic dimers, to observe effects on conduction velocity and arrhythmogenicity. It may be necessary to cause insult to the heart, either before or after peptide treatment, as we hypothesize the peptides likely don't have a major effect when perinexii are largely intact. The next step would be a fully *in vivo* model. Those experiments would most likely be completed in a mouse model, with either a one-time IP injection of peptide or a slow-release mechanism to have continuous peptide treatment available to the heart. In these experiments, we would be monitoring the mouse for signs of arrhythmias, seizures, and sudden cardiac death since initial experiments with high doses of  $\beta$ adp1 resulted in spontaneous ventricular arrhythmias (Veeraraghavan et al., 2018). The study analysis would include fixing heart tissue for immunofluorescence microscopy to determine the presence and effects on  $\beta$ 1/ $\beta$ 1B,  $\text{Na}_v1.5$ , and Cx43, electron microscopy to measure changes to the perinexii in the heart, and tissue collection for WB to further investigate the effects on  $\beta$ 1/ $\beta$ 1B.

Once these experiments are completed, there are numerous likely fruitful directions, with the method of  $\beta$  subunit modulation through mimetic peptides of the adhesion domain applicable to both the other  $\beta$  subunits and other cell-adhesion molecules that are present in the intercalated disc and throughout the body.

The future work detailed in this section will help to advance our understanding of the structure and function of the proteins found in the perinexus. With the new information described here, it is unclear how SCN1B-mediated adhesion is maintained and regulated in the perinexus. While  $\beta$ 1B has been shown to be retained at the membrane when co-expressed with  $\text{Na}_v1.5$  (Patino et al., 2011), it is unclear whether that is through a direct interaction with the  $\alpha$  subunit, through interaction with another scaffolding protein found at the perinexus, or perhaps the putative transmembrane region initially described in  $\beta$ 1B (Qin et al., 2003). A better understanding of the role of the perinexus and the molecular players involved will eventually result in more targeted and efficient peptides or drugs that can prevent or treat arrhythmias.

The overall conclusion of this dissertation is that SCN1B ( $\beta$ 1/ $\beta$ 1B) mimetic peptides not only have therapeutic potential through modulation of  $\beta$ 1/ $\beta$ 1B-mediated adhesion, regulated intramembrane proteolysis of  $\beta$ 1, and effects on sodium current, but they have the ability to provide the field with a greater knowledge base when it comes to how the SCN1B ( $\beta$ 1/ $\beta$ 1B) proteins function and where they are found in the heart and beyond.

## REFERENCES

- Angsutararux, P., Zhu, W., Voelker, T.L., and Silva, J.R. (2021). Molecular Pathology of Sodium Channel Beta-Subunit Variants. *Front Pharmacol* 12, 761275.
- Beneski, D.A., and Catterall, W.A. (1980). Covalent labeling of protein components of the sodium channel with a photoactivable derivative of scorpion toxin. *Proceedings of the National Academy of Sciences* 77, 639-643.
- Bouza, A.A., Edokobi, N., Hodges, S.L., Pinsky, A.M., Offord, J., Piao, L., Zhao, Y.-T., Lopatin, A.N., Lopez-Santiago, L.F., and Isom, L.L. (2021). Sodium channel  $\beta$ 1 subunits participate in regulated intramembrane proteolysis-excitation coupling. *JCI Insight* 6.
- Brackenbury, W., and Isom, L. (2011). Na<sup>+</sup> Channel  $\beta$  Subunits: Overachievers of the Ion Channel Family. *Front Pharmacol* 2.
- Cortada, E., Brugada, R., and Verges, M. (2019). Trafficking and Function of the Voltage-Gated Sodium Channel  $\beta$ 2 Subunit. *Biomolecules* 9.
- Cusdin, F.S., Clare, J.J., and Jackson, A.P. (2008). Trafficking and Cellular Distribution of Voltage-Gated Sodium Channels. *Traffic* 9, 17-26.
- Edokobi, N., and Isom, L.L. (2018). Voltage-Gated Sodium Channel  $\beta$ 1/ $\beta$ 1B Subunits Regulate Cardiac Physiology and Pathophysiology. *Frontiers in Physiology* 9.
- Haworth, A.S., Hodges, S.L., Capatina, A.L., Isom, L.L., Baumann, C.G., and Brackenbury, W.J. (2022). Subcellular dynamics and functional activity of the cleaved intracellular domain of the Na<sup>+</sup> channel  $\beta$ 1 subunit. *Journal of Biological Chemistry* 298, 102174.

Kazarinova-Noyes, K., Malhotra, J.D., McEwen, D.P., Mattei, L.N., Berglund, E.O., Ranscht, B., Levinson, S.R., Schachner, M., Shrager, P., Isom, L.L., *et al.* (2001). Contactin Associates with Na<sup>+</sup> Channels and Increases Their Functional Expression. *The Journal of Neuroscience* 21, 7517-7525.

Malhotra, J.D., Kazen-Gillespie, K., Hortsch, M., and Isom, L.L. (2000). Sodium Channel  $\beta$  Subunits Mediate Homophilic Cell Adhesion and Recruit Ankyrin to Points of Cell-Cell Contact\*. *Journal of Biological Chemistry* 275, 11383-11388.

McEwen, D.P., Chen, C., Meadows, L.S., Lopez-Santiago, L., and Isom, L.L. (2009). The voltage-gated Na<sup>+</sup> channel  $\beta$ 3 subunit does not mediate trans homophilic cell adhesion or associate with the cell adhesion molecule contactin. *Neuroscience Letters* 462, 272-275.

Namadurai, S., Yereddi, N.R., Cusdin, F.S., Huang, C.L.-H., Chirgadze, D.Y., and Jackson, A.P. (2015). A new look at sodium channel  $\beta$  subunits. *Open Biology* 5, 140192.

O'Malley, H.A., and Isom, L.L. (2015). Sodium channel  $\beta$  subunits: emerging targets in channelopathies. *Annu Rev Physiol* 77, 481-504.

Patino, G.A., Brackenbury, W.J., Bao, Y., Lopez-Santiago, L.F., O'Malley, H.A., Chen, C., Calhoun, J.D., Lafrenière, R.G., Cossette, P., Rouleau, G.A., *et al.* (2011). Voltage-gated Na<sup>+</sup> channel  $\beta$ 1B: a secreted cell adhesion molecule involved in human epilepsy. *J Neurosci* 31, 14577-14591.

Qin, N., D'Andrea, M.R., Lubin, M.L., Shafae, N., Codd, E.E., and Correa, A.M. (2003). Molecular cloning and functional expression of the human sodium channel beta1B subunit, a novel splicing variant of the beta1 subunit. *Eur J Biochem* 270, 4762-4770.

Ratcliffe , C.F., Westenbroek , R.E., Curtis , R., and Catterall , W.A. (2001). Sodium channel  $\beta$ 1 and  $\beta$ 3 subunits associate with neurofascin through their extracellular immunoglobulin-like domain. *Journal of Cell Biology* 154, 427-434.

Rhett, J.M., Ongstad, E.L., Jourdan, J., and Gourdie, R.G. (2012). Cx43 associates with Na(v)1.5 in the cardiomyocyte perinexus. *J Membr Biol* 245, 411-422.

Veeraraghavan, R., Hoeker, G.S., Alvarez-Laviada, A., Hoagland, D., Wan, X., King, D.R., Sanchez-Alonso, J., Chen, C., Jourdan, J., Isom, L.L., *et al.* (2018). The adhesion function of the sodium channel beta subunit ( $\beta$ 1) contributes to cardiac action potential propagation. *Elife* 7, e37610.

Wong, H.-K., Sakurai, T., Oyama, F., Kaneko, K., Wada, K., Miyazaki, H., Kurosawa, M., De Strooper, B., Saftig, P., and Nukina, N. (2005).  $\beta$  Subunits of Voltage-gated Sodium Channels Are Novel Substrates of  $\beta$ -Site Amyloid Precursor Protein-cleaving Enzyme (BACE1) and  $\gamma$ -Secretase\*. *Journal of Biological Chemistry* 280, 23009-23017.

Xiao, Z.-C., Ragsdale, D.S., Malhotra, J.D., Mattei, L.N., Braun, P.E., Schachner, M., and Isom, L.L. (1999). Tenascin-R Is a Functional Modulator of Sodium Channel  $\beta$  Subunits\*. *Journal of Biological Chemistry* 274, 26511-26517.

Yereddi, N.R., Cusdin, F.S., Namadurai, S., Packman, L.C., Monie, T.P., Slavny, P., Clare, J.J., Powell, A.J., and Jackson, A.P. (2013). The immunoglobulin domain of the sodium channel  $\beta$ 3 subunit contains a surface-localized disulfide bond that is required for homophilic binding. *The FASEB Journal* 27, 568-580.